Doctoral Thesis

Characterization of nuclear envelope proteins NPP-16 and LEM-2 and identification of interaction partners

Adela Morales Martínez

Director: Peter Askjaer

Tutor: Manuel J. Muñoz

December 2013

“Somos naturaleza,

Poner al dinero como bien supremo

Nos conduce a la catástrofe”

José Luis Sampedro

A mis padres

Hace un poco más de 4 años empecé este proyecto que ahora termina, lo cual no hubiera sido posible si el apoyo y el aliento de muchas personas.

En primer lugar quiero agradecer a Peter, mi jefe, por darme esta oportunidad y por estar a nuestro lado cada día dispuesto a ayudarnos y a transmitirnos el amor por la ciencia y todo ello siempre con un sentido exquisito de la honradez y la justicia. A mis maestros o hermanos mayores, Eduardo, que aunque está a miles de km me responde siempre en un minuto, a Cristina González siempre con una sonrisa para animarte y a Machupi a la que echo de menos cada día en el laboratorio. A Cristina Ayuso por aguantar mi desorden y estar siempre dispuesta a ayudar. A Aga, compañera de tesis, por su cercanía y cariño y a Gina por su apoyo y comprensión.

También han sido fundamental para este trabajo los demás gusaneros, no puedo olvidarme de Antonio Miranda y su grupo, especialmente Nando, Fran y María por tantas risas y buenos momentos compartidos. Gracias a mi gusanologa Mercedes y su pareja, Carlos por su sonrisas permanente y por compartir conmigo su afición por la escalada, el deporte y por la vida. Y, aunque llevan aquí poquito, gracias a Roxani, Ann, Artur y Marta por compartir pared y vivencias día a día.

Pero no sólo de gusanos vive la ciencia y en CABD hay mucha gente estupenda q me ha acompañado estos años. Especialmente mis “supergirls” María, Mª Ángeles e Inés y (super-boy) Manolo, con quienes empecé un master y acabé compartiendo cuatro años. También agradecer a Ozren sus ánimos y su ayuda con la traducción, a Rocío Polvillo por sus consejos de pasillo y a David y Paco Corín. A, Lesly y Katy por estar siempre dispuestas a ayudar.

Cuatro años son muchos días y horas en el laboratorio y para mí ha sido muy importante el apoyo de muchas personas fuera de este. Gracias a mi compi de piso Alfonso por echarme una mano con el inglés, a mis “gallinitas” Chana, Isa, Carmen, Triana y Rocío, por su apoyo constante. También a mis biólogos Helia y A. Merino. A Carmen Lampaya por su ejemplo de mujer que puede con todo. A mis trianeros queridos, especialmente a Paco y Vero por sus palabras de ánimo y su comprensión. Y a Jose Manuel porque aunque nos conocemos de poco no ha dejado de animarme a llegar donde quiera ni un solo día. Agradecer también a mis niñas Reyes, Patri y Tere

con las que he compartido muchos cafés, momentos de agobio y de felicidad por estar siempre a mi lado.

Como no podía ser de otra forma, agradecer a mi Sarahita por creer en mí y compartir tantos años de nuestras vidas.. Y a Carlos por “aguantarme” estos meses, mimarme, apoyarme en cada paso y sacarme siempre una sonrisa.

Y por último y no por ello menos importante, quería dar las gracias a mi hermano Jose, por sus consejos y a mis padres Rosarito y Pepe, que me han acompañado durante cada día, mostrándome los caminos más justos con su forma de actuar, pero respetando también mis decisiones. Sin vosotros nada de esto hubiera sido posible, gracias por estar siempre en la recámara dispuestos a ayudarme y aconsejarme siempre que lo necesito, gracias por quererme tanto.

INDEX

FIGURES INDEX

TABLE INDEX

Abbreviations:	
Aa	amino acid
Amp	Ampicillin
Bp	base pair
Carb	Carbenicillin
DNA	Deoxyribonucleic acid
dsRNA	double stranded RNA
Emb	Embryonic lethality
EMR-1	Emerin
ER	Endoplasmatic Reticulum
GFP	Green Fluorescent Protein
Gro	Growth defects
IF	Immunofluorescence
INM	Inner Nuclear Membrane
KD	Kilo Dalton
LMN-1	Lamin
Lva	Larval arrest
Lvl	Larval lethality
mRNA	messenger RNA
Muv	Multivulva
NE	Nuclear Envelope
NGM	Nematode Growth Medium
NPC	Nuclear Pore Complex
NPP	Nucleoporin (*C. elegans* nomenclature)
Nup	Nucleoporin (Vertebrate and yeast nomenclature)
ONM	Outer Nuclear Membrane
ORF	Open Reading Frame
PCR	Polymerase Chain Reaction
Pvl	Protruding vulva
Rb	Reduced brood progeny
RdRP	RNA dependent RNA Polymerases
RNA	Ribonucleic acid
RNAi	RNA interference
RT-PCR	Reverse Transcription Polymerase Chain Reaction
Sck	Sick
siRNA	small interference RNA
Ste	Sterility
Stp	Sterility progeny
Tet	Tetracycline
Unc	Uncoordinated
Wt	wild type
α-tub	alpha tubulin
β-tub	beta tubulin

Resumen

Caenorhabditis elegans, primer organismo multicelular cuyo genoma fue secuenciado y publicado en 1998 (Consortium 1998), es un nematodo transparente de vida libre, perteneciente a la familia Rhabditidae. Su tamaño no supera el mm y, aunque su dieta natural es bastante variada, *C. elegans* se alimenta en el laboratorio de la bacteria *Escherichia coli*.

Su población es fundamentalmente hermafrodita y sólo un 1% de los animales son machos, presentando un claro dimorfismo sexual en la mayoría de los tejidos. Pese al reducido número de células somáticas (959 en hermafroditas y 1031 en machos), todas ellas con un destino fijo e invariable entre individuos, este nematodo presenta algunos órganos completamente formados así como un sistema nervioso bastante complejo. Todo esto, además de su fácil y asequible mantenimiento en el laboratorio, hacen de *C. elegans* un organismo modelo idóneo para estudiar diferentes procesos en un organismo completo. Fue en 1963 cuando Sydney Brenner propuso este nematodo como organismo modelo y desde entonces cada día es más usado en gran diversidad de estudios.

Una de las ventajas de *C. elegans* es que permite trabajar con técnicas moleculares de manera muy efectiva. Una de ellas es el ARN de interferencia (del inglés interfering Ribonucleic Acid or RNAi) que permite el silenciamiento de un gen determinado bloqueando la expresión del ARN mensajero (ARNm) resultante de su transcripción. Esta técnica se basa en un fenómeno que inicialmente fue descrito en plantas y hongos (Napoli, Lemieux et al. 1990, Cogoni, Irelan et al. 1996) y posteriormente se desarrolló en *C. elegans* (Fire, Xu et al. 1998). Aunque pueden observarse ciertas diferencias entre los distintos organismos, todos coinciden en que la introducción de moléculas de ARN bicatenario (del inglés double stranded RNA dsRNA) induce el proceso de ARNi causando una reducción drástica de los niveles de ARNm, produciéndose el silenciamiento del gen y por tanto un fenotipo en el propio animal/individuo y en toda su progenie (Fire, Xu et al. 1998, Agrawal, Dasaradhi et al. 2003).

La aplicación de este proceso natural a la ciencia ha llevado a usar la interferencia por ARN como una técnica fundamental en diversas investigaciones. Esta técnica se utiliza para determinar la función de un determinado gen observando qué efectos

tiene su silenciamiento en el desarrollo del organismo, ayudando a definir así su función mediante lo que se considera genética reversa. En este nematodo las moléculas de ARN interferente pequeño (del inglés small interfering RNA o siRNA) pueden ser también introducidas de forma exógena en el adulto mediante diversos métodos, de manera que el siRNA llega a las células produciendo la destrucción del ARNm complementario. Los métodos utilizados en *C. elegans* son inyección (Fire, Xu et al. 1998), osmosis (Tabara, Grishok et al. 1998) y alimentación(Timmons and Fire 1998).

Aunque los tres métodos son utilizados en multitud de estudios, el que parece combinar mejor efectividad, simplicidad y asequibilidad económica es el RNAi por alimentación. Este método además posibilita hacer estudios a gran escala (Boutros and Ahringer 2008) como el que se ha realizado en esta tesis.

Combinado el uso de *C. elegans* como organismo modelo y la interferencia por ARN como una de las técnicas más efectivas en la determinación de funciones génicas, hemos estudiado una de las estructuras fundamentales en la célula eucariota, la envoltura nuclear (NE). Esta estructura está compuesta por dos membranas lipídicas, la membrana interna (INM) la membrana externa (ONM) que se fusionan en numerosos lugares, generando poros que están ocupados por grandes canales macromoleculares llamados complejo del poro nuclear (NPC). La NE delimita el núcleo separándolo del citoplasma, por lo que posibilita la maduración del ARN mensajero antes de ser traducido a proteínas este proceso de maduración no se presenta en procariotas), pero además esta estructura aparece cada vez más relacionada con la regulación del material genético y su distribución dentro del núcleo (Hetzer 2010). Los NPCs juegan un papel fundamental en la regulación del transporte núcleo-citoplasma de multitud de moléculas, y se relacionan cada vez más con la regulación de la expresión del material génico (Kalverda, Pickersgill et al. 2010).

Por todo ello la NE y sus componentes son esenciales para la célula y por ende para los organismos, de hecho multitud de enfermedades han sido relacionadas con defectos en esta estructura. Las laminopatías (Worman and Bonne 2007) son, por ejemplo, enfermedades relacionadas con mutaciones en la proteína lámina que forma

la capa subyacente a la NE y que interviene en el mantenimiento de la estructura del nucleoesqueleto. Pero estas enfermedades también están relacionadas con defectos en proteínas de la NE como es el caso de Emerin, proteína de la INM, relacionada en el síndrome de distrofia muscular Emery- Dreifuss (EDMD).

Uno de los objetivos principales de esta tesis es describir dos proteínas de la NE, la nucleoporina NPP-16 que forma parte de los NPCs y la proteína transmembrana LEM-2 que se encuentra situada en la INM. Además de describir características como su localización, dinámica y posibles funciones, en la primera parte del proyecto se realizó una búsqueda en el genoma completo de *C. elegans* (del inglés genome wide screening) mediante la técnica de ARNi y usando la librería del laboratorio de Julie Ahringer(Kamath, Martinez-Campos et al. 2001). Tras analizar el efecto del ARNi de ~17,000 genes en la línea silvestre (wt) y dos líneas mutantes, un mutante de *npp-16* y otro de *lem-2*, obtuvimos 1,016 genes que fueron sometidos a dos rondas de validación. Finalmente se obtuvieron 40 genes que mostraban algún tipo de interacción con *lem-2* y 13 genes con *npp-16*.

En la segunda parte de esta tesis, además de analizar los genes obtenidos con cada proteína, se llevaron a cabo distintos experimentos para caracterizar y describir la función de NPP-16 y LEM-2.

NPP-16, Nup50 en mamíferos, es una nucleoporina que forma parte de la NE y que en mamíferos (Fan, Liu et al. 1997)se ha relacionado con mecanismos de transporte nuclear (Lindsay, Plafker et al. 2002, Matsuura and Stewart 2005, Pumroy, Nardozzi et al. 2012) y regulación de la expresión génica (Fan, Liu et al. 1997, Kalverda, Pickersgill et al. 2010). En este trabajo utilizamos el mutante *tm1596* para caracterizarla, que, teniendo en cuenta los resultados obtenidos en inmunofluorescencias, parece no ser una mutación completamente nula. Utilizando una línea transgénica que expresa GFP::NPP-16 se caracterizó su expresión en todas las células del nematodo y su localización sub-celular, que está restringida a la envoltura nuclear y en el nucleoplasma, aunque presenta variación entre los distintos tipos celulares y fases embrionarias. Otra característica estudiada fue su movilidad, superior a la de otras nucleoporinas como NPP-19. Respecto los resultados obtenidos en la búsqueda

genética, uno de los candidatos que mostró un fenotipo más severo y reproducible en el mutante *tm1596* fue NPP-2 (Nup85 en mamíferos) cuyo ARNi tanto en el silvestre como en el mutante NPP-16 produce una reducción en el tamaño del núcleo, pero además produce casi un 100% de letalidad embrionaria en el mutante, fenotipo prácticamente ausente en la línea silvestre alimentada con el mismo ARNi Mediante el estudio de distintos genes reporteros y anticuerpos, describimos que la falta de ambas nucleoporinas produce graves defectos en la segregación del ADN y la estabilidad de la NE.

La otra proteína objeto de estudio en esta tesis, LEM-2, pertenece al grupo de proteínas transmembranas de la NE (NETs) y tiene, al igual que otras proteínas de esta zona, un dominio llamado LEM que media la interacción con la proteína BAF que se une a ADN (Brachner, Reipert et al. 2005). Confirmamos su localización en la envoltura nuclear así como en el retículo endoplasmático (ER) y la letalidad sintética que esta proteína muestra con emerin (Gruenbaum, Lee et al. 2002, Liu, Lee et al. 2003, Ikegami, Egelhofer et al. 2010), uno de nuestros controles en la búsqueda genética. Aunque aparentemente el mutante *lem-2(tm1582)*, consistente en una mutación nula, no presentaba ningún fenotipo, en el presente trabajo se ha descrito que la ausencia de LEM-2 afecta a la circularidad y forma de la envoltura nuclear. Además, este mutante muestra un defecto en la separación de los núcleos en la segunda división embrionaria (AB) y en el comportamiento de los centrosomas durante la misma.

Respecto a los resultados de la búsqueda genética, de los 40 genes que mostraron una interacción con la línea *tm1582*, seleccionamos *ubc-12*, cuyo ARNi produce una letalidad significativamente mayor en el mutante *lem*-2 que en la línea silvestre, y además en ausencia de LEM-2, causa fenotipos post-embrionarios severos como letalidad larvaria y esterilidad en aquellos embriones que logran eclosionar. Para estudiar la relación entre estas dos proteínas profundizamos en la ruta de nedilación, el proceso en el que interviene UBC-12, y que se trata de una ruta de modificación post-traduccional de proteínas similar a la ubiquitinación. En el caso de la nedilación la molécula que se añade al sustrato es NED-8 y conlleva distintos tipos de modificaciones estructurales, activaciones o represiones de las mismas (Rabut and Peter 2008). Realizando experimentos de RNAi en el mutante *lem-2*, vimos que el RNAi

de *ned*-8, gen codificante para la molécula que se añade al sustrato en esta ruta, produce una letalidad embrionaria significativamente superior en el mutante *lem*-2 en comparación con la línea silvestre, indicando que el LEM-2 puede tener un papel concreto en esta ruta.

En conclusión, en esta tesis hemos profundizado en el conocimiento y la caracterización de dos proteínas de la envoltura nuclear, NPP-16 y LEM-2, así como en sus posibles funciones. Además hemos encontrado 13 proteínas que muestran relación con NPP-16 y 40 con LEM-2, profundizando en la descripción de dos de ellas, NPP-2 en el caso de NPP-16 y UBC-12 en el caso de LEM-2.

Resumen

I. Introduction

Introduction

1.1 *Caenorhabditis elegans*, a research nematode

Caenorhabditis elegans is a free-living, transparent nematode that belongs to the Rhabditidae family and to the *Caenorhabditis* genus, which geographical distribution includes North Africa, Madeira, Europe, Hawaii, Asia and Australia. Although the habitats where this genus of nematodes can be found are very diverse, some species, like *C.* elegans, have only been isolated from anthropogenic habitats (as compost). *Caenorhabditis* nematodes are colonizers of nutrient and microorganism-rich organic material so when an ephemeral resource appears, this is populated rapidly and the local population reaches high densities (as observed at the laboratory).

It is well known that *C. elegans* feeds on the bacterium *Escherichia. coli* but its food sources are in general more variable. In 1991 Grewal (Grewal 1991) analyzed 10 bacterium strains that grow together with *C. elegans* in mushrooms compost; only 5 out of those 10 sustained growth and reproduction of *C. elegans* for many generations in monoxenic culture. In parallel it was also shown that this nematode can also feed on *amoebae* of the slime mold *Dictyostellum discoideum* (Pukatzki, Tordilla et al. 1998).

Moreover, as many other nematodes, *C. elegans* associates with invertebrates as millipedes, isopods, insects, snails and slugs, by a phoretic association, and it is thought that its resistance stage could feed dead matter.

One important thing for researches, is that *C. elegans* was the first multicellular organism to have its genome completely sequenced and published in 1998 (Consortium 1998). This genome is around 100 million base pairs (bp) long, distributed in six chromosomes (named I, II, III, IV, V and X) with over 19,000 genes.

Proposed as a model organism in 1963 by Sydney Brenner, this animal has several characteristics that make it a great model organism: is simple, easy to grow in bulk populations, strains are cheap and they can be frozen, allowing long-term storage. Another relevant property for work with *C. elegans* is its transparency, which facilitated the study of cellular differentiation and other developmental processes in the intact organism.

This nematode, which presents a clear sexual dimorphism, has only 959 somatic cells (1031 in the male) and the invariant patterns of cell lineages between individuals. It has a nervous system and other organs completely formed a feature that allows for studies of different processes in the entire organism (Figure 1).

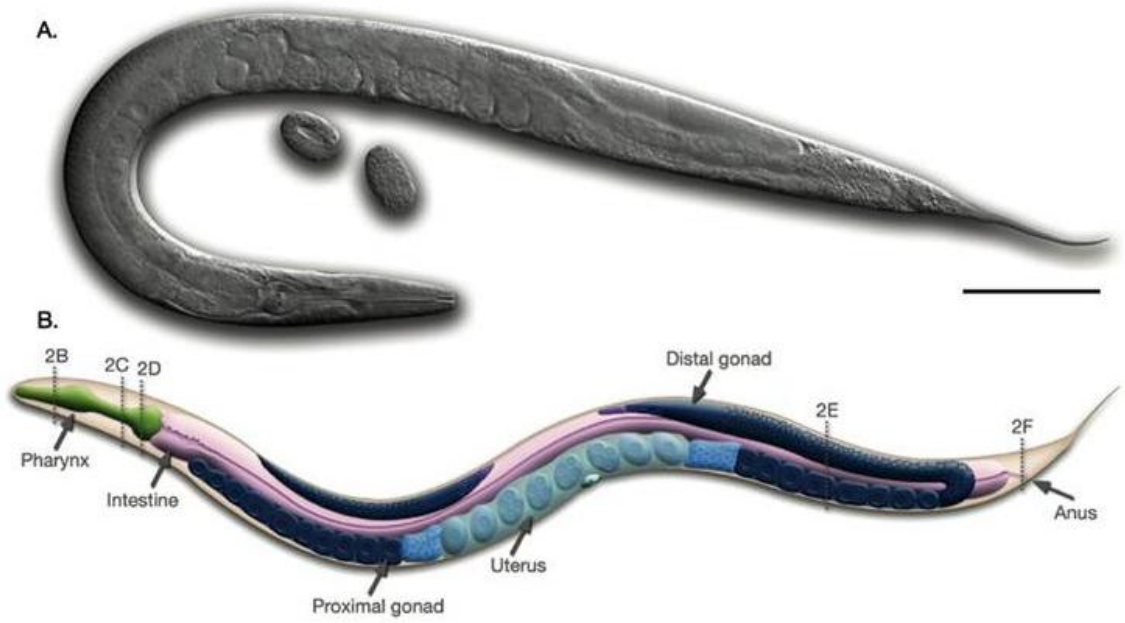

Figure 1: Anatomy of an adult hermaphrodite *C. elegans*. A) DIC image of an adult hermaphrodite, left lateral side. Scale bar 0.1 mm. B) Schematic drawing of anatomical structures, left lateral side, where are visible the different of alimentary system and reproductive system in an adult hermaphrodite. The dotted lines and numbers correspond to different body sections showed in Figure 2. Scale bar 0.1 mm. Adapted from (Altun 2009).

1.1.1. <u>Anatomy</u>: *C. elegans* has a cylindrical, un-segmented body composed of two concentric tubes separated by the pseudocelomic space (Figure 1 and 2). The body wall (outer tube) is composed of the cuticle, hypodermis, excretory system, neurons and muscles; whereas the inner tube consists of the pharynx, intestine and gonads. The osmoregulatory system allows regulating the internal hydrostatic pressure in all these tissues. All tissues, with the exception of the pharynx and the excretory system exhibit some degree of sexual dimorphism (Figure 3). Both the nervous and the muscle systems are additionally related with sex-specific morphogenesis and behavior (Altun 2009).

- **Cuticle**: the cuticle is the exoskeleton of the nematode and is very flexible and resistant, allowing the locomotion via muscle attachment. The cuticle provides environmental protection and has molting process allowing the growing of the animal, in fact it is synthesized five times, once in the embryo and then at the end of each larval stage. This cuticle is secreted by the underlying epithelium, and is composed mainly by collagens, but also by insoluble proteins called cuticlins, associated with glycoproteins and lipids. Through this cuticle there are various tissue openings: the excretory pore (on the ventral side of the head), the vulva (ventral side of the midbody), and the anus (ventral opening before the tail whip) and there are other smaller openings related with the sensillia.

- **Epithelial System**: the epithelial system in *C. elegans* is formed by the hypodermis and other specialized epithelial cells. The hypodermis is composed by cells that are syncytium structures; this organ forms the external surface of this nematode, secretes the cuticle, establishes the basic body form of the animal, acts as a nutrient storage and has phagocytosis activity for up-take of apoptotic cells corpes. The main body syncytium is hyp 7; there are five smaller syncytial cells in the head, three mononucleated and one syncytial cell in the tail. The hypodermis and the inner tissues are connected by specialized epithelial cells that connect the latter to the outside (Figure 2).

Some of the specialized epithelial cells are related with the nervous system, acting as potential guides for axon outgrowth, protectors of neuronal sensory receptors, or as linker cells to hold various portions of the hypodermis together. Others form specialized adaptations of the cuticle, allowing the formation of holes or ridges in it. Inside this group of cells there are 3 subcategories:

- Seam cells that are present in the apical midline (left and right sides) of the hypodermis.

- The interfacial epithelial cells are in the junctions where hypodermis meets another type of tissue. This group also contains the socket cells that are related with the

secretion of the cuticle in the region near the opening of several sensilia, and the glial-like sheath cells that provide a protective environment for the cilium.

- Others epithelial cells that are present between the junctions of hypodermal/epithelial and other tissues. are arcade cells of the nose, two interfacial epithelial cells (the excretory duct cell and the excretory pore cell) that connect the excretory system to the ventral opening at the excretory pore, and cells of the different epitheliums: pharyngeal, rectal, vulval, cloacal (in male) and marginal cells of pharynx.

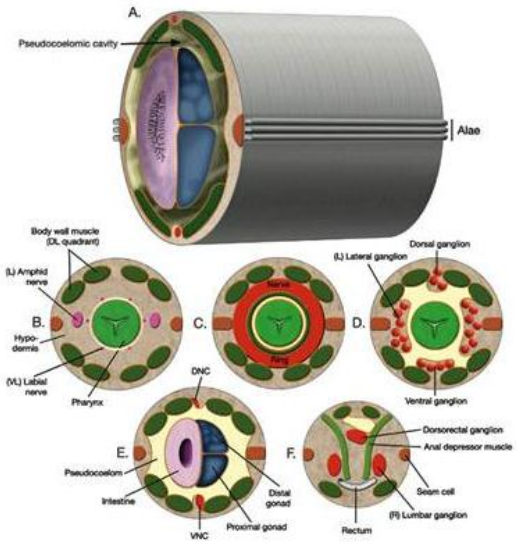

Figure 2. Cross sections from head to tail of the nematode body plan. A) Section of the posterior body region, the outer tube (body wall) and the inner tube (alimentary system, gonad) are concentric and separated by a psedocoelom. The orange lines represent basal laminae. B) Section through anterior head. The narrow space between the pharynx and the surrounding tissues anterior to the NR can be considered an accessory pseudocoelom since the main pseudocoelom is sealed off by the GLRs at the NR level. C) Section through the middle of head. D) Section through posterior head. E. Section through posterior body. DNC: Dorsal nerve cord; VNC: Ventral nerve cord. F. Section through tail, rectum area. Adapted from (Altun 2009).

- **Nervous system**: **i**s the most complex tissue of *C. elegans*, not only in terms of numbers (302 neurons and 56 glial cells, which correspond to 37% of the somatic cells in hermaphrodite) but also in diversity (118 morphologically distinct neuron classes). This system is organized in several ganglia localized in the head, tail and into a spinal cord-like ventral and dorsal nerve, formed by cell bodies that lie at the midline, adjacent to ventral hypodermis. Moreover, two small posterior lateral ganglia can be found, as well as some scattered neurons along the lateral body (Figure 2).

The information from most neurons travels through both the ventral and dorsal nerve cord, and it is projected to the nerve ring in the head (major neutrophil in this animal). Most of the neurons show complex patterns of wiring to other neurons, and often express a large number of signaling molecules.

Muscle system: in *C. elegans*, this system is separated from the neurons and hypodermis by a thin basal lamina. The striated body wall muscles are organized in quadrants, two dorsal and two ventral, along the whole length of the animal (Figure 2). The striated muscles contain several to many sarcomeres repeated in regular order in one cell. Non-striated muscles are found in the pharynx, around the vulva, intestine and rectum, and have at least one well-structured sarcomere (pharyngeal muscle, anal depressor muscle and vulval muscles) or in other cases myofilament networks that are less organized, such as the contractile gonadal sheath.

- **Excretory system**: this system handles the osmoregulation and waste disposal and is formed by four distinctive cell types: one pore cell, one duct cell, one canal cell and a fused pair of gland cells (Figure 2). The excretory canal cell acts as a kidney, excreting saline fluid via the duct and the pore, maintaining the salt balance and removing metabolites. The excretory gland cell secretes, to the same duct, materials from large membrane-bound vesicles. All these secretions empty through a cuticle-lined excretory duct and pore, on the ventral side of the head.
- **Pseudocelomatics cavity organs**: the coelomocyte system, is formed by three pairs of coelomocytes that are located in the pseudocelomic cavity, adjacent to the somatic musculature. Coelomocytes act as scavenger cells that take up a variety of molecules from the body cavity fluid and are suggested to comprise a primitive immune system in *C. elegans*.
- **Alimentary system:** in the worm the alimentary system is formed by a two lobed pharynx that passes ingested and ground food into the intestine via the intestinal pharyngeal valve. The intestine is made of 20 cells organized to form a tube with a central lumen and numerous microvilli of these cells. The intestinal contents are excreted to the exterior via a rectal valve, connecting the gut to the rectum and anus (Figure 1 and 2).

- **Hermaphrodite germ line**: is one of the most sexually dimorphic tissues in the nematode (Figure 1). As mentioned before *C. elegans* population is 90% hermaphrodite. A hermaphrodite is considered a specialized self-fertile female (because the soma is female) that it is able to produce a fixed number of male gametes before switching to the sole production of female gametes (oocytes). The hermaphrodite produces mature gametes and creates the proper conditions for fertilization and egg-laying. It is composed by two symmetrical U-shaped tubes, composed by the somatic gonad and germ line, joined to a uterus and egg-laying apparatus that open in the midbody through the vulva. The organization of the hermaphrodite adult germ line is in a distal-to-proximal manner, so that germ cells in the distal part are mitotic and undifferentiated, and as they move proximally they pass through all the phases reaching meiosis in the proximal arm of the gonad. There, the oocytes undergo maturation and are ovulated in single-file, arriving to the sperm-containing spermatheca where they are fertilized. The embryos then move into the uterus and the egg-laying apparatus forces their exit to the environment through the vulva. Approximately 300 embryos are produced by self-fertilization.

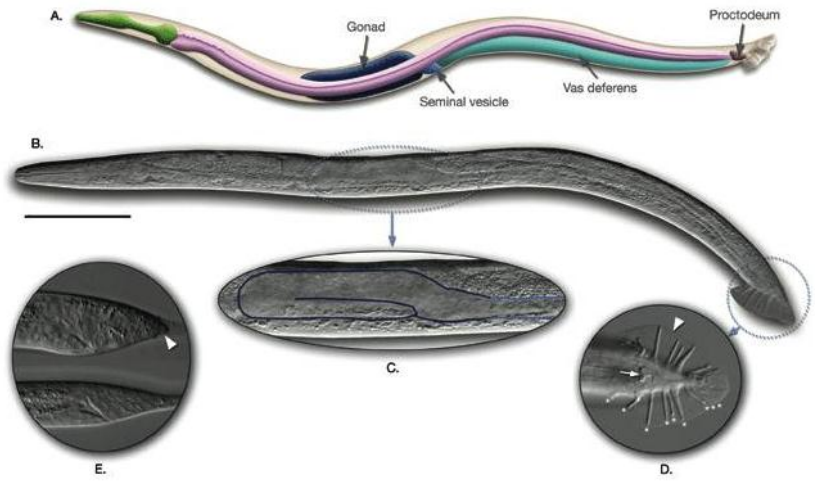

Figure 3. *C. elegans* male. A) Schematic drawing of anatomical structures, left lateral side. B) DIC image of an adult male, left lateral side. Scale bar 0.1 mm. C) The unilobed distal gonad of the animal in B is shown as enlarged. D) The adult male tail, ventral view. Arrow points to cloaca, arrowhead marks the fan. Rays 1-9 are labeled with asterisks on the left side. E) L3 tail, bottom, is starting to bulge. Tail hypodermis has retracted in L4 tail (arrowhead), top. Adapted from (Altun 2009).

- **Male anatomy:** initially the male *C. elegans* larval show the same body plan as the hermaphrodites; it is from L2 stage when its copulatory apparatus starts to develop in the posterior part of the body. It consists of a single armed gonad that opens to the exterior at the cloaca via the proctodeum, which includes two sclerotic sensory spicules that the male uses during mating to locate the hermaphrodite vulva and to hold it open during sperm transfer (Figure 3).

1.1.2. **Live cycle:** *C. elegans* has a live cycle composed of embryogenesis, four larval stages (L1-L4) and adulthood (Figure 4). At 22º this live cycle last 55h

Embryogenesis is divided in two stages:

- **Proliferation** (0 to 330-350 min at 22º): from a single cell to a 558 cells ("16 E stages"). This stage, which starts with the zygote, comprises of the generation of embryonic founder cells and the bulk of cell division and gastrulation are covered. (Figure 5

Many researches are focused in the early embryo divisions of the embryo making very relevant to know the different features of this developmental stage (Figure 4). The zygote experiment a series of asymmetric cell divisions critical in setting up the anterior/posterior, dorsal ventral, and left/right axes of the body plan (Gonczy and Rose 2005). When the sperm fertilizes the egg, the sperm nucleus and centrosomes are deposited within the egg, producing a cytoplasmic flux that causes the movement of the sperm pronucleus towards one pole. The first division of the one cell embryo produces two distinctly different blastomeres, termed AB and P1. When the sperm fertilizes the egg, the sperm nucleus and centrosomes are deposited within the egg. This causes a cytoplasmic flux resulting in the movement of the sperm pronucleus and centrosomes towards one posterior pole (Goldstein and Hird 1996, Cowan and Hyman 2004). After the establishment of this polarity several proteins present in the zygote, called the PAR proteins (partitioning –defective) are distribute in a polarized manner in the zygote establishing cell polarity during development (Cheeks, Canman et al. 2004). The orientation in which the division occurs is also an important factor determinate by the

mitotic spindle that must be oriented correctly to ensure that the proper cell fate determinants are distributed appropriately to the daughter cells. PAR proteins regulate the positioning of the centrosomes along the A/P axis as well as the movement of the mitotic spindle along the A/P axis (Gonczy and Rose 2005).Following this first asymmetric division, the AB daughter cell divides symmetrically, giving rise to ABa and ABp, while the P1 daughter cell undergoes another asymmetric cell division to produce P2 and EMS. This division is also dependent on the distribution of the PAR proteins (Schneider and Bowerman 2003).

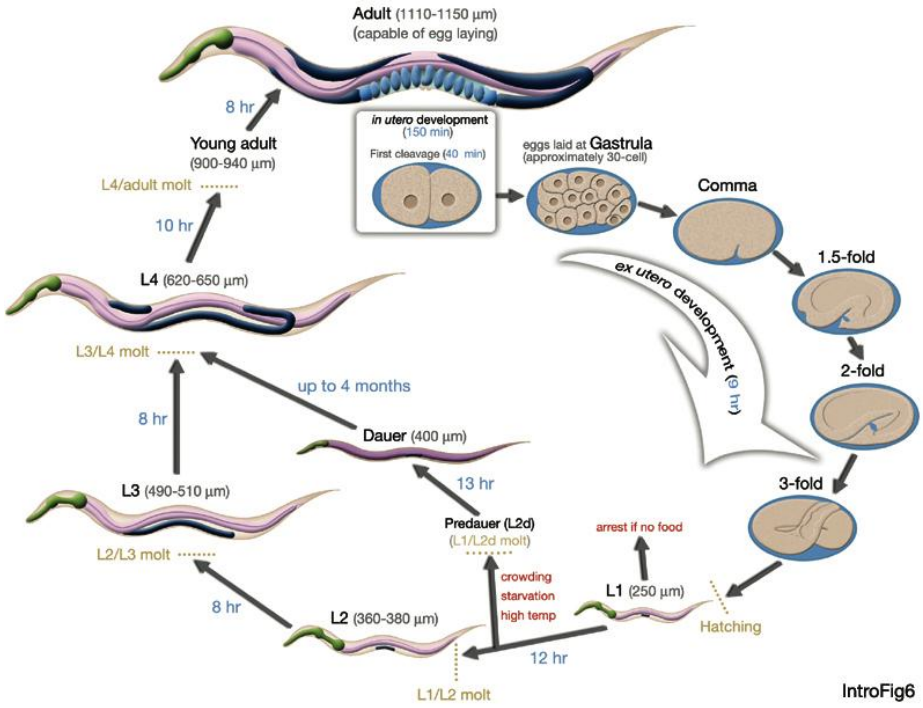

Figure 4. Life cycle of *C. elegans at 22ºC*. After fertilization(0 min) the embryo develops and hatches after 9h. The post-embryonic development consists in four larval stage: L1, L2, L3 and L4, becoming a young adult after 38 h and reaching the adult stage 8 h latter. After L2 if the environmental conditions are not the right ones the worm enters in a resistant stage called Dauer, resuming the cycle when the stress conditions disappear. Numbers in blue along the arrows indicate the length of time the animal spends at a certain stage. First cleavage occurs at about 40 min. post fertilization. Eggs are laid outside at about 150 min. post fertilization and during the gastrula stage. The length of the animal at each stage is marked next to the stage name in micrometers. Adapted from (Altun 2009)

- **Organogenesis and morphogenesis** (330-360 min to 720-840 min): in this stage terminal differentiation of cells occurs without additional cell division and the embryo elongates threefold. Later, the worm can move inside the egg and start pharyngeal pumping 40 min before the hatching, at 800 min. At the end of the embryogenesis, the

main body plan is already established and it does not change during postembryonic development.

Post-embryonic development is triggered by feeding of the larval after hatching, and three hours later the developmental program begins. There are four larval stage (L1-L4), and through them the different organs and structures of the nematode acquire their final morphology. If a L2 larva encounters environmental conditions that are not favorable for growth, the worm will enter in a resistance stage called Dauer, characterized by feeding arrest and a markedly reduced locomotion. This state ends when the animal experiences favorable conditions, and after 10 h of feeding molts in L4 stage (Figure 4).

About 45-50 h. after hatching, at 22-25º, the worm reaches adulthood. Hermaphrodites produce oocytes for about four days and live after that for an additional period of 10-15 days. By self-fertilization, the adult hermaphrodite produces about 300 progeny, however if mating with a male occurs, the progeny number can reach 1200-1400.

The short live cycle is another feature that facilitates the use of this nematode for researches as the one presented in this thesis.

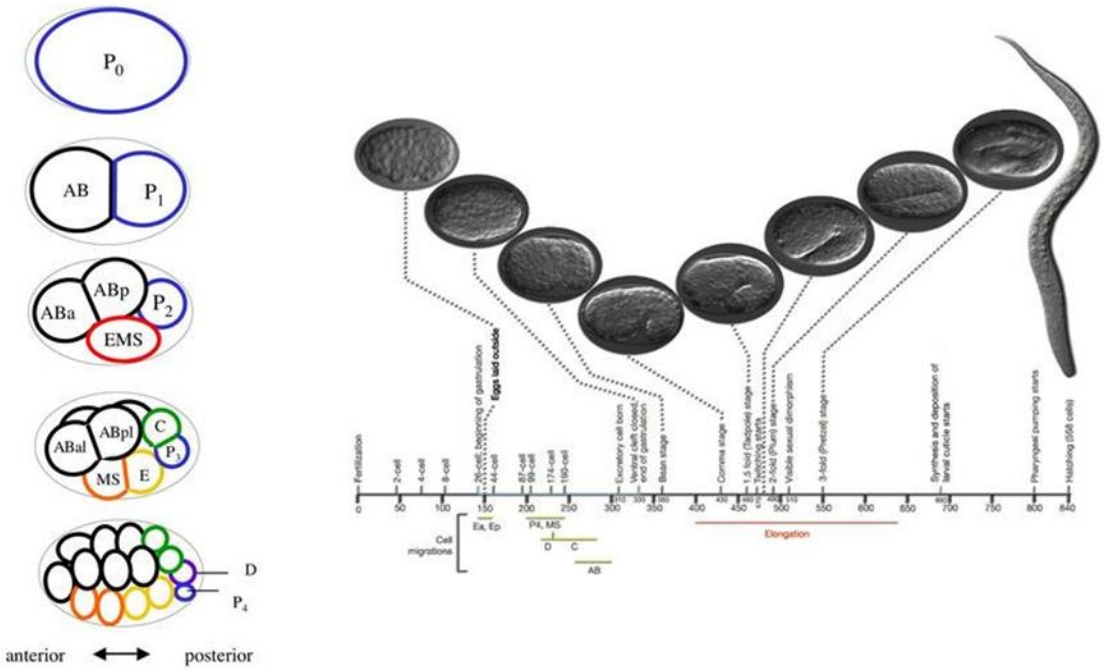

Figure 5. Embryonic stages of development. A) Generation of founder cells in the early embryo. The AB lineage produces hypodermis, neurons, anterior pharynx and other cell types; MS produces the somatic gonad, muscle, the majority of the pharynx, neurons and gland cells; E produces all intestine; C produces muscle, hypodermis and neurons; D produces muscle; P4 is the germ-line precursor. The 16-cell embryo shown in (e) is simplified and does not show the daughters of the 4th AB cell division, which occurs at approximately the same time as the P3 division. Adapted from (Gonczy and Rose 2005)B) Different stage in C. elegans embryos after fertilization., the first cleavage occurs at approximately 40 min. after fertilization. Then starts gastrulation process that finish with the neuroblast division. After that the hypodermal cells spread over the ventral surface from both sides and meet each other along the ventral midline to cover the surface of the embryo and complete the epithelium formation. Then starts the elongation that takes place between 400-640 min and the embryo becomes threefold thinner and its length increases about fourfold. Before the hatching (840 min, 558 cells) several process such as the deposition of the larval cuticle and the pharyngeal pumping start. Adapted from (Altun 2009)

1.2. RNA interference (RNAi)

One of the advantages of *C. elegans* as model organism is that several molecular genetic techniques work really well on it. For example RNA interference, that has become a widely used method for studying gene function and the main technique used in this thesis.

RNA interference has been one of the most used tools in the area of cell biology during the last years. One of the reasons is that it allows selectively disrupting of a specific gene's activity and to observe how this affects to the cell or organism.

In 1990 Richard Jorgensen observed the result of the introduction of exogenous transgenes in petunias, with the goal of alter their pigmentation (Figure 6) Surprisingly, the flower color was not deepened as expected; the result was a variegated pigmentation, even the loss of color in some cases. This result suggests not only that the transgenes introduced were inactive, but also that the introduced DNA affected in some way the endogenous loci (Napoli, Lemieux et al. 1990). This phenomenon was called co-suppression (Hannon 2002).

At the same time several groups showed that plants responded to RNA viruses by targeting viral RNAs for destruction (Hannon 2002).

In the fungus *Neurospora crassa*, the phenomenon was called quelling and was discovered during attempts to boost the production of an orange pigment produced by the gene al1 (Cogoni, Irelan et al. 1996). When *N. crassa* was transformed with a plasmid containing a 1,500 bp fragment of this gene, instead of enhanced pigmentation, an albino phenotype was observed and at the same time the levels of the mature al1 mRNA were highly reduced.

Surprisingly, in *C. elegans* not only antisense but also sense RNAs blocked gene expression resulting in both cases in a penetrant loss-of-function phenotype (Guo and Kemphues 1995). In 1998, the work of Andrew Fire et al (Fire, Xu et al. 1998), demonstrated the biochemical nature of the inducer of gene silencing by introducing purified double-stranded RNAs (dsRNA), directly into the gonad or body cavity of an adult (Figure 6). The main conclusions were:

(a) dsRNAs are the inducers of the RNAi process, because they could trigger gene silencing in a more efficient way than the sense and antisense single-stranded RNA.

(b) A catalytic amount of dsRNA can induce the silencing and produce the phenotype in the adult and in its whole brood of the next generation, suggesting that RNAi is a heritable and amplified process (Sijen, Fleenor et al. 2001).

(c) The level of the target mRNA is drastically reduced.

The gene used in this study was *unc-22*, which encodes an abundant, but non-essential, myofilament protein. Repression of *unc-22* produces a twitching phenotype that was reproducible in a weak manner in the injected worms; meanwhile this phenotype was stronger in the progeny of the injected adult. Similar loss of function individuals could also be generated with dsRNA for other 4 nematodes genes, producing a very specific phenotype (Fire, Xu et al. 1998).

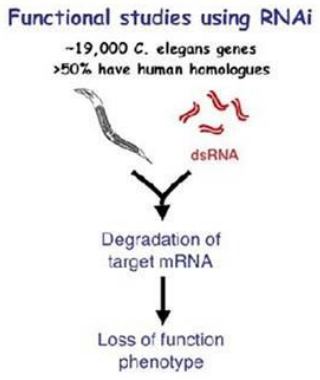

Figure 6. RNAi reveals the function of genes. A) Experiments carry on petunias with RNAi. White sections in petunia flowers represent areas where RNAi has silenced a gene involved in flower coloration (Grosshans and Filipowicz 2008). B) the introduction of dsRNA in worms cause the depletion of a determinate target mRNA producing a phenotype that allow to determinate the function of the gene (http://www.gurdon.cam.ac.uk/~ahringerlab/pages/res_rnai.html) .

This technic, termed as reverse genetics, has several advantages over forward or classical genetics, for example the sequences of all identified genes are immediately known and lethal mutations are easy to identify because it is not necessary to recover the mutants.

1.2.1. The RNAi pathway in *C. elegans*:

1.2.1.1. **Delivery of dsRNA into the worm:** in *C. elegans*, in addition to injection, the RNAi can also be initiated by soaking the worms in a solution containing dsRNA (Tabara, Grishok et al. 1998) feeding the worms with *E. coli* that expresses the dsRNA (Timmons, Court et al. 2001) or by expressing dsRNAs from a transgene (Timmons, Court et al. 2001)

As Fire et al suggested, the RNA can spread from one tissue to another, meaning that the molecules are transported between cells, which has been referred as RNAi spreading (Tijsterman, May et al. 2004).

Several genes are involved in this step. The first one to be described was *sid*-1, which encodes a transmembrane protein that facilitates the transport of long dsRNAs. *sid-1* (systemic RNAi deficient) was identified in a genetic screen for RNAi spreading insensibility, but is not required when the dsRNAs is provided in the target tissue. This indicates that the function of SID-1 involves dsRNA transport (Winston, Molodowitch et al. 2002).

Other groups have shown that knockdown of other genes, some of them related to intracellular vesicle transport, affects RNAi efficiency,(Saleh, van Rij et al. 2006). It has been recently shown that sid-1 is not required for the export of RNAi from tissue, (Jose, Smith et al. 2009).

Other genes suggested to be related with the RNAi transport are known as *rsd* (RNA spreading defective). These mutants are resistant to feeding but sensitive to RNAi by injection (Tijsterman, May et al. 2004). As well, several members of the ATP-binding-cassette (ABC) transporter genes superfamily seem to be implied in the RNAi transport, considering that, their mutations causes RNAi-deficient phenotypes (Sundaram, Echalier et al. 2006).

1.2.1.2. Inside the cell: once inside the cell, the dsRNA must be processed to produce small interfering RNA molecules (siRNA) that will bind the mRNA causing the silencing. In this pathway there are two essential features:

- A very small amount of dsRNA is able to silence the expression of a particular gene and the effect can be transmitted to the entire brood of its progeny(Fire, Xu et al. 1998). The big difference between the quantity of trigger RNA versus target mRNA was

the reason why was thought that the initial trigger signal may be amplified to elicit silencing. RNA Dependent RNA Polymerases (RdRP) mediate this step.

- Three main protein complex implicated in this process have been described:

- DCR-1 which, with its dsRNA-binding partner (RDE-4) that processes the dsRNA into siRNAs.

-RNA-induced silencing complex (RISC), composed of endonucleases that bind the primary siRNA (Grishok, Pasquinelli et al. 2001).

- A group of worm specific Argonautes, WAGO, that binds the secondary siRNA (Yigit, Batista et al. 2006).

The processing steps that the dsRNA molecules suffer are the followings (Figure 7):

1) **Processing of exogenous dsRNA**: *rde-4* gene was identified in a genetic screen looking for RNAi deficient mutant. This gene encodes a protein with two dsRNA binding motifs (Tabara, Sarkissian et al. 1999), and is required for the accumulation of trigger-matched siRNAs by processing of dsRNA; in fact rde-4 mutants show a low level of trigger-matched siRNAs (Pak, Maniar et al. 2012). However *rde-4* mutants retain residual ability to trigger silencing(Parrish and Fire 2001), which could mean an alternative pathway for siRNA production.

The enzyme that generates the siRNAs from the dsRNA, termed as Dicer, was first identified in Drosophila S2 cells(Bernstein, Caudy et al. 2001). Tabara et al. showed that RDE-4 interacts with DCR-1, the only homolog of Dicer in C. elegans (Tabara, Yigit et al. 2002). The siRNAs molecules have 20-23 bp and 5´-monoP.

2) **Processing of siRNA molecules:** *rde-1* gen, which encodes RDE-1 Argonaute protein that form part of the RISC complex (Yigit, Batista et al. 2006), was found in a genomic screening. In *rde-1* mutant the amount of primary siRNA, after dsRNA injection, was comparable to that of wild-type, but if siRNAs were injected in *rde-1* mutant, the RNAi effect was not present, indicating that this gene functions downstream of the siRNA formation(Parrish and Fire 2001). Yigit et al.(Yigit, Batista et al. 2006) also showed

that *rde-1* complex only was found with single stranded siRNAs, implying in these process two helicase, DHR-1 and DHR-2 (Duchaine, Wohlschlegel et al. 2006) that acts over the double stranded siRNA producing single stranded siRNA, upstream of RDE-1. Once that RDE-1 has bound the guide strain of the primary siRNA (the passenger strain is degraded), this complex localizes and bind the complementary mRNA forming a duplex.

3) **Secondary siRNA and mRNA target degradation:** the duplex siRNA-mRNA bind to the enzyme RDE-1 can be processed in two different ways:

- Some Primary siRNAi-RDE-1RISC complexes destroy the RNA targets by an endonucleolytically way (Pak, Maniar et al. 2012).

- Other siRNA-RDE-1 complexes bind the RdRP enzyme directing it throw the RNA targets, using them to generate secondary siRNA molecules These molecules are short 5´-PPP transcripts that complexes with the WAGOs, worms specific Argonautes, down regulating the target RNA via an unknown mechanism. (Sijen, Fleenor et al. 2001, Pak, Maniar et al. 2012). This amplification process is not universal and seems to be restricted to some nematodes, fungi and plants, but not in mammals or flies (Sijen, Fleenor et al. 2001).

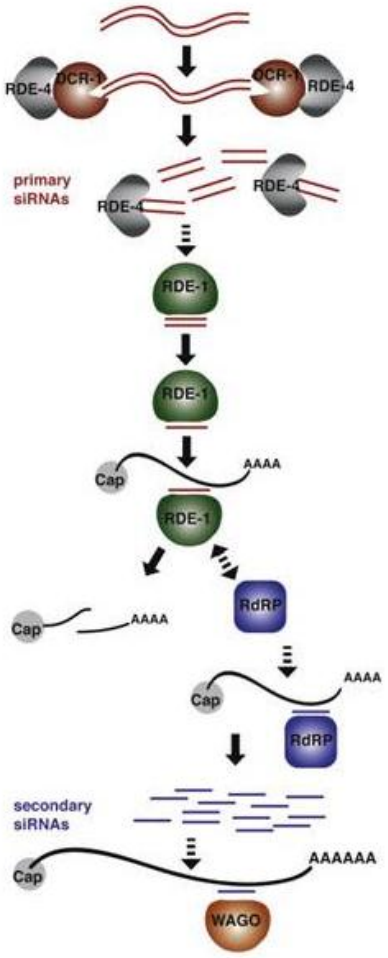

Figure 7. RNAi pathway in *C. elegans*: Model for RNAi in *C. elegans.* Exogenous dsRNA is processed by DCR-1 and RDE-4 into primary siRNAs. Short dsRNAs are then delivered to RDE-1, which cleaves the passenger strand, allowing subsequent maturation into active RISC.
The RDE-1 RISC then recruits the RdRP (RRF-1 or EGO-1) to the target RNA where the latter engages in secondary siRNA synthesis with the target as template.
Primary siRNA-complexes RDE-1 may endonucleolytically destroy target RNAs, whereas secondary siRNAs complex with the WAGOs and presumably further
down regulate the target RNA via an unknown mechanism (Pak, Maniar et al. 2012).

As described before, RNAi is a very potent method that, in some organism such as *C. elegans*, only required catalytic amounts of dsRNA per cell to silence gene expression. In spite of that there are differences between biological organisms, almost all the eukaryotes, have converged on a universal paradigm of gene regulation with several common components that are:

- The inducer is the dsRNA.
- The target mRNA is degraded in a homology-dependent form.
- Degradative machinery requires a set of proteins which are similar in structure and function across most organisms.

1.2.2. RNAi methods: as has been mentioned previously, three techniques exist to induce RNAi in *C. elegans*: injection(Fire, Xu et al. 1998), soaking (Tabara, Grishok et al. 1998)and feeding (Timmons and Fire 1998) (Figure 8). All three can produce efficient gene knockdowns and each of them has its advantages and disadvantages.

- **RNAi by injection**: dsRNA produced *in vitro* is injected into young adult hermaphrodites whose progeny will be scored for mutant phenotype. To obtain the dsRNA is necessary to do a transcription reaction that produces 5–10 µg dsRNA, which is sufficient to conduct many experiments. This method provides very reliable gene inhibition from worm to worm; the disadvantage is that it is more labor intensive than other methods.

- **RNAi by soaking**: in this case the worms are soaked in a high concentration dsRNA solution and later, they or their progeny scored for phenotypes. This methods required more dsRNA than for injection (5–10 µg per experiment). Worms of any stage can be soaked, but overall this way is useful for treating a large number of animals (e.g., tens to hundreds).

- **RNAi by feeding:** this is the method that has been used mainly in this thesis. Bacteria producing the dsRNA molecules are fed to worms and either they or their progeny are scored. As by the soaking, worms of any stage can be subjected to this technique. RNAi by feeding is the least labor intensive and most inexpensive method, but produces slightly more variable results than the two previous methods. It is suitable both to knock down a single gene in a large number of animals and for high throughput screening, using agar plates or liquid culture (Figure 8).

There is another method that is in vivo production of dsRNA from transgenic promoters (Tavernarakis, Wang et al. 2000) that follow to increase the heritability of RNAi effect and to produce a strong effect in late-acting genes that are generally less consistent than that of embryonically expressed genes.

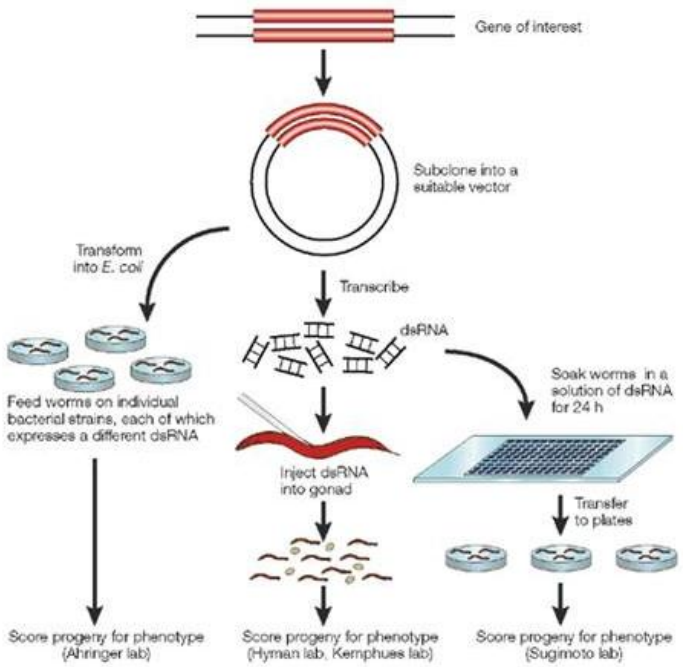

Figure 8. RNAi methods in *C. elegans*: method available to introduce the dsRNA in C. elegans to do RNAi technique. From left to right, the RNAi by feeding consists in fed worms with E. coli strains that express the dsRNA. The injection method introduces the dsRNA produced in vitro in the adult body using a micro-injector. The soaking method consists in soak the worms in a high concentration dsRNA solution. In all the case the adult worms and their progeny will be check looking for phenotypes (Kim 2001).

1.2.3. <u>Biological functions</u>: RNAi is a silencing phenomenon very relevant in eukaryotic organisms, one of the main functions of this mechanism is to participate in the immune response to viruses and other foreign genetic material, *C. elegans* Argonautes proteins are up regulated in response to viruses, and worms that overexpress components of the RNAi pathway are resistant to viral infection (Wilkins, Dishongh et al. 2005).

1.2.4. <u>Research and technological applications</u>: RNAi causes a drastic decrease in the expression of the target gene and thereby provides information on its effects and physiological role in the organism. However RNAi does not totally abolish expression of the gene so is termed as “knockdown” instead of “knockout” in which expression of the gene is completely eliminated.

The versatility of RNAi allowed systematic functional analyses of the entire *C. elegans* genome. On the other hand, RNAi has also disadvantages due to the fact that not all the genes are so sensitive to the RNAi; there is variability and incomplete or

interspecific knockdown. For these reasons it is vital to make a good design of the screening to obtain a successful experiment (Boutros and Ahringer 2008).

The library that has been used mostly for genome wide RNAi screening, and the one that has been used in this thesis, is the one generated by the Julie Ahringer laboratory. This library opened the possibility to perform high-throughput reverse genetic studies on an animal model organism and provided the first systematic functional analysis in *C. elegans* (Kamath, Fraser et al. 2003). A lot of screenings have been performed using RNAi technique, supposing a high progress for molecular biology.(Simmer, Moorman et al. 2003, Poole, Bashllari et al. 2011, Fievet, Rodriguez et al. 2013).

In medicine, RNA interference opens new possibilities in cancer´s treatment, by silencing genes differentially up regulated in tumor cells or genes involved in cell division (Izquierdo 2005). Related with this, a central area of research is the development of a safe delivery method of RNAi, involving viral vector systems(Li, Parker et al. 2006).

In biotechnology RNAi has been related with the engineering of food plants that produce lower levels of natural plant toxins, decreased the precursors of likely carcinogens in tobacco plant or the allergens in tomato plants (Gavilano, Coleman et al. 2006, Le, Lorenz et al. 2006). These approaches are still at an experimental stage.

1.3. The Nuclear Envelope

The Nuclear Envelope (NE), also known as nuclear membrane, is the double lipid bilayer which surrounds the genetic material and nucleus in eukaryotic cells. This structure is the physical barrier between the nucleus and the cytoplasm, and it was first described as a lipid bilayer 60 years ago in studies performed on amphibian oocytes (Callan and Tomlin 1950). The NE allows the existence of two compartments inside the cell with different compositions (Figure 9): the nucleus, which contains the DNA, and the cytosol with the cytoplasmic material. These membranes have also a relevant role in the organization and transcription of DNA.

The NE is composed of two membranes: the outer nuclear membrane (ONM) and the inner nuclear membrane (INM). The ONM is continuous with the endoplasmic reticulum (ER) and has proteins that are implicated in nuclear positioning (related with polarity and pronuclear migration). The INM is highly specified, encloses the nucleoplasm, and is covered by the nuclear lamina, a mesh of intermediate filaments which stabilize the nuclear membrane as well as being involved in chromatin function and gene expression (Hetzer 2010) (Figure 9

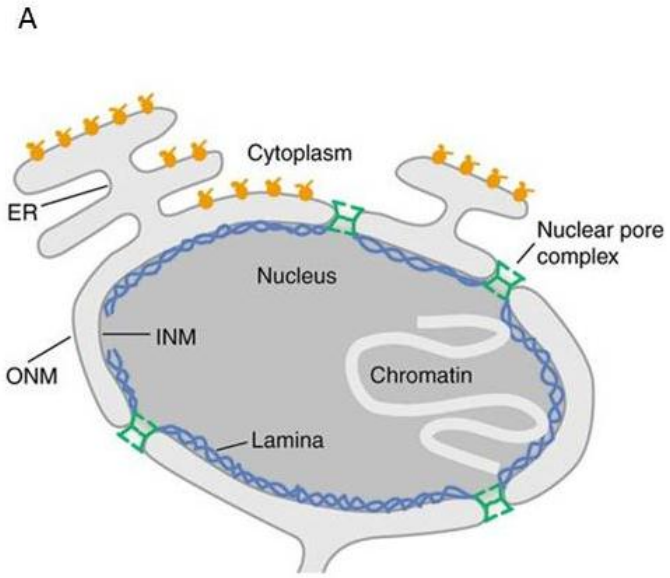

Figure 9: NE structure. Scheme of the NE structure that separates the nucleus from the cytoplasm in eukaryotic cells. NE is formed by two lipid membranes, the ONM and INM. The 1st one is continuous with the ER, while the INM is in the interior part in contact with the nuclear lamina that links chromatin to the NE. NPC span the NE at the sites where the INM and the ONM fused together. Adapted from (Schirmer and Gerace 2002).

Between these two membranes resides the lumen, where proteinaceous bridges that could establish physical connections between the cytoskeleton and chromatin have been found. They could be related to the DNA repair mechanism, replication or to the transcriptions process (Tzur, Wilson et al. 2006)

Both membranes, the INM and the ONM, form two concentric lipid bilayer, over the entire nuclear surface, but there are places where they are continuous with each other. In these regions huge multi-subunit protein complexes are found, termed nuclear pore complex (NPC), which connect the nucleoplasm with the cytoplasm, being the

gatekeepers that regulate the transport. These structures are built of around 30 different proteins, termed nucleoporins, that are organized into several subcomplexes that assemble into a ring-shaped structure with eightfold rotational symmetry (Hetzer and Wente 2009) (Figure 10). The NPCs have a molecular mass estimated at ~66 MDa in yeast and ~100 MDa in vertebrates.

In the NE, diverse groups of proteins are present. The first ones are nucleoporins or Nup, which form part of the NPC. The second group is NE transmembrane proteins or NETs that include proteins such as lamin-B receptor (LBR) or emerin (EMR-1) and are present in the INM. A third class or NE proteins, present in the ONM, seems to interact with proteins of the INM and regulate nuclear positioning (Figure 11). The final group of proteins constitute the lamina that it is critical for nuclear stability and plays important roles in chromatin function and gene expression (Hetzer 2010). This work is focused on NE proteins that belong to the two first groups, the nucleoporin NPP-16 and the NET protein LEM-2.

1.3.1. Nucleoporins: proteins of the NPC : nucleoporins or Nups are the proteins that form the NPC and they can be classified in three types according to their structure, function and position in the NPC (Figure 10):

- Transmembrane Nups: integral proteins of the pore membrane present in the contact region between ONM and INM, anchoring the NPC to the NE.
- Scaffold Nups: they form a cylinder coating the curved region of the NE and they are among the most stable proteins in the cells, persisting for months or years in nondividing cells, and even remaining in stable NPC once they are associated with these NPC (Rabut, Doye et al. 2004, Savas, Toyama et al. 2012).
- FG Nups: they are responsible for the transport and establishment of the permeability barrier. They spend seconds to minutes of residence time in the NPC being highly dynamic (Rabut, Doye et al. 2004).

In addition, filamentous appendices extend to both sides of the pore (nuclear basket and cytoplasmic filaments) (Doucet and Hetzer 2010).

One of the most characteristic domains of the Nups are the Phenylalanine-glycine (FG) repeats that are mainly present in FG Nups (reason for this group´s name) but also in some TM Nups and in cytoplasmic filaments, and are essential for NPC functions. These domains establish the nuclear permeability barrier and facilitate receptor-mediated transport of selected cargo molecules. While ions and small molecules diffuse through NPCs freely, macromolecules (larger than 30 kDa.) are restricted in diffusion by the FG repeats meshwork. For these processes are essential the shuttling nuclear transport receptors (Figure 10). There are several models for FG-based permeability restriction and protein translocation, which are discrepant in the spatial distribution of FG repeats along the pore, the biophysical contacts between FG motives, and the structural consequences of receptor FG binding. However all of them agree that FG repeats are essential for both transport and barrier function of the NPC, and that the selective passage is possiblw e due to the interactions between nuclear transport receptors and FG motifs. (Rothballer and Kutay 2013).

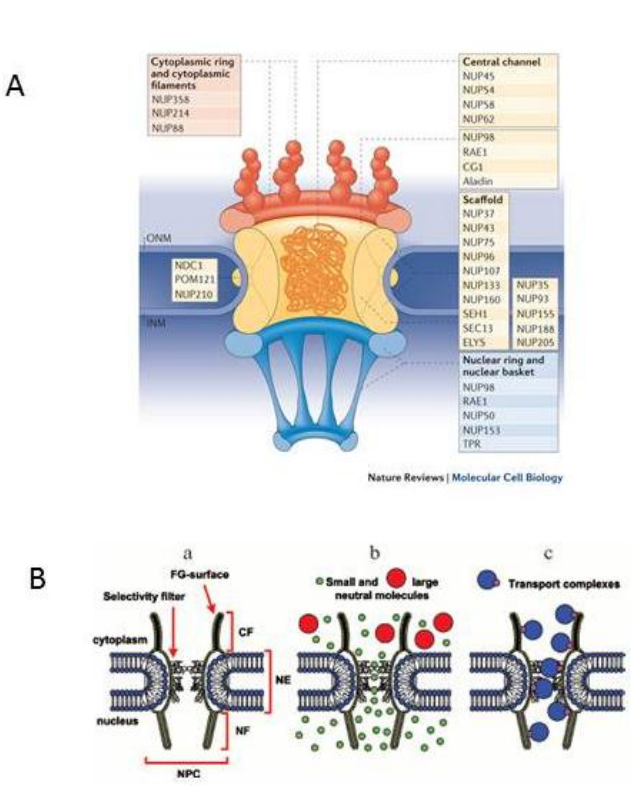

Figure 10. NPC structure and it role in nuclear transport. A) NPCs are huge multi-subunit protein complexes. They are built of around 30 different proteins, termed nucleoporins organized into several subcomplexes that assemble into a ring-shaped structure with eightfold rotational symmetry. There is a central structure composed that is form by an scaffold structure and conform the central channel, which regulates the transport. In the cytoplasm side it is found the cytoplasmic ring and cytoplasmic filaments, whereas in the nucleoplasm it is found the nuclear ring and the nuclear basket. On each structure are indicated the nucleoporins (NUPs in mammals) that form part of them. (Raices and D'Angelo 2012)B) The NPC communicates the nucleus with the cytoplasm being the main transport channel. This transport is mainly mediated by the FG-nucleoporins, and the molecules pass throw a filter in the center part of the NPC (a). Depending of the molecules the transport is free in the case of small and large neutral molecules, or require energy and transport complex, in the case of charged molecules (b and c) (A. V. Sorokin 2007)

1.3.1.1. NPP-16/Nup50: as has been previously mentioned in, this thesis is centered on two proteins. One of them, the nucleoporin NPP-16, termed Nup50 (originally NPAP60) in mammals, is a FG-repeats containing mobile nucleoporin that has a MW of around 50kD (Rabut, Doye et al. 2004, Tran and Wente 2006). The homologous protein in yeast is called Nup2p, and even though having very low similarity with animal Nup50 (14%), it has been suggested that the role of both Nup50 and Nup2p proteins, in the terminal stage of nuclear import, is conserved from yeast to vertebrates (Matsuura, Lange et al. 2003).

This protein was first described in 1996 (Fan, Liu et al. 1997) and it was shown that its expression levels are about 10-20 times higher in rat testes than in somatic tissues and also, NPAP60 colocalizes with NPC markers. In mice, Nup50 expression is also higher in adult testes and in the embryonic neural tube (Smitherman, Lee et al. 2000).

With respect to its subcellular localization, using different techniques, it has been determined that Nup50 localizes in the nucleoplasmic fibrils of the NPC, but also in the nucleoplasm (Guan, Kehlenbach et al. 2000, Smitherman, Lee et al. 2000, Rabut, Doye et al. 2004, Kalverda, Pickersgill et al. 2010). This localization has also been seen for others nucleoporins such as Tpr or Nup96 (Cordes, Reidenbach et al. 1997, Fontoura, Blobel et al. 1999).

- **Role of Nup50 in nuclear transport**: Nup50 was described as a Ran binding protein and a cofactor for importin-α: β mediated nuclear protein import. In mammals Nup50 has three domains, the C-terminus that binds importin-β through RanGTP, N-terminus that binds the C-terminus of importin-α, and the central domain that binds importin-β (Lindsay, Plafker et al. 2002). Disagreement related to the functional role of these interactions exists in the current literature. In 2002 Lindsay et al proposed that Nup50 acts as a tri-stable switch that alternates between different simultaneous binding modes of Nup50 to importin-α and to NLS-cargo during nuclear import (Lindsay, Plafker et al. 2002). Conversely, Matsura and Stewart showed that the binding of Nup50 and NLS-cargo were mutually exclusive, meaning that the main role of Nup50 could be related to displacing import complex and recycling importin-α to the cytoplasm (Matsuura and Stewart 2005) but it may still contribute to this process. More recent

studies have shown that Nup50 alone is insufficient to dissociate an importin-α-NLS cargo complex on the time-scale of nuclear transport (Sun, Yang et al. 2008). Apart from this, Pumroy et al. showed that Nup50 prevents cargo re-binding to importin-α, stabilizing its closed conformation for adaptor recycling (Pumroy, Nardozzi et al. 2012). Related to the different models, it is important to note that in humans, two isoforms of Nup50 have been described, a longer one that promotes the release of NLS cargo from importin-α and the shorter isoform (found only in humans) that accelerates nuclear import of classical NLS cargos (Ogawa, Miyamoto et al. 2010).

It has also been shown that Nup50 interacts with CRM1, the export receptor for leucine-rich export sequencing (Fan, Liu et al. 1997) and with $p27^{kip1}$, a member of CDK family proteins. Depletion of Nup50 affects the distribution of $p27^{kip1}$ in the Central Nervous System (CNS), which agrees with the strong defects presented in the neural tube of Nup50 null mice that also showed a late embryonic lethality (Smitherman, Lee et al. 2000). It was shown in the same study that the absence of Nup50 did not have effects on other tissues like muscles, where another protein could play a redundant role.

- **Role of Nup50 in nuclear pore assembly and abscission checkpoint process:** cytokinesis is the final stage of cell divisions and its correct execution is essential. During this stage the midbody, a protein-rich structure that stabilizes an intercellular bridge is formed, and ultimately resolved to create two daughter cells through the membrane abscission process. Mackay et al. showed that the depletion of Nup50 does not affect the localization of other proteins in this area, like Nup153 or Tpr, but it produces an increase in the number of midbody-stage cells and ectopic cytoplasmic foci of Aurora B, the molecule that activates the abscission checkpoint during cytokinesis (Mackay, Makise et al. 2010). This suggests that defects in Nup50 and other proteins of the NPC, especially in the basket structure, during cytokinesis activate the Aurora B-mediated abscission checkpoint, ensuring that daughter cells are generated only when fully formed NPCs are present.

- **Nup50 directly stimulates expression of developmental and cell-cycle genes inside the nucleoplasm:** the "gene-gating" hypothesis proposes that active genes associate with NPCs in order to increase the efficiency of nuclear export of transcribed mRNA(Blobel 1985) Evidence in favor of this hypothesis has been found in the budding yeast *Saccharomyces cerevisiae* (Blobel 1985, Casolari, Brown et al. 2004). However, several bodies of evidence (Kalverda, Pickersgill et al. 2010) indicate that the nucleoplasmic pool of nucleoporins has a role in transcription. With the idea of elucidating these interactions and differentiate them from those at the NPC, Kalverda et al. analyzed, in *Drosophila* cells, the genomic interactions of several full-length and truncated nucleoporins, that localize to the NPC and in the nucleoplasm, like Nup50 and Nup98, using the in vivo mapping technique DamID (van Steensel, Delrow et al. 2001). Mainly they work with several Nup98 constructions, analyzing if there was any difference between the genes which activation was related with the Nup98 NPC pool, and the ones that depend on the Nup98 nucleoplasmic pool. Their result indicates was the nucleoplasmic Nup98 domain construction the one that affect the expression of more genes. In the case of Nup50 the experiment was done with the full length protein and, although there was a clear effect on Nup50 in the transcription of a set of genes, it is not possible to say if is the nucleoplasmic or the NPC pool of Nup50 the one that it is relate with this expression control. Most of these genes are implicated in developmental and cell cycle processes (Kalverda, Pickersgill et al. 2010).

- **Nup50/NPP-16 in *C. elegans*:** in *Caenorhabditis elegans,* Nup50 is called NPP-16 and is present in two isoforms made up of 512 and 497 amino acids, respectively. Until now, it has been described that this nucleoporin, together with CDK-1, plays a role in a prophase checkpoint in the *C. elegans* embryo when there is a natural stressor, such as oxygen deprivation, regulating a cell cycle arrest. In anoxia conditions, a WT strain has its CDK-1 protein inactive, arresting the prophase until normal air conditions are restored. However, in a *npp-16* mutant the CDK-1 protein remains active. CDK-1 is known to regulate the phosphorylation of several proteins before Nuclear Envelope Breakdown (NEBD), implying that in anoxia conditions and in the absent of NPP-16, CDK-1 continues promoting NEBD (Hajeri, Little et al. 2010). Related to this, as it was mentioned before, Nup50 was shown to interact with $p27^{kip1}$, a CDK/cyclin inhibitor

reaffirming a role of this nucleoporin with cell cycle checkpoints (Smitherman, Lee et al. 2000).

1.3.2. LEM-domain proteins: the INM is characterized by a specific set of transmembrane proteins, known as NETS (nuclear envelope transmembrane proteins) that interact with chromatin and/or the nuclear lamina (Figure 11), which is a filamentous meshwork formed by type V intermediate filaments including B- type lamins, expressed in all cells and essential for viability, and A-type lamins, only expressed in differentiated cells (Brachner, Reipert et al. 2005).

Several of these NETS are termed LEM-domain proteins because they share a common structural motif of 40 aa at their N-terminus, called the lamina- associated polypeptide-emerin-MAN-1 domain (LEM domain). This region mediates the interaction with the DNA binding protein barrier to autointegration factor (BAF) This group consists of several proteins such as: LAP2, emerin, MAN-1, the *Drosophila*-specific otefin, the *C. elegans* LEM-3, a mammalian orthologue of Ce-LEM3, and the recently characterized LEM2, LEM3 and LEM5 (Lee and Wilson 2004, Brachner, Reipert et al. 2005). On the basis of their interaction with BAF and DNA, the LEM-domain proteins may have a role in chromatin organization (Liu, Lee et al. 2003) .

The study and knowledge about these proteins is very relevant because mutations in their genes have been causally linked to a series of human diseases, many of them affecting cardiac and skeletal muscle. Some of these defects are called laminopathies (Figure 11), at least there are 14 diseases in this group, caused by a defect in the A-type lamin gene (LMNA) or other NE genes, such as Emery-Dreifuss muscular dystrophy (EDMD), the Hutchison-Gilford progeria syndrome and atypical Werner syndrome (Worman and Bonne 2007).

1.3.2.1. LEM-2 protein: while NPP-16 protein has been largely described in mammals and only in few observations made in *C. elegans*, LEM-2 has been studied in the nematode since the beginning of LEM-2 research and, nowadays, is an essential model for studying most of the diseases previously named.

LEMD2 (human LEM-2), which shows a high identity and similarity between human and mouse, is a LEM-domain protein that was first described in 2005 by Brachner et al. like a structurally related MAN-1 protein that, although lacks the MAN1- specific C-terminal RNA- recognition motif (RRM), it contains a N-terminal LEM motif, two predicted transmembrane domains and a MAN1-Src1p C-terminal (MSC) domain highly homologous to MAN1. For this reason, these two proteins are considered as a subfamily within the LEM-domain proteins characterized by the presence of the MSC domain and perhaps, they have a common ancestor in evolution (Brachner, Reipert et al. 2005). This protein in *C. elegans* was originally considered as an othologue of the human MAN1 (hMAN1), known as Ce-MAN1 (Lee, Gruenbaum et al. 2000), but it is more homologous in the N-terminus and in the region between the transmembrane domains to the human LEMD2 than to hMAN1, concluding that the *C. elegans* protein LEM-2 is orthologous to LEMD2.

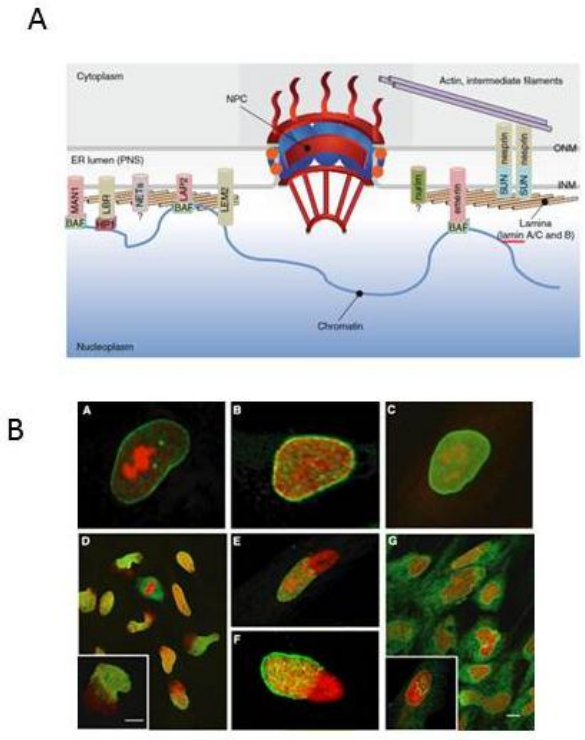

Figure 11: INM transmembrane proteins are related to laminopathies: A) in the NE there are several groups of proteins, the NETS are proteins of the INM that are characterized by the LEM-domain. These domains interact with the protein BAF and with the chromatin. LBR, LAP2, LEM-2, MAN-1 and EMR-1 are LEM-2 proteins. (Hetzer 2010) B) Micrographs of normal (A–C) and laminopathy (D–G) human fibroblasts. Cultured fibroblasts from a patient with lethal homozygous LMNA mutation (Y259X) that were null for lamins A/C were immunostained with antibodies to lamin B2 (D), the nuclear pore complex protein p62 (E), lamin B1 (F), and emerin (G). Note the abnormal shape of the nuclei and the discontinuous abnormal localization of the lamin-associated proteins in the laminopathy cells. (Broers, Ramaekers et al. 2006)

LEM-2 is ubiquitously expressed and different techniques, as immunofluorescence microscopy or digitonin treatments, allow determining that this protein subcellular localization is in the NE and in a lesser manner in the ER. (Gruenbaum, Lee et al. 2002, Brachner, Reipert et al. 2005, Ikegami, Egelhofer et al. 2010). The C-terminus is located in the nucleoplasm, being a transmembrane protein of the INM associated with the nucleoskeletal- lamina network.

Experiments in mouse and human cells and nematodes have shown that in the presence of mutated *lamins*, LEM-2 is misslocalized in the NE and diffuse to the ER (Liu, Lee et al. 2003, Brachner, Reipert et al. 2005, Ulbert, Antonin et al. 2006). This localization of LEM-2 in a lamin dependent manner is mediated by the retention domain inside the N- terminus domain of LEM-2 (Brachner, Reipert et al. 2005). Studies in a ΔK46 *C. elegans* lamin mutant (corresponding to EDMD- linked ΔK32 in human *lamins* A and C) have shown that this lamin mutation alters the lateral assembly of dimeric head-to-tail polymers, producing an abnormal organization of tetrameric protofilament (basic structures of the muscles) and causing aggregates of LEM-2, which correspond with GFP::ΔK4 lamin aggregates, and also mislocalization of emerin, which has problems in associating with lamin filaments (Bank, Ben-Harush et al. 2011).

- **LEM-2 affects NE integrity:** the overexpression of LEMD-2 in stable cell lines produces patchy structures in which LEM-2 is accumulated. This overexpression produces a dramatic reorganization of BAF and emerin, weaker in the case of A- type lamins, in LEM-2 clusters. In contrast B-type lamins and their interaction partner LBR are not affected. From these patches, finger-type invaginations of the nuclear membranes are formed. These are found between nuclei of adjacent cells that have completed cytokinesis. These structures seem to be stable and can be maintained for a long time and apparently, they do not affect cell-cycle progression. In these tubular formations, lamin A, emerin (Brachner, Reipert et al. 2005) and BAF are also accumulated, which could cause abnormalities of the NE, leading to the formation of extra membrane sheets extending from the chromatin attached nuclear membranes (Brachner, Reipert et al. 2005). Similar to this, it has been observed in fission yeast that overexpression of

the distantly related homologs Lem2 and Man1 causes the formation of membrane stacks in the NE (Gonzalez, Saito et al. 2012).

The absence of LEMD-2, by RNAi, has also a strong effect on the growth of cells, and after 48 h the cells showed a delay in proliferation rate and after 96 h, they showed abnormally shaped nuclei with large invagination of the NE membranes, as well as lobulations. In some cases, cells with two nuclei interconnected with thick chromatin bridges inside one cell were found, indicating segregation defects. On the contrary, the effect seen in the lamin- A, emerin and BAF localization, when LEM-2 is overexpressed, have not been observed in the absent of LEM-2(Ulbert, Antonin et al. 2006).

- **LEM-2 attaches chromosome arms regions to the NE:** Ikegami et al. using ChIP-chip experiments (Ikegami, Egelhofer et al. 2010) observed that left and right arms of all five autosomes of C. elegans have LEM-2-associated regions termed as "LEM-2 domains", while central regions of the autosomes are almost completely devoid of LEM-2 association. These results demonstrate a model in which the arm regions are attached to the nuclear membrane, and the central regions are likely to loop out. In the case of the X chromosome, only the left arm shows LEM-2 associations. The regions that associate with LEM-2 have high repeat density, low gene density and also silent or more inactive genes, whereas gaps between these regions are enriched in active genes. This result, which has not been tested in human cells and mouse, and neither with other INM protein as emerin, present a role of LEM-2 protein in the attachment of DNA to the NE.

In *S. pombe*, which does not have BAF protein, the Lem2 molecule has a domain called HEH that is predicted to bind directly to chromatin. The excess of this protein causes chromatin hypercompactation and the dissociation of chromatin from the nuclear periphery (Gonzalez, Saito et al. 2012). Moreover, it has been indicated that *S. pombe* Lem2, and also Man1, binds to telomeric and subtelomeric regions of the chromosomes, being essential for telomere anchoring at the NE.

- **LEM-2 and emerin proteins have overlapping functions: relevance in development muscle functions and mitosis:** in 2003 Liu et al., based on the results of single and double RNAi experiments against LEM-2 and emerin, showed that these two NET proteins have overlapping functions required for viability in early embryos. In the absence of both of them, the embryonic lethality was near 100 %, meanwhile, there was no embryonic lethality in the absence of only one of these genes (Liu, Lee et al. 2003). In double null mutants, resulting from crosses of single *lem2*$^{-/-}$ and *emr*$^{-/-}$ strains, the phenotype is delayed until postembryonic stage because of maternal contribution. These worms displayed a larval arrest in L2 and showed several developmental and physiological phenotypes in dividing and non-dividing cells. Hypomorphic strain (*lem2*$^{-/-}$ and *emr*$^{-/+}$) was viable, indicating that one copy of emr-1 is sufficient to maintain the viability of *lem2*$^{-/-}$ *emr* $^{-/+}$animals, reaffirming their overlapping functions (Barkan, Zahand et al. 2012).

- **Chromatin organization and cell proliferation:** the Lem-domain, as mentioned before, of these two proteins, interacts with the DNA crosslinking protein BAF, explaining that the absence of LEM2 and emerin produces defects in chromatin organization. Immunofluorescence with lamin and NPCs antibodies showed that double null mutant animals presented defects in the chromatin organization, nuclear intermediate filaments, and NPCs. They also showed defects in mitosis, not only during embryogenesis but during post-embryonic development in mitotic cells, too (Liu, Lee et al. 2003, Barkan, Zahand et al. 2012).

Both proteins are also required for cell proliferation of the postembryonic M lineage and for maintaining the expression of the HLH-8 transcription factor, required for the proper patterning of M lineage (Barkan, Zahand et al. 2012).

- **Muscle integrity:** LEM-2 and emerin are also required for striated muscle formations (Huber, Guan et al. 2009), normal motility, proper localization of muscle cells, normal sarcomeres and correct attachment to hypodermis. In double null mutants, different phenotypes related to these processes appear, such as the mislocalization of components of the hemidesmosomas, which are responsible of the

hypodermis attachment of the muscles (Barkan, Zahand et al. 2012). This was also hypothesized by Bank et al., who observed that ΔK46 *C. elegans* lamin mutant (corresponding to EDMD-linked ΔK32 in human lamins A and C) had problems in swimming motility, which reminded of phenotypes due to the lacks of MUA protein (Bercher, Wahl et al. 2001). This could reveal that this mutant lamin disrupts attachment of the muscle or other underlying tissues to the cuticle (Bank, Ben-Harush et al. 2011).

- Extracellular signaling: a shared role of LEM-2 and emerin in the extracellular-signal regulated kinase (ERK) signaling during mouse myoblast differentiation, also indicates the relevance of these two proteins in muscle development. In this sense, it has been shown that null mutant of LEM-2 has reduced lifespan and pumping rate, indicating that this protein could have a slightly more important role in myoblast differentiation (Huber, Guan et al. 2009, Barkan, Zahand et al. 2012).

1.4. Objetives:

1. Conduct a genome-wide RNAi screen in *Caenorhabditis elegans* to identify genes that interact with nuclear envelope-related genes *npp-16* and/or *lem-2*.

2. Characterize the localization, function and behavior of the nucleoporin NPP-16.

3. Describe the relation between *npp-16* and the genes retrieved from the genome-wide RNAi screen.

4. Characterize the behavior and function of inner nuclear membrane protein LEM-2 and its relation with emerin.

5. Describe the interaction between *lem-2* and the genes retrieved from the genome-wide RNAi screen.

2. Results

2.1. A Genome Wide RNAi screen reveals genes that show interaction with *lem-2* or *npp-16*

As mentioned in the Introduction, this project is focused in the description of two proteins of the NE. One of our goals was to identify genes that interact with *lem-2* or/ and Nup50/*npp-16*.

Following this idea we have performed a genome wide RNAi screen, through almost the entire genome of *C. elegans* (Figure 12). Although highly effective RNAi injection and soaking screens have been performed (Gonczy, Echeverri et al. 2000, Maeda, Kohara et al. 2001) we have chosen the feeding method because of the availability of libraries, the low cost and the ease of application and scaling.

We used the RNAi feeding library of Julie Ahringer (Kamath, Martinez-Campos et al. 2001, Kamath, Fraser et al. 2003) that contains 16,757 bacterial strains targeting 86% of the predicted genes.

In this screen two mutant strains were used, *lem-2(tm1582)* and *npp-16 (tm1596)*, as well as the wild type strain (wt). The *tm1582* is a null mutant while *tm1596* is a strong loss of function mutant (Figure 13). These strains are described in Result sections 2 and 3.

This screening has been performed based on Julie Ahringer and Michael Boutros review on designing RNAi screen experiments (Boutros and Ahringer 2008), trying to find the best compromise between specificity and practicality. It comprises three steps: a genome wide screen made in liquid culture and two rounds of validation of the candidates obtained in the genome wide screen, both of them performed in RNAi plates.

2.1.1 Our goal: Identify interactions proteins of LEM2 or/and NPP-16:

the goal of the screening was to identify proteins that show any interaction with *lem-2* or/ and *npp-16*. For that we have paid attention to those genes whose RNAi cause a phenotype in any of the mutant strains but not in the wt.

The main phenotype that we were looking for was embryonic lethality (emb) but also we chose as possible interactors the genes whose RNAi produced phenotypes such

as adult sterility (Ste), protruding vulva (Pvl), multi vulva (Muv), larval arrest (Lva), larval lethality (Lva), sick (Sck), growth defects (Gro) or reduced brood size (Rb).

2.1.2. Controls and scoring of the results: Positive and negative controls in a screening are very important because they give relevant information on the reproducibility, ease and robustness of the assay. Positive controls should achieve high signal while low noise should be obtained with the negative controls.

In our screening we used as positives controls two genes, *emr-1* and *npp-5* whose RNAi produces about 100% of embryonic lethality in *lem-2(tm1582)* and *npp-16(tm1596)* mutant strains respectively. As negative control we used the empty vector RNAi (named as #2 corresponding to L4440 vector empty) that does not produce any phenotype in any of the three strains. These controls were performed along all the steps of the screening to ensure that the phenotypes observed were specific and consistent.

As mentioned before, the main phenotype we were looking for was embryonic lethality and we designed a number code that corresponds to the different possible outputs during the first stage of the screening:

0: no growth in any of the strains
1: equal growth in all
2: superior growth in wt strain
3: superior growth in *tm1596* strain
4: superior growth in *tm1582* strain
5: superior growth in wt and *tm1596*
6: superior growth in wt and *tm1582*
7: superior growth in *tm1596* and *tm1582*

We selected genes that showed phenotypes 2, 5 and 6. We proceed to validate these genes in individual plates, and also we looked for other possible phenotypes, which were scored following the nomenclature depicted above.

2.1.3. Steps of the screen: this screen, as described in Material and methods, has been performed in three steps using the RNAi technique in different media, liquid or RNAi plates (Figure 12)

- **1st step: Genome wide screen in liquid culture: The screening of 16,757 genes resulted in 1,015 candidates genes:** about 86% of *C. elegans* genes were analyzed in the genome wide screening in liquid cultured. RNAi against 550 genes show growth defects in *tm1582* mutants, 445 RNAi genes caused growth defects exclusively in the *tm1596* mutants, and 20 RNAi genes produce growth defects in both mutant strains, while the wt strain did not show any phenotype or it was much weaker.

In this first round non-restrictive requirements were applied when considering a gene as candidate to avoid ruling out possible true interactors.

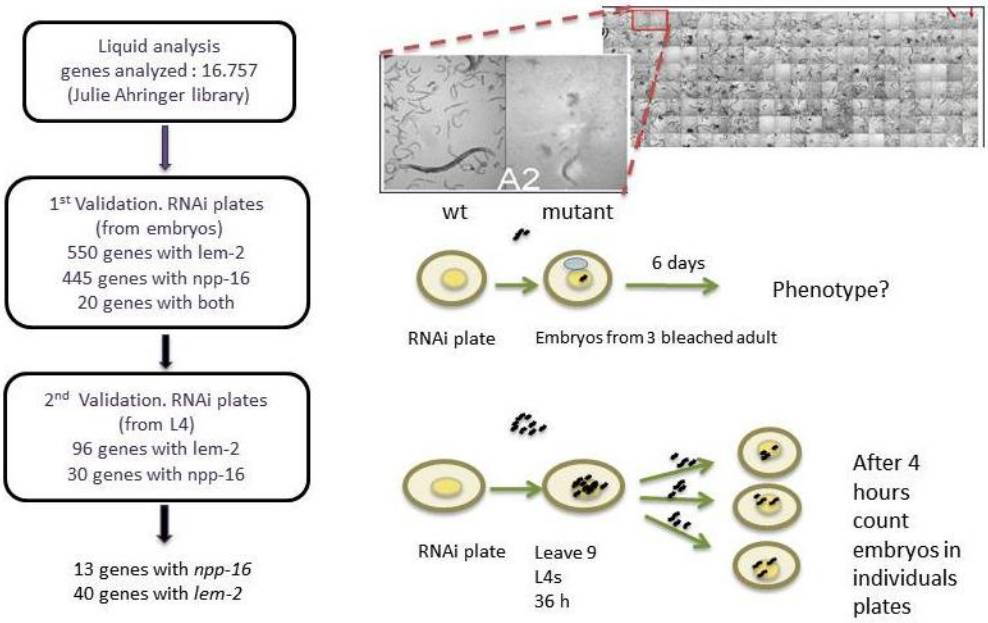

Figure 12. Genome wide RNAi screen: the screening performed has three steps, the initial screening using the J. Ahringer library that check 16. 757 genes in the wt and the mutant strains *tm1596* (BN11) and *tm1582* (BN19), in liquid using 96 flat well plates. From them 1015 genes show phenotypes such as Embryonic lethality or Sterility in one or both mutant strains but not in the wt. To validate this results the RNAi was repeated in plates and only 126 genes confirm their effect in the mutant strains. Finally a 2nd validation of these genes was made in RNAi plates checking carefully the phenotype observed. 53

- **2nd step: Validation: 126 genes validated the results**: we screened again the 1,015 genes that were retrieved in the liquid culture assay to validate genuine candidates and to discard false positives. In this case the RNAi was made on plates,

which were seeded with the bacteria strain of each candidate gene (Material and methods). In the case of the genes that showed a phenotype only with one of the mutant strains, the assay was performed with the corresponding mutant and the wt strain. The assay was repeated with the three strains in those genes that showed growth problems with both mutants. Worms were fed with the RNAi from embryos, and effects in these animals and their progeny were evaluated.

We obtained a total number of 126 genes that reproduced the previous phenotypes, 96 of them corresponding to genes whose RNAi cause problems in the *lem-2(tm1582)* mutant, and 30 genes whose RNAi produce problems in *npp-16(tm1596)* mutant.

In this validation step, we also look for several RNAi phenotypes in plates, such as Emb, Lva, Lvl, Ste, Muv or Pvl.

- **3rd step: Re-validation step: A second validation resulted in 53 candidates genes:** we decided to do a second validation of the 126 genes resulted for the previous step, repeating the RNAi experiment in plates. However, in this occasion each experiment was done by triplicate and the worms of the different strains were fed with RNAi bacteria form L4 stage, analyzing their progeny for the same phenotypes previously mentioned. At this stage, the embryonic lethality was also quantified.

As a result of the re-validation we obtained 53 genes that recapitulate the effect of their RNAi phenotype from the initial screening, 40 genes that showed interactions with the *tm1582* mutant, and 13 with the *tm1596* mutant. Candidate genes have been classified in functional categories according to annotations in Worm Base (Table 1)

Functions	*npp-16* candidates	*lem-2* candidates
Cell cycle related genes	*cye-1*	*coh-1*
Nucleoporins and NE proteins	*npp-2, npp-21*	*npp-17, emr-1*
Ubiquitination related genes.	*skr-1*	*ubc-12, skr-6*
Ribosomal related genes	*rpl-1, rps-14*	*pro-1, rskn-1*
Receptors	*srd-22, srw-87, srw-15*	*srw-3, sru-39, T06E4.5*
Transcription/translation factors		*taf-1, sago-2, tbc-11*
Others	*ncbp-1*	*apm-3, cuti-1, UPRTase, oac-22, ceh-45, lipl-2, zig-3,* T14G8.3, *fbxa-114, nas-21,* T07H6.1, K10B3.6, *dhs-6, sem-5, pkc-3, unc-98, add-1*
Unknown	Y71F9AL.12/13, ZK809.5, C14F11.2	W04A4.5, K05C4.7, D2096.9, C27B7.7, ZK896.4, VY35H6BL.2, C03B1.3, Y57G11B.5, T28F2.2, F4719

Table 1. 53 genes resulted from the genome wide RNAi screening: after the different steps of the screening 53 candidates were obtained, of these 13 genes show a possible interaction with the *npp-16* and 40 with *lem-2*. They were classified in functional groups related with different process such as cell cycle or ubiquitination and interestingly, several unknown genes were identified as well.

Despite the fact that the final candidates were selected because they caused phenotypes in the three screening steps, we noticed high variability for some of them. We speculate that these are candidates whose depletion by RNAi is inefficient and therefore create a spectrum of phenotypes. We have worked hard to elucidate the main causes for RNAi *varia*bility and the different conclusions appear in a sub-section of Materials and Methods. Considering the high reproducibility in other candidates, we decided to focus our work in two of them, the nucleoporin NPP-2 that in *the npp-16* mutant causes a high Emb, and the neddylation protein UBC-12 that produces high Emb and Lvl in the *lem-2* mutant.

2.2. NPP-16 is a mobile nucleoporin localized in the NPC

NPP-16, as mentioned in the introduction, is predicted to be the *C. elegans* ortholog of mammalian Nup50 that forms part of the NPC basket and is also present in the nucleoplasm. We have characterized this protein in *C. elegans*.

2.2.1. <u>Characterization of NPP-16 mutant allele *tm1596*:</u> to study the function of NPP-16 in *C. elegans*, we have combined RNAi experiments with other genetic approaches. Initially we characterized the mutant allele *tm1596* (provided by Dr. Shohei Mitani) that has a 382 bp deletion, which affect the second intron and the third exon of the gene (Figure 13).

The wt *npp-16* allele is predicted to encode a 55 KDa protein that contains 8 FG repeats domains. Eight independent reverse transcriptase PCR (RT-PCR) assay was performed to analyze the complementary DNA (cDNA) of *tm1596* mutants, and 7 of these reactions showed a premature termination codon (PTC) resulting in a putative 26 KDa protein of 236 amino acid, which lacks 7 out of 8 FG repeats present in the wt npp-16 allele. In the remaining cDNA a cryptic splice site in exon 3 is activated, resulting in an intact ORF encoding a protein of 389 aa (43 KDa) that lacks 6 FG repeats. (Figure13).

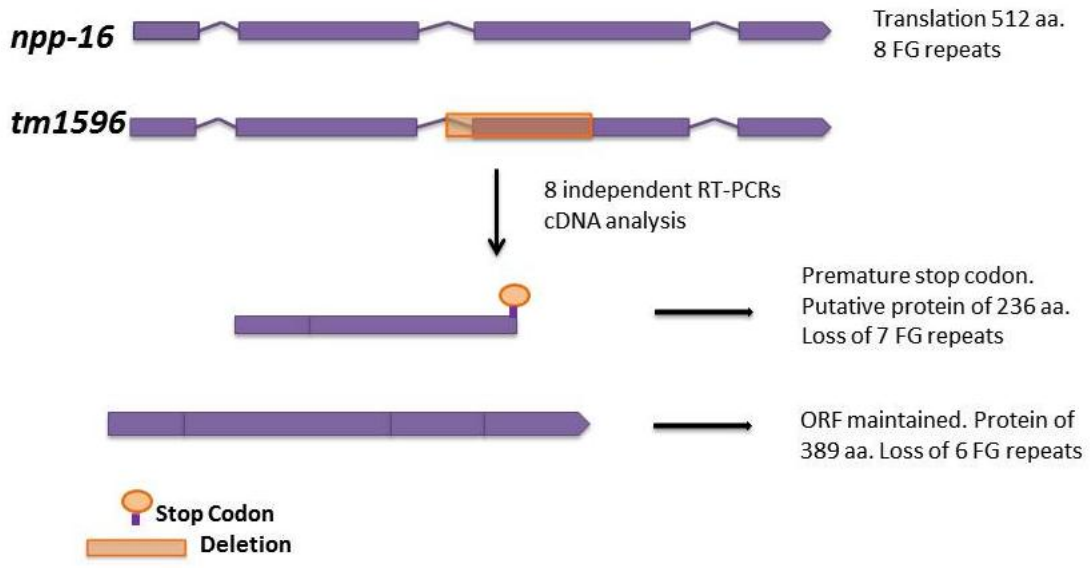

Figure 13. Schematic representation of *C. elegans* NPP-16 and deletion allele *npp-16(tm1596)*: exons and introns are indicated by purple boxes and lines, respectively. In the mutant strain (BN11) there is a deletion of 382 bp that affects the 2nd intron and the 3rd. exon. Eight independent RT-PCR analysis were performed to analyze the cDNA resulting from the mutant allele. Seven of them have a premature stop codon, and the ORF is disrupted resulting in a putative protein of 236 aa that lost 7 out of 8 FG repeats present in the wt *npp-16* allele. In the other cDNA a cryptic splice site in exon 3 is activated, resulting in an intact ORF encoding a protein of 389 aa that misses 6 FG repeats.

We raised antibodies against a peptide from the N-terminus of NPP-16 protein (present in wt and mutant alleles) that were used in Western blot analysis of wt and mutant samples (see Material and Methods). This revealed a prominent band of the expected size (55 KDa) in the wt sample treated with control RNAi , a weaker band in the wt treated with *npp*-16 RNAi, while it was absent in *tm1596* treated with control and with *npp-16* RNAi (Figure 14). Due to the presence of several cross-reacting bands of ~20-45 KDa we cannot conclude from our Western blots if truncated NPP-16 polypeptides are produced from the two mutant transcripts isolated from *tm1596* animals. Moreover this analysis also indicates that the *npp-16* RNAi is not completely efficient and does not remove all NPP-16 protein expression in the wt strain. NPP-16 antibodies raised in Jason D. Lieb´s laboratory allowed them to detect the *npp-16*(*ok1839)* band of around 27 KDa (Gerstein, Lu et al. 2010).We plan to test these antibodies in our mutant strain. The *npp-16*(*ok1839)* allele has a 1120 bp deletion that affects the 2nd, 3rd and 4th exons, producing a 253 aa (27KDa) protein.

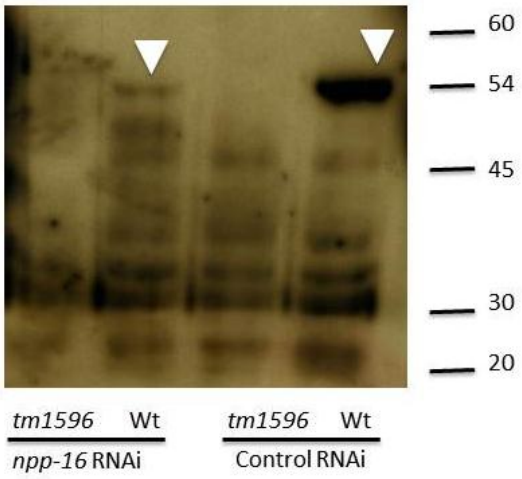

Figure14. Western blot of control and *tm1596* strains fed with control and *npp-16(RNAi)* using NPP-16 Abs: a 55 kDa band, which corresponds to the predicted molecular weight of NPP-16 (arrow-head), appears in wt embryos from animals fed with control RNAi. The band is strongly diminished in the wt embryos from animals fed with *npp-16(RNAi).* As expected, the band is absent in the *tm1596* (BN11) embryos in both RNAi conditions.

Immunofluorescence (IF) assays with the same NPP-16 antibodies showed that low amounts of truncated NPP-16 are expressed in the *tm1596* mutants. IF was performed in wt and *tm1596* embryos treated with control and *npp-16* RNAi. As shown in Figure15, NPP-16 localizes in the nucleoplasm and in the NE in wt embryos treated with control RNAi. This provides an important support to the notion that NPP-16 is a nucleoporin, orthologous to human Nup50. Immunofluorescence signal also appears in the *tm1596* embryos but it is much weaker, and mainly present in the NE (Figure 15). On the other

hand, wt embryos treated with *npp-16* RNAi showed a weaker signal, evidencing that the RNAi is effective but not 100%. In the *tm1596* embryos treated with *npp-16* RNAi the signal is not reduced compared with the same strain fed with control RNAi.

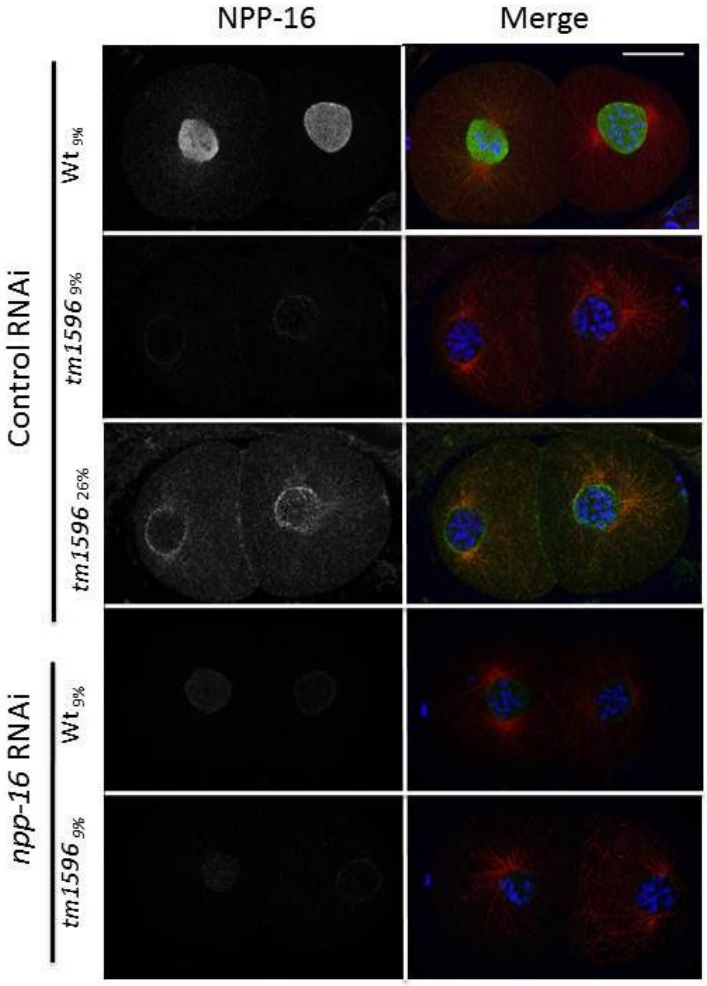

Figure 15. NPP-16 localizes in the NE and in the nucleoplasm: NPP-16 antibodies were used to study the NPP-16 localization in the wt (N2)and *tm1596* strains (BN11). In control RNAi conditions the antibodies show staining in the NE and in the nucleoplasm in the wt (upper row) In the mutant strain(second row) there is less protein but it localizes properly in the NE. This signal that is nearly invisible with 9% laser power (the same used in wt), is readily visible when increasing the laser power to 26% (third row). The two last rows show embryos of both strain treated with *npp-16* RNAi, in the case of the wt the signal was clearly reduced but not in the case of the mutant embryos. Scale bar 10 µm

2.2.2. **NPP-16 localization varies between cell and tissue types**: to study the localization of NPP-16 in living samples we made a transgenic strain that contain Pnpp-16::GFP::NPP-16; Plmn-1::mCherry::HIS-58 in *npp-16(tm1596)* background. In these strain the Plmn-1::mCherry::HIS-58 marker helps us to identify the cells and their nuclei. This GFP::NPP-16 construction rescues completely the embryonic lethality showed when *tm1596* mutants were fed with *npp-5* RNAi demonstrating that the transgene is biologically active (Figure 16). Next we analyze the localization of NPP-16

in early embryos as well as in different tissues. GFP::NPP-16 embryos were recorded from the pronuclear stage until 4-cell stage, as well as larvae of different stages and adults. All recordings were performed using a Nikon A1R confocal microscope.

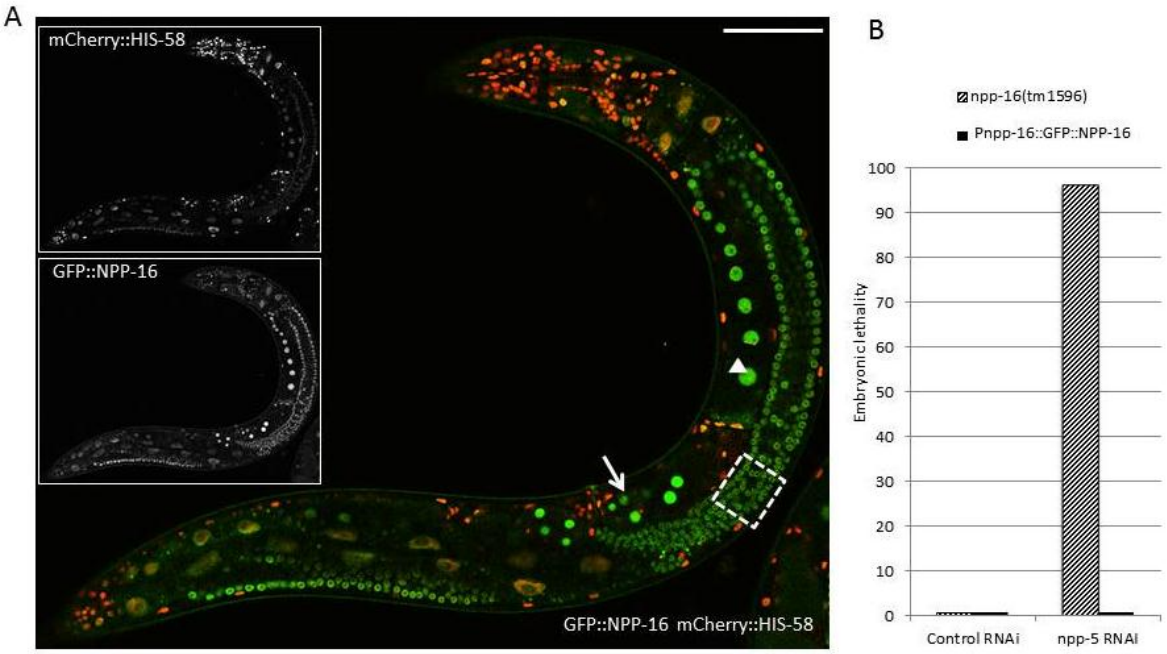

Figure 16. NPP-16 is ubiquitously expressed in *C. elegans* with strong levels in the germ cells: expression and localization of NPP-16 was studied using a *npp-16(tm1596*) mutant strain that carries Pnpp-16::GFP::NPP-16 and Plmn-1::mCherry::HIS-58 transgenes (BN192). A) This protein is expressed ubiquitously in the nematode but can be observed (GFP::NPP-16 and merge image) that its level expression is higher in embryos (arrow), germ line (dashed square) and oocytes(arrow head). Scale bar 0.1 mm. B) This transgenic strain recovers completely the synthetic lethal phenotype showed in the background *tm1596* when it is fed with *npp-5* RNAi demonstrating that the transgene is biologically active.

As shown in Figure 16, NPP-16 is ubiquitously expressed in all the cells with high expression levels in the germ line, oocytes and embryos. The subcellular localization (Figure 17) slightly changes between the different cell types, showing a uniform nuclear distribution in the head cells, while intestine and tail cells show also accumulation in the NE. In germ line cells, oocytes and embryos, NPP-16 is strongly expressed in the nucleoplasm.

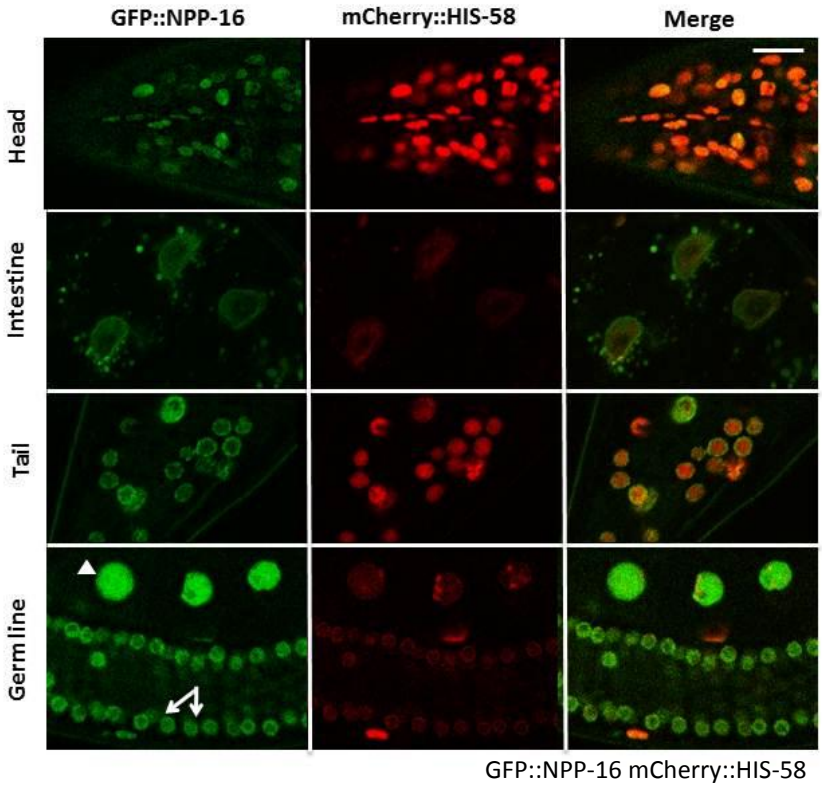

Figure 17. NPP-16 expression pattern in different cell types: NPP-16 is expressed in all the cells of the animals and localizes in the nucleus, but depending of the cell type its intranuclear distribution changes. In the head (upper row) NPP-16 shows a uniform nuclear distribution. Cells of the intestine (2nd row) and the tail (3rd row) show in addition to nucleoplasmic localization also accumulation in the NE. NPP-16 is strongly expressed in the nucleoplasm in germ line cells (arrows) and oocytes (arrow heads) (lower row). Strain used BN192. Scale bar 50µm.

In embryos NPP-16 is highly expressed but its distribution change from pronuclear stage, where the concentration is mainly in the nucleoplasm, to older embryos, where NPP-16 increases its localization in the NE (Figure 18). To check this difference we measured the distribution of NPP-16 (using it fluorescence value) along a cross section in nuclei of different stages (Figure 18). In pronuclear stages this nucleoporin is distribute along the nucleoplasm in a regular manner, whereas in the nucleus of 16-cell stage embryos the distribution has two peaks that correspond to the NE.

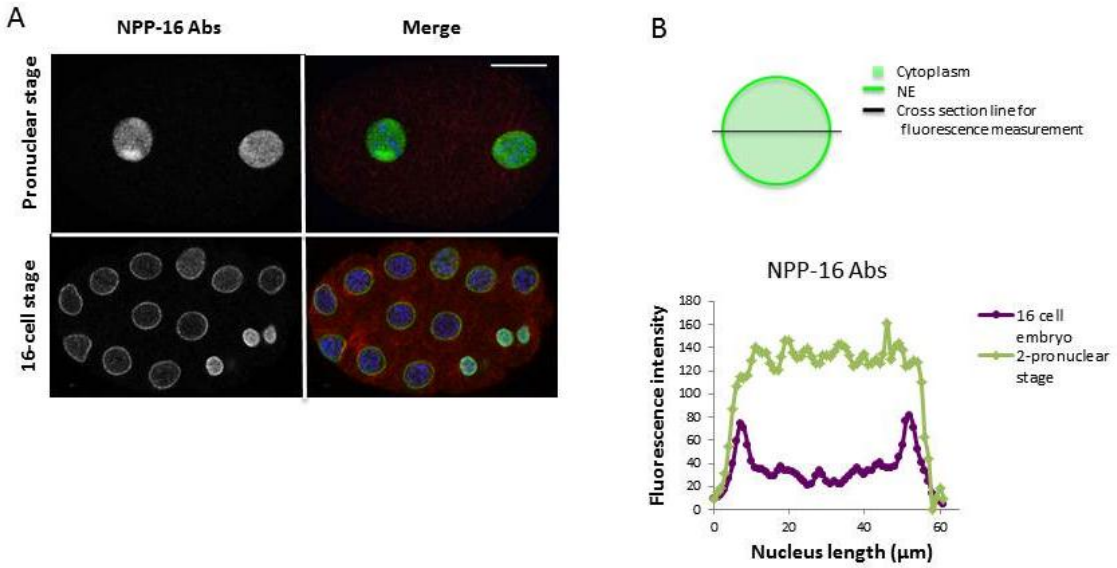

Figure 18. NPP-16 distribution depends on embryonic stage: A) Immunofluorescence images using NPP-16 antibody show a regular distribution in pronuclei (upper row), whereas its localization becomes stronger in the NE as the embryo develops (lower row; 16-cell stage embryo). B) Scheme for measure the fluorescence intensity distribution in a nucleus (top). Measurements in NPP-16 in pronuclei and nuclei of older embryos (n=4 of each class) evidence the different distribution pattern of NPP-16 in both cases. In pronuclear stage the fluorescence intensity is uniformly distributed while in 16-cell embryos there are two fluorescence peaks that correspond to the NE (bottom). Strain used N2. Scale bar 10 µm.

NPP-16 also changes its localization in the different cell cycle stage. As shown in Figure 19, NPP-16 localizes to the nucleoplasm and accumulates at the NE during interphase. When the cell enters mitosis and the NE breaks down, NE localization of NPP-16 is lost whereas signal in the nucleoplasm is maintained. During pro-metaphase NPP-16 remains in the vicinity of the condensed chromosomes, it is dispersed completely at anaphase onset, and is recruited again to the reforming nuclei in telophase.

This means that NPP-16 has not only a NE but also a nucleoplasm localization, which is in agreement with what has been previously described with Nup50 in mammals (Smitherman, Lee et al. 2000, Kalverda, Pickersgill et al. 2010).

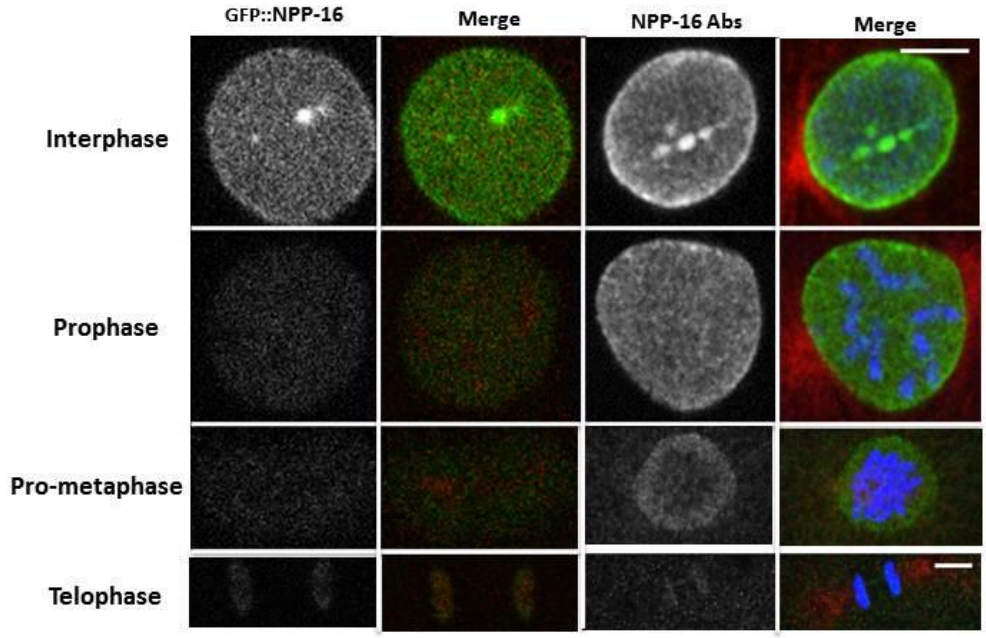

Figure 19. NPP-16 localization in embryos: Images showing the localization of NPP-16 in the different cell cycle phases. The two first columns correspond to still images from an *in vivo* recording of a transgenic strain that expresses GFP::NPP-16 and mCherry::HIS-58 (BN192). The last two columns correspond to immunofluorescence images using the NPP-16 antibodies and Hoechst to visualize the DNA in wt embryos. In both cases the images correspond to two-cell embryos. During interphase NPP-16 localizes in the NE but also in the nucleoplasm (1st row), then accumulates in the nucleoplasm when the cell enters prophase (2nd row). The 3rd row shows that during pro-metaphase NPP-16 accumulates around the DNA. Note that in the immunofluorescence images the metaphase plate is observed from the centrosome angle, explaining the circular aspect of the DNA. Finally, in late anaphase and telophase (4th row) NPP-16 is recruited to the reforming nuclei. Scale bar 5 µm.

2.2.3. **<u>NPP-16 is a mobile nucleoporin</u>:** one of the characteristics of a protein is its mobility. Information about whether a protein is localized to a given position for a prolonged time or rather display a dynamic on/off binding may provide insight into which kind of process the protein is involved. To study this feature in NPP-16, FRAP analysis (Fluorescence Recovery After Photo-bleaching) was performed in four cell embryos of the GFP::NPP-16 strain. Using the Nikon A1R microscope, selected areas of the NE of several nuclei where bleached with a strong excitation laser during one second. After that, we measure the time necessary for the recovery of the fluorescence in the bleached area, which corresponds to the time required for unbleached GFP::NPP-16 molecules, from outside the region, to replace bleached GFP::NPP-16 molecules (Figure 20). The mobility rate of NPP-16 obtained ($t_{1/2}$ = 53

sec), corresponds to the time required for the recovering of half of the max fluorescence value obtained in the experiment. As a comparison, we also performed FRAP experiments with GFP::NPP-19. In the case of GFP::NPP-19, the recovery is slower than GFP::NPP-16 and the fluorescence intensity do not even reach a clear plateau, making it difficult to obtain its mobility rate. However looking at the graph it is evident that GFP::NPP-16 has faster fluorescence recovery than GFP::NPP-19 implying that it is more mobile. FRAP images of nucleus of both nucleoporins also show this difference (Figure 20). This result is in agreement with the previous designation of NPP-19 (human Nup35) as an structural adaptor of the NPC (Rabut, Doye et al. 2004, Rodenas, Klerkx et al. 2009) that should be more static than a FG nucleoporin as Nup50/NPP-16 that localizes in the nuclear basket and in the nucleoplasm.

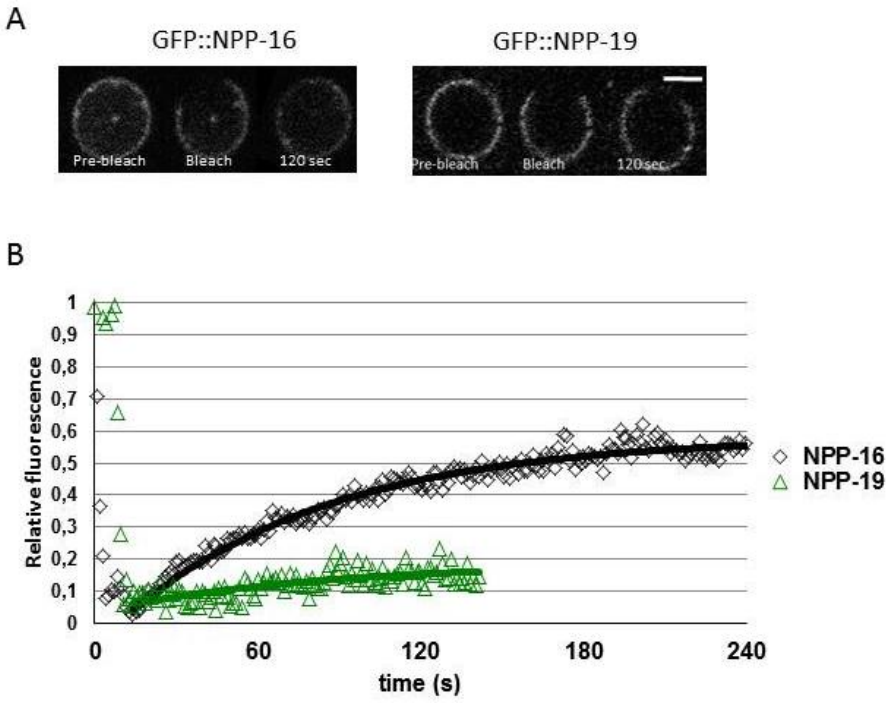

Figure 20. NPP-16 is more mobile than NPP-19: A) Images from FRAP experiments of BN192, GFP::NPP-16 (left panel) and BN46, GFP::NPP-19 (right panel) illustrating NE accumulation before, immediately after and 120 sec after bleaching. Scale bar 5 µm. B) Measurement of the fluorescence intensity every sec was used to calculate the $t_{1/2}$ of GFP::NPP-16 recovery (53 sec). In the case of GFP::NPP-19 the fluorescence recovery is slower and it does not reach a clear plateau, what make difficult to calculate its mobility rate. n= 8 in each strain.

2.2.4. **<u>NPP-16 is dispensable for nuclear import</u>:** knowing that Nup50, the human orthologous gene of NPP-16, play an important role in nuclear import (Lindsay, Plafker et al. 2002, Matsuura and Stewart 2005), we decided to analyze if the transport

of the nuclear protein PIE-1 is affected by the absence of NPP-16. For that we use a transgenic strain that expresses the protein PIE-1 tagged with GFP (GFP::PIE-1) and we compared the nuclear accumulation of this molecule in embryos treated with the control RNAi vector and with *npp-16* RNAi. In wt, GFP::PIE-1 localizes in the cytoplasm and in large cytoplasmic granules (P granules) during cell division, and it is rapidly imported to the nucleus when the NE is completely formed, where it accumulates in numerous fine nuclear foci (Ghosh and Seydoux 2008). In these experimental conditions we did not observe any statistically significant difference in the import of this fluorescent protein between control and *npp-16* RNAi (Figure 21), implying that NPP-16 is not related with this specific transport pathway. This result does not discard the possibility that NPP-16 play a role in other nuclear import pathways.

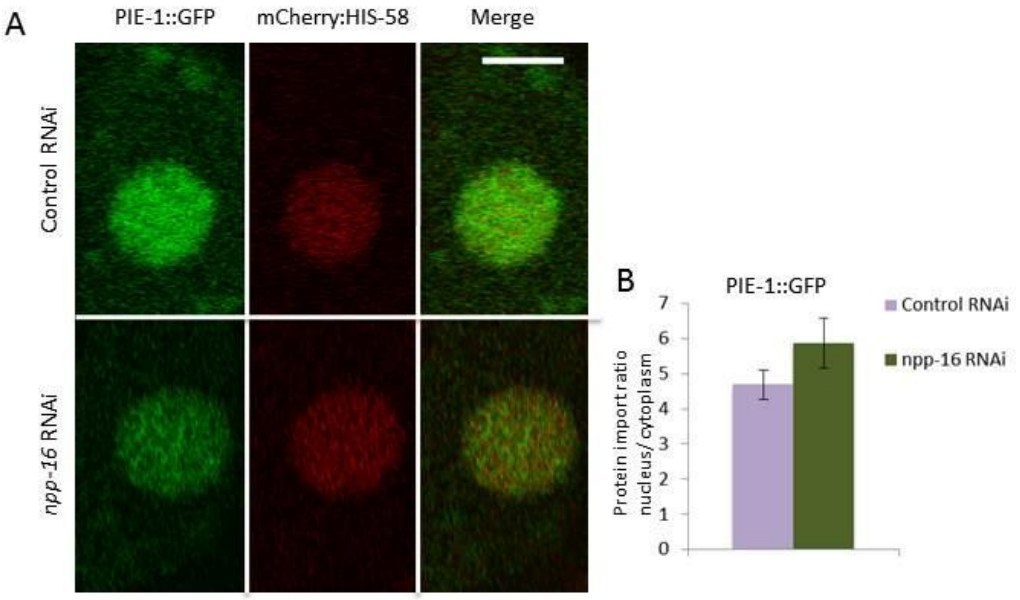

Figure 21: Nuclear import of PIE is not affected by the absent of NPP-16. A) PIE-1::GFP localizes in the cytoplasm during telophase and is imported to the nucleus during interphase. Both in the control (upper panel) and in the *npp-16* RNAi treatment (lower panel), PIE-1 localizes properly in the nucleoplasm. Shown are P2 nuclei of four-cell stage embryos. Scale bar 5 µm. B) Quantification of nuclear PIE-1::GFP in control and *npp-16(RNAi)* embryos showed no significant difference in nuclear import, suggesting that this nucleoporin is not affecting the PIE-1 transport pathway. n= 6 embryos in each strain. Error bars indicate the standard error of the mean. Strain used JH1327

2.2.5. ***npp-16* and *npp-5* show a synthetic lethality interaction**: one of the positive controls used in our screening was *npp-5* (Nup107), encoding a nucleoporin that forms part of the Nup107-160 complex (Rodenas, Gonzalez-Aguilera et al. 2012). This control was chosen because a former member of the laboratory studied its interaction with *npp-16*, showing that depletion of *npp-16* by RNAi in wt worms did not cause any evident phenotype, while depletion in npp-5(*ok1966)* mutants produced a high frequency of embryonic lethality. When we performed the reciprocal experiment, that is depletion of NPP-5 by RNAi, we observed >95% of embryonic lethality and larval arrest in *npp-16(tm1596)* mutant whereas no phenotype was detected in wt worms (Figure 16). To analyze if the synthetic lethal interaction induces severe defects in early embryogenesis, transgenic strains expressing mCherry::HIS-58, and GFP::α-tubulin in wt and *tm1596* backgrounds, were fed with *npp-5* and control RNAi. The images obtained did not show a clear phenotype in relative young embryos (~8-16 cell) (data not shown).

2.2.6. ***npp-16* shows interaction with 13 genes:** as mentioned in the screening results, we found 13 different possible interactors with *npp-16*, whose RNAi produce a more severe phenotype in *tm1596* mutants than in wt animals. Among those interactors, there are genes related with the cell cycle, serpentine receptors and other processes, but also we obtained three unknown genes that potentially could be nucleoporins that have been already described in other model organisms but not in *C. elegans* (Table 1). It is important to note that screening with *npp-16(tm1596)* also yielded two nucleoporin genes, *npp-21* and *npp-2.* Based on their common localization to the NPC, we indeed expected to retrieve *npp* genes.

In some of the cases, the RNAi phenotypes observed in the *npp-16* mutant were embryonic lethality or adult sterility but for others we also were able to observe post-embryonic phenotypes such as larval lethality, larval arrest, and protruding vulva or growth defects (Table 2)

After the two validation rounds, we analyze the 13 candidates more in detail, specially focusing in the genes that are still unknown and those that showed a high

embryonic lethality in the mutant compared to the WT. Using WT and *tm1596* mutant strains expressing EMR-1::mCherry, we look for early embryonic phenotypes. Some of them, such as *skr-1,* did not show any early embryonic phenotype, while others, such as Y71F9AL-1 showed dramatic effects of the RNAi also in the wt background. In the case of *npp-21*, which show 100% embryonic lethality in the second validation round, its RNAi stop showing any phenotype and, although we have tried to reproduce the phenotype changing different conditions (Material and methods), we were not able to reproduce it again. After all these analysis we decided to focus in the nucleoporin *npp-2*, which RNAi produces 99.6 % embryonic lethality in the *tm1596* strain and this phenotype was highly reproducible (Figure 22).

NPP-16	Emb	Lva/Lvl	Ste	Stp	Pvl/Muv	Gro/Unc/Rb
ncbp-1						
cye-1	32 % (24%-36%)					
npp-2	100%					
skr-1	80%* (48%-88%)					
rpl-1	62 % (5%-84%)					
npp-21	100 %					
rpl-1						
ZK809.5	30 %* * (9%-61%)					
srd-22	20 % (0%-50%)					
srw-87						
srw-15						
C14F11.2						
rps-14	37.6%* (27%-50%)					

Table 2. 13 candidates genes resulted from the genome wide screening with the npp-16 mutant: we observed embryonic lethality (Emb) in some of them(the average percentage and the range, in brackets are indicated), while in others the absence of both genes caused post-embryonic phenotypes such as larval lethality (Lvl), larval arrest (Lva), sterility (Ste) or growth defect (Gro).
*Emb is also present in the wt.
**Emb in the wt 62%

2.2.6.1. NPP-16 and NPP-2 absence produce severe phenotypes in embryogenesis: among the 13 genes resulted in the screening, in the case of NPP-16 we chose other nucleoporin, NPP-2 (Nup85 in mammals), which mutant strain *npp-2(tm2199)* is lethal but its RNAi only causes low embryonic lethality (~1%) and other defects such as nuclear size defects in wt worms. In contrast *tm1596* strain fed with *npp-2* RNAi showed ~100% embryonic lethality (Figure 22).

- **Absence of NPP-16 and NPP-2 causes strong defects in early embryonic development.** Next we analyze the effect that the absence of both nucleoporins produces in young embryos. For that we used different transgenic strains in the wt and *tm1596* backgrounds.

First, we checked the effect of depletion of *npp-2* by RNAi in the DNA and in tubulin, using mCherry::HIS-58 and GFP::α-tubulin as markers and as it is shown in the Figure 22 the *npp-2* RNAi in the NPP-16 mutant caused severe defects, starting by an abnormal behavior of the two pronuclei that do not juxtapose correctly (data not shown), and problems during the alignment and segregation of chromosomes during the following cell division. We could observe also a delay in the P1 division. These defects are not observed in the wt background strain fed with the same RNAi. Next, we decided to check what happens with other cell structures in these conditions. To visualize the defect that the absence of these two Nups can produce in the NE we used the EMR-1::mCherry as a marker in wt and mutant backgrounds (Figure 23) . While the wt strain fed with the *npp-2* RNAi show small nuclei, defect described before in embryos treated with this RNAi (Galy, Mattaj et al. 2003), the NPP-16 mutants also showed defect in the NE reformation and the same delay in P1 division observed with the other transgenic strain.

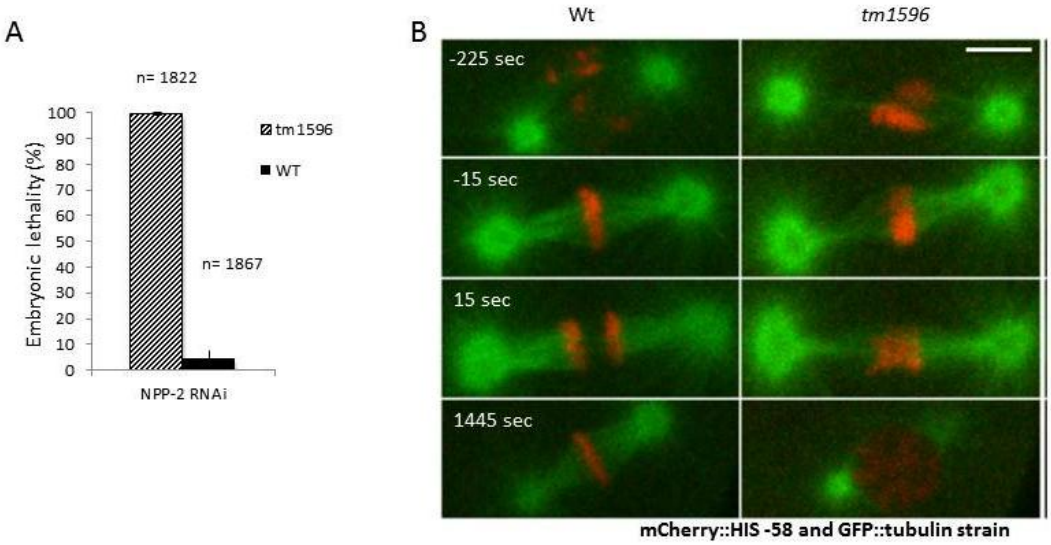

Figure 22. Depletion of *npp-2* causes embryonic lethality and cell division defects in *npp-16* mutants: A) Depletion of *npp-2* by RNAi causes very low embryonic lethality in wt animals but ~100% lethality in *tm1596* mutants. B) Still images from time lapse confocal microscopy of control and *tm1596* embryos depleted for *npp-2* by RNAi and expressing GFP::tubulin (green) and mCherry::HIS-58 (red). Specific defects in the *tm1596* embryo include premature separation of centrosomes prior to the first mitotic division (-225 sec), failure to align chromosomes properly on the metaphase plate (-15 sec), and chromosome missegregation (15 sec). Moreover, division of the P1 cell is delayed (1445 sec; mitotic spindle has been formed in the wt embryo, whereas the nucleus is still intact in the tm1596 embryo). Error bars indicate the standard error of the mean. Strain used BN192. Scale bar 5 µm.

- **The *npp-2* RNAi in *tm1596* embryos causes strong defects in NPP-7 and other FG Nups.** Trying to elucidate the phenotype observed in the absence of *npp-16* and *npp-2* and how this affects NPC structure, we performed immunofluorescence experiments using antibodies against NPP-7 (Nup153 in mammals) that also localizes in the NPC basket, and mAb414 antibodies that bind to FG nucleoporins. *npp-2* RNAi causes defects in the NE structure and both NPP-7 and mAb414 signals are affected appearing in clumps instead of a continuous NE. Moreover in the *tm1596* mutant strain the *npp-2* RNAi produces strong defects in the embryos, which show NE completely broken, DNA trapped and, enucleated cells (Figure 23).

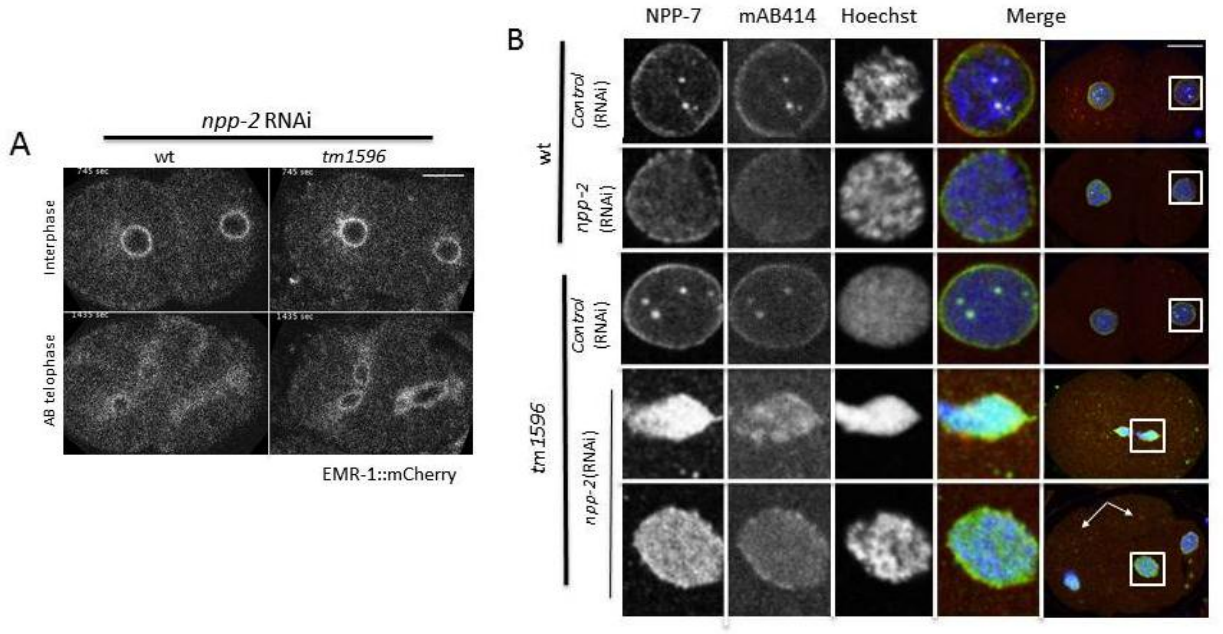

Figure 23. The *npp-2* RNAi causes dramatic effects in the NE and DNA segregation, in the npp-16 mutant: A) Still images from time lapse confocal microscopy in wt and *tm1596* strains expressing EMR-1::mCherry (BN142 and BN231 respectively) fed with npp-2 RNAi. During two cell embryo stage the mutant strains is similar to wt (first row) while during the AB division (2nd row) the mutant show defects in the nuclear separation and consequently it is affected the nuclear shape (arrow). In the mutant strain, the distribution of EMR-1 is not affected by the *npp-2 RNAi*

B) Immunofluorescence using antibodies against NPP-7 (1st column) a nucleoporin of the nuclear basket, mAb414 (2nd panel) that allow to visualize several FG nucleoporins, and DAPI to visualize the DNA (3rd panel). In the wt strain fed with the *npp-2* RNAi the NE is affected showing a more diffuse localization of the NPP-7 and mAB414 signals that in the same strain fed with the control RNAi (1st panel) has a continuous and enhanced localization. In the *tm1596* (BN11) fed with the control RNAi (3rd panel), the different structures looks like the wt strain in the same conditions, whereas in the NPP-16 mutant fed with *npp-2* RNAi (4th and 5th panels) the NE is dramatically affected and there are defects in the DNA segregations. Also, how is shown in the 4-cell embryo of the last panel, depletion by RNAi of *npp-2* in *tm1596* strain, produce cells that seems to lose all the nuclear structure, even their DNA. Scale bar 10 µm.

- **Lamina structure is less affected than NE in embryos fed with *npp-2* RNAi:** immunofluorescence images using lamin/LMN-1 antibody to visualize the effect of *npp-2* RNAi on the nuclear lamina of WT and *tm1596* embryos, showed that this structure is less affected than the NE by the absent of one or both nucleoporins (Figure 24). However when *npp-2* is depleted by RNAi there is an accumulation of lamin signal around the centrosomes in WT and mutant embryos, which is absent in the same strains fed with the control RNAi. Moreover the *npp-16* mutant embryos fed with *npp-2* RNAi showed, as in the previous experiments, DNA segregations problems and DNA trapped phenotypes.

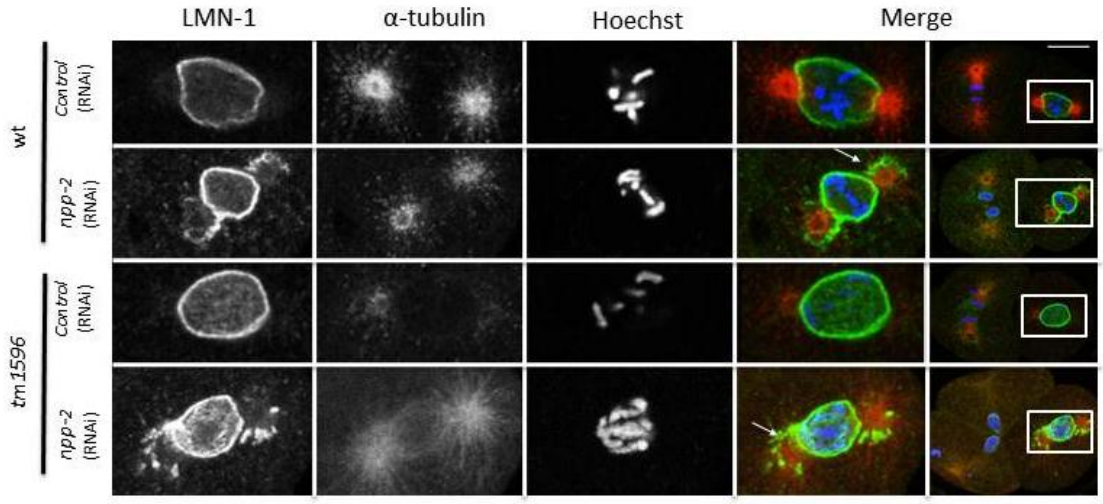

Figure 24. *npp-2* RNAi causes lamina aggregations around the centrosomes: Immunofluorescence using, tubulin, DAPI and lamin-1 antibody (LMN-1) to visualize if npp-2 RNAi also affects the lamina structure. Both in the wt and the mutant strain these structure is less affected than the NE, but it shows aggregations surrounding the centrosomes (arrows ,4th column of 2nd and 4th row of panels). DAPI show defects in the DNA segregation and DNA trapped in the *tm1596* strain fed with the *npp-2* RNAi (last row).Strain used N2 and BN11 Scale bar 10 µm.

- **The *npp-2* RNAi in *tm1596* strain produce an embryonic lethality around the 300 cell stages**. To check when the *npp-16* mutant embryos died with *npp-2* depleted by RNAi stops their development, we recorded early embryos expressing mCherry::HIS-58 and GFP::α-tubulin. As control we also recorded the development of *tm1596* embryos fed with the control RNAi. These results (Figure 25) confirmed the high embryonic lethality showed before, but also showed that the mutant embryos

when fed with *npp-2* RNAi died in ~300 cell stage, around 5 h from the fertilization. Most of the wt embryos fed with *npp-2* RNAi were able to hatch, and those who died did so in an older stage of development.

A

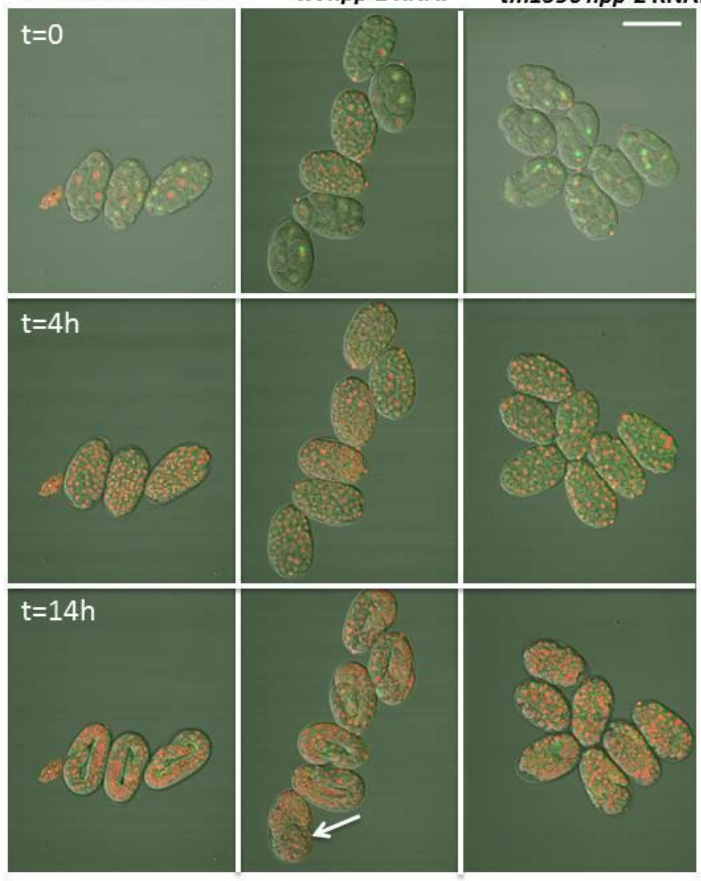

Figure 25. *npp-2* RNAi produces early embryonic lethality in npp-16 mutants: A) still images from a recording of strains expressing mCherry::HIS-58 and GFP::tubulin. The mutant strain fed with control RNAi behave as a wt and all embryos completed embryogenesis (1st column). In the wt strain fed with *npp-2* RNAi, 5 out of 6 embryos hatched (2nd column). Finally, all the *tm1596* embryos depleted for NPP-2 arrested in a relatively early stage after ~5h (3rd column). Compared with these embryos, the single wt embryo that died (arrow) reached the bean stage. Scale bar 50 µm. B) Number of recorded and dead embryos for each strain. Strain used BN245 and BN247

B

Strain/ RNAi	Embryos recorded	Dead embryos
wt/ *npp-2*	11	3
tm1596/ control	6	0
tm1596/ *npp-2*	14	14

- **NPP-16 mobility is affected by *npp-2* RNAi:** to understand better the interaction between NPP-16 and NPP-2 proteins FRAP analysis was performed in a strain expressing GFP::NPP-16, to study how the mobility of NPP-16 is affected when *npp-2* is depleted by RNAi. Figure 26 shows that depletion of *npp-2* by RNAi results in a faster recovery of the fluorescence in the bleached area, showing a six times fold increase of the mobility rate compared to control RNAi ($t_{1/2}$ control RNAi 42 sec versus $t_{1/2}$ *npp-2* RNAi:7 sec). The distribution of NPP-16 also seems to be affected by *npp-2* RNAi. The nuclei of embryos treated with control RNAi showed a stronger recruitment

of NPP-16 in the NE while the nuclei of embryos treated with *npp-2* RNAi showed a uniform distribution along the nuclear surface (Figure 26). These results imply that the depletion of *npp-2* by RNAi increased the mobility of the NPP-16 pool bind to the NPC.

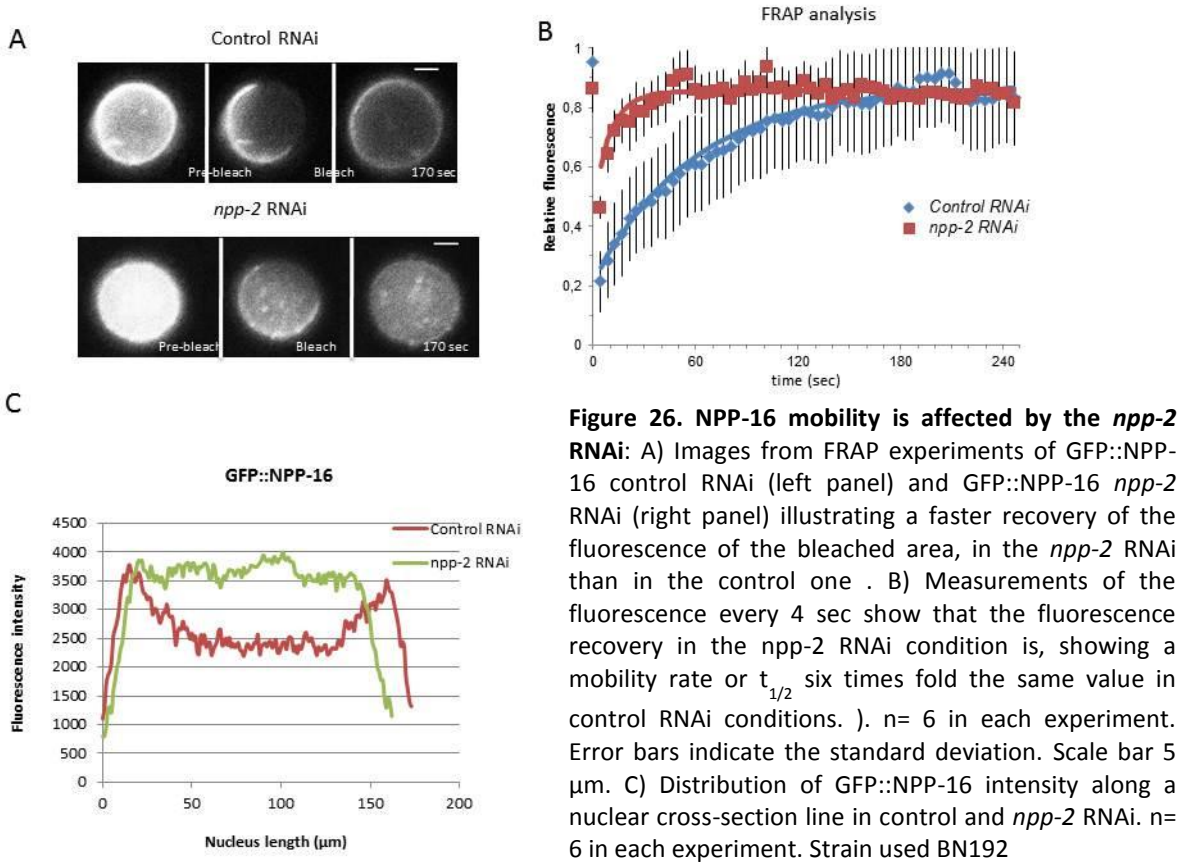

Figure 26. NPP-16 mobility is affected by the *npp-2* RNAi: A) Images from FRAP experiments of GFP::NPP-16 control RNAi (left panel) and GFP::NPP-16 *npp-2* RNAi (right panel) illustrating a faster recovery of the fluorescence of the bleached area, in the *npp-2* RNAi than in the control one . B) Measurements of the fluorescence every 4 sec show that the fluorescence recovery in the npp-2 RNAi condition is, showing a mobility rate or $t_{1/2}$ six times fold the same value in control RNAi conditions.). n= 6 in each experiment. Error bars indicate the standard deviation. Scale bar 5 µm. C) Distribution of GFP::NPP-16 intensity along a nuclear cross-section line in control and *npp-2* RNAi. n= 6 in each experiment. Strain used BN192

2.3. LEM-2 is an integral membrane protein related with centrosome and nucleus behavior

2.3.1. LEM-2 expressed and localizes in the NE: as mentioned in the introduction LEM-2 is a INM protein that is ubiquitously expressed in all kind of cells, and also localizes in the ER but in a lesser manner. As it has been previously shown, there is an overlapping function between LEM-2 and emerin/ EMR-1. To clarify the relationship between these two proteins, we expressed both of them in a transgenic strain using GFP and mCherry markers (LEM-2::GFP; EMR-1::mCherry). After the first mitotic division, when nuclei are reassembling, it was observed (Figure 27) that LEM-2 is recruited to the NE earlier than EMR-1. Moreover, it was observed that both proteins were expressed in most of the tissues but in different proportion, in the case of LEM-2 its expression is enriched in germ line and intestinal cells (Figure 27).

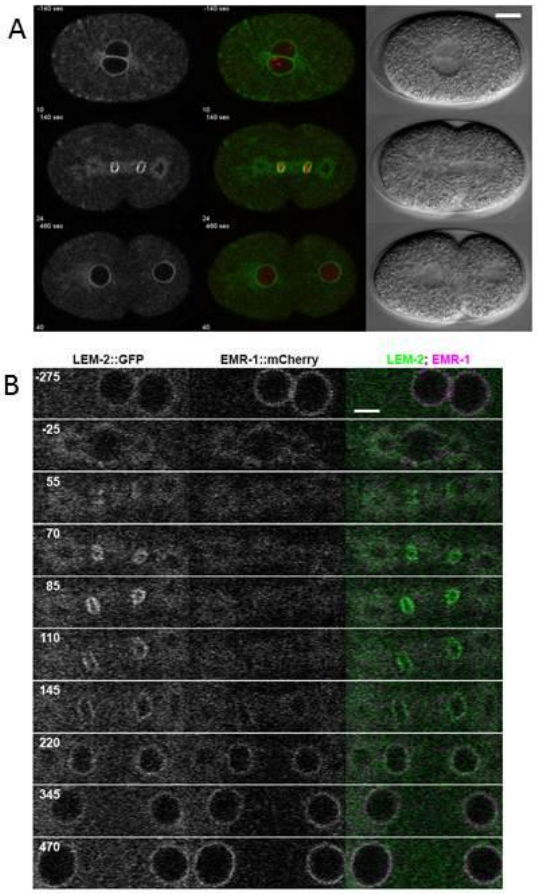

Figure 27. LEM-2 localization and expression pattern: A) Still images from time-lapse confocal microscopy of a transgenic strain expressing GFP::LEM-2 and mCherry::HIS-58 (OD83) show that LEM-2 localizes in the NE with higher intensity during telophase and in a lesser manner in the ER. Scale bar 10 µm B) Images of a strain expressing LEM-2::GFP and EMR-1::mCherry showing the recruitment of the two proteins from pronuclear meeting and during the first division. In the merged images (last column) is shown that the recruitment of LEM-2 (green) to the NE occurs earlier than the recruitment of EMR-1 (magenta) Strain used BN227. Scale bar 5 µm. C) Both proteins are ubiquitously expressed but LEM-2 is enriched in the germ line and intestine relative to EMR-1. Strain used BN227. Scale bar 0.1 mm.

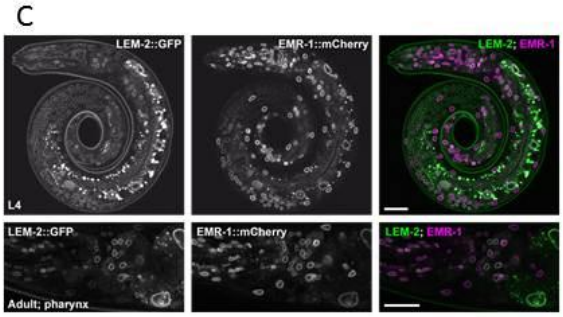

2.3.2. **<u>LEM-2 and EMR-1 are synthetically lethal</u>:** emerin, as it was mentioned before, is also an INM protein that has the LEM-domain, and it has been previously described to have overlapping functions with LEM-2. In the screening we used emerin / EMR-1 RNAi as positive control due to the strong effect that the absent of both NETs proteins have in development. Depletion of *emr-1* by RNAi in the null LEM-2 mutant strain *tm1582* causes ~100% embryonic lethality versus ~0% emb observed when individual *emr-1* or *lem-2* were depleted, confirming the results of previous studies (Liu, Lee et al. 2003). The phenotype observed in *tm1582* mutants depleted of *emr-1 by* RNAi was a complete collapse of the NE and that the DNA is trapped in the center of the cell as can be observe in the Figure 28. The Emb phenotype was completely rescued by expression of LEM-2::GFP from a single-copy transgene which both confirms that the phenotype is due to the *lem-2(tm1582)* allele and demonstrates that the transgene is biologically active.

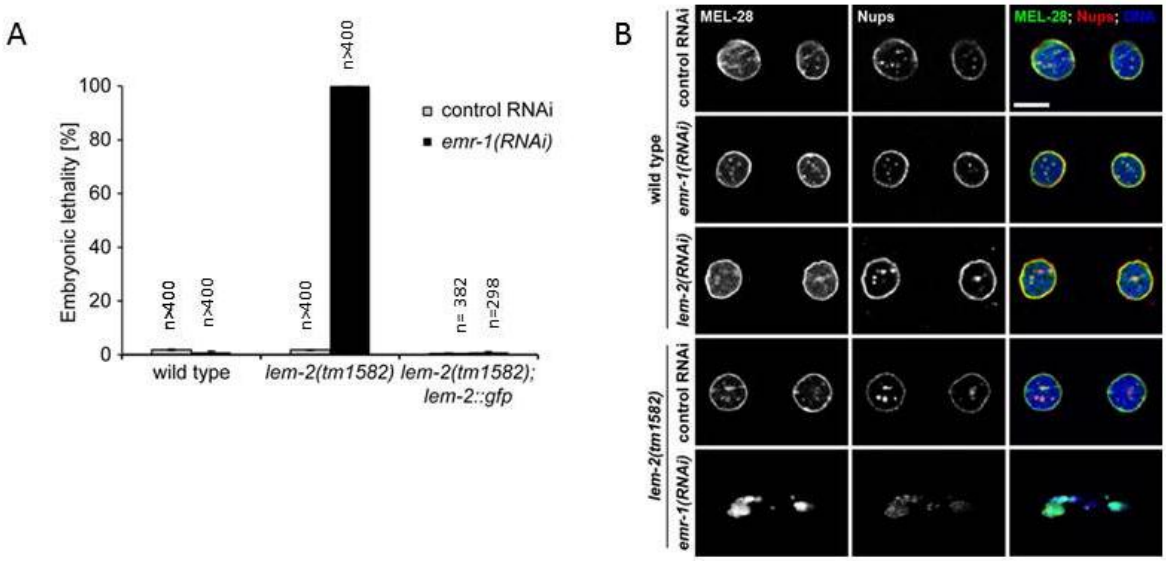

Figure 28. LEM-2 and EMR-1 show a synthetically lethal interaction: A) *emr-1* RNAi causes ~100% emb in *tm1582* strain, but no lethality in the wt strain. The introduction of a single-copy *lem-2::gfp* transgene restore the embryonic viability in the *lem-2* mutant confirming the functionality of this fusion gene. B) Depletion of EMR-1 by RNAi in *tm1582* causes severe defects such as incomplete NE assembly and DNA missegregation (last row). In single mutants or single RNAi depletions these phenotypes are not present (2^{nd}, 3^{rd} and 4^{th} panels). . Strain used N2 and BN19. Error bars indicate the standard error of the mean. Scale bar 5 µm.

2.3.3. <u>Loss of LEM-2 does not affect the short-term dynamics of EMR-1 although long-term turn-over of EMR-1 is increased in *lem-2* mutants</u> : To better understand the relationship between LEM-2 and EMR-1, both of them ubiquitously expressed and with a different localization Pattern (Figure 29), we performed FRAP analysis to check if the absence of LEM-2 affects the mobility of EMR-1. A total of 8 nuclei (from different 4 cell embryos) were bleached in a selected area and we measured the recovery time of the mCherry::EMR-1 molecules in the wt and in the *tm1582* background. The difference between both strains was very small, t½ is 37±6 sec for the wt; 35±7 sec for *tm1582* mutants. Results that indicate that LEM-2 does not affect the dynamics of EMR-1 (Figure 29).

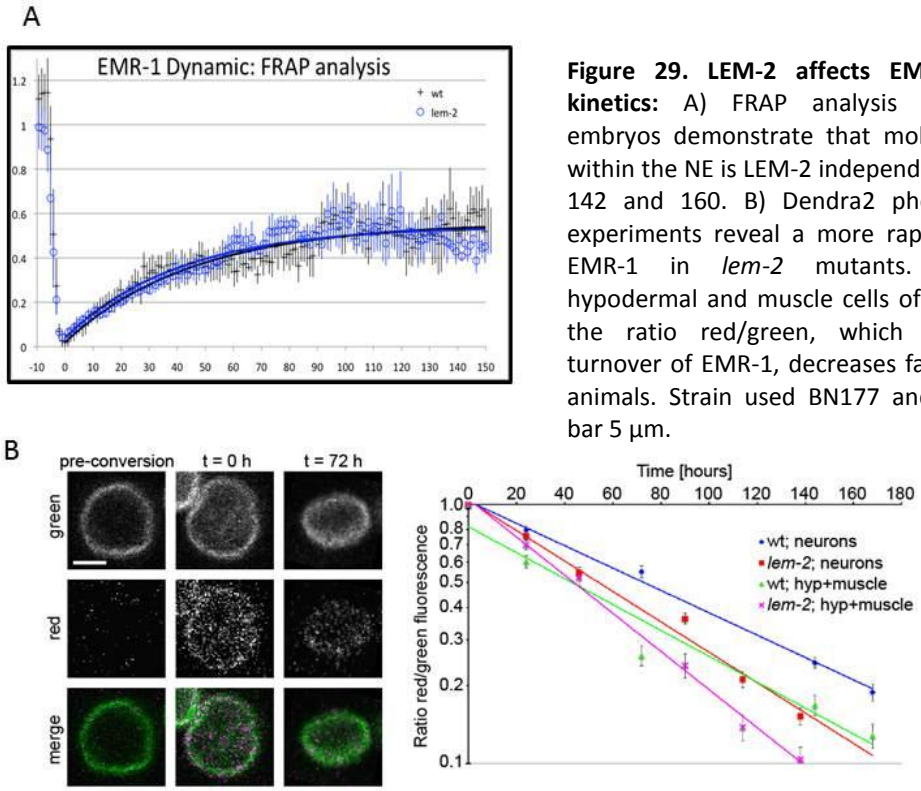

Figure 29. LEM-2 affects EMR-1 long-term kinetics: A) FRAP analysis in 4-cell-stage embryos demonstrate that mobility of EMR-1 within the NE is LEM-2 independent. Strain used 142 and 160. B) Dendra2 photo conversion experiments reveal a more rapid turn-over of EMR-1 in *lem-2* mutants. In neurons, hypodermal and muscle cells of *lem-2* mutants the ratio red/green, which expresses the turnover of EMR-1, decreases faster than in wt animals. Strain used BN177 and BN190. Scale bar 5 µm.

We also performed Dendra photo conversion experiments, and the results in this case show that the turnover of EMR-1 is faster in *lem-2* mutant than in wt neurons, muscle and hypodermal cells. Dendra2 is a photo switchable (green to red), monomeric fluorescent protein very commonly used to study the mobility and turnover of proteins.

This reporter binds to the protein producing a green signal and when receives a specific light irradiation changes to red. In this experiment Dendra2 was fused to *emr-1* and, after the UV irradiation, we measured the ratio between the value of red (old protein) and green protein (new protein synthetized) (Figure 29).

2.3.4. **Depletion of LEM-2 affects nuclear shape:** another phenotype observed in *tm1582* mutant embryos is that their NE shape and circularity were affected. Considering that several studies have previously shown that the absence of LEM-2 affects the nuclear shape (Brachner, Reipert et al. 2005, Ulbert, Antonin et al. 2006) we decided to measure the NE circularity index in 4 cell embryos in wt and *tm1582* strains using mCherry::EMR-1 as a NE marker. We measure this value using the formula $4\pi A/perimeter^2$ and the average of the wt nuclei was 0.91 with and standard deviation of 0.012 while in the mutant the average was 0.89 with a standard deviation of 0.029. These results are statistical significant, indicating there is a significant difference between WT and mutant nuclear circularity. We also measured the nuclear circularity in *emr-1* mutants (GFP::LEM-2) and the results indicated that their nuclear circularity was not different from the wt (Figure 30).

Furthermore we observed that the nuclei of *tm1582* strain showed intranuclear NE invaginations, which agrees with the results of previous studies (Brachner, Reipert et al. 2005) and gives more evidence about the relevance that LEM-2 has for the integrity of NE.

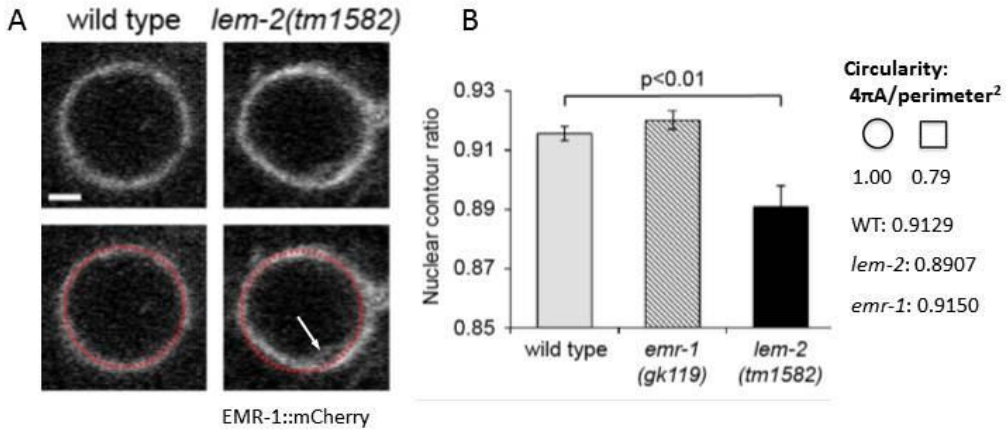

Figure 30. The absence of LEM-2 affects NE circularity and shape: A) Images of nuclei from 4 cell embryos expressing EMR-1::mCherry in *tm1582* and wt background. The *tm1582* nuclei show defects in NE shape and circularity, as well these nucleus present fingers-like invaginations (arrow) in the nucleoplasm. EMR-1 is localized along all the NE and also in this aberrant structures. B) Measurements of the circularity of wt and mutant nuclei (n=8) show that the difference is statistically significant. The relevance of this observation is more evident if we compare the circularity values of a perfect square and a circle. n=17 nuclei in all the experiments. Error bars indicate the standard error of the mean. Strain used BN142, BN160 and XA2524. Scale bar 3 µm.

2.3.5. <u>LEM-2 affects the nuclear separation after mitosis</u>: another phenotype that we also observed in the *tm1582* mutants was that there were defects in the nuclear separation during AB cell division (Figure 31). Measurement of the distance between the AB nuclei (taking as time 0 the anaphase onset, at 20 sec intervals) in wt and mutant strain, confirmed this phenotype showing not only a delay in the separation of the nucleus but also a defect in this process. In the cases of the mutant the nucleus starts to separated, then stop, move one to the other a little bit and them they continue the separation process in a normal way. This phenotype has been observed in several strains (EMR-1::mCherry , GFP-tub; mCherry-HIS-58 and GFP::y-tub; GFP::HIST) to ensure that is not an effect of the transgenic markers.

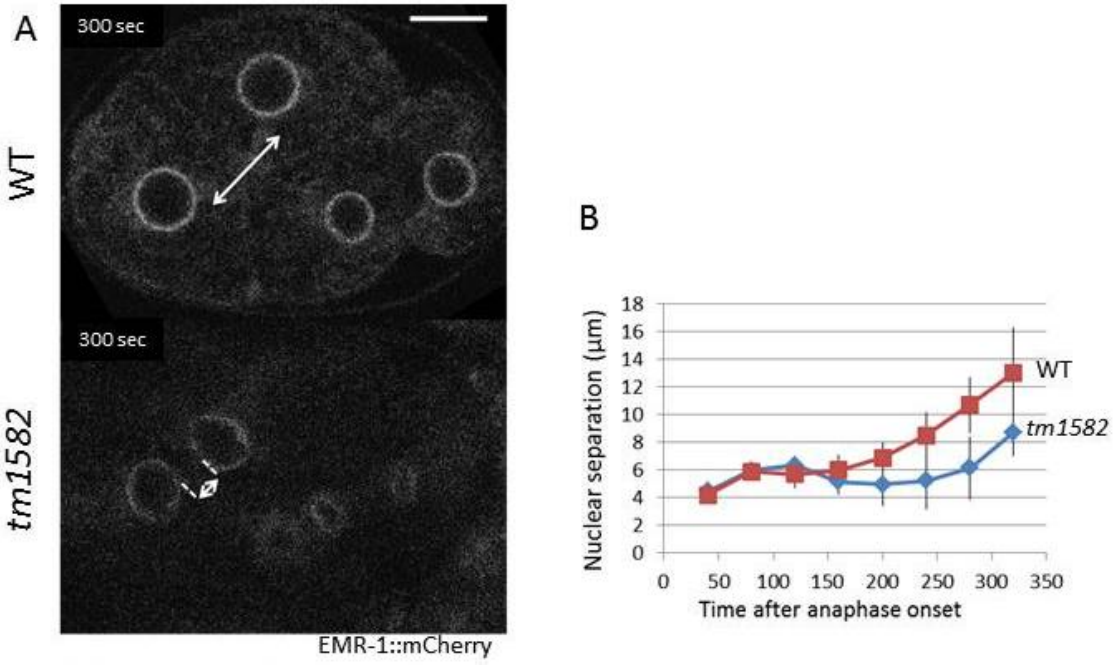

Figure 31. LEM-2 absence causes a nuclear separation phenotype: A) Still images from time lapse confocal microscopy of wt(bBN142) and *lem-2* (bn160) mutant strains expressing EMR-1::mCherry. The *tm1582* strain shows a defect in AB nuclear separation and, how is shown in the images, 300 sec after anaphase onset while in the wt the AB nuclei are positioned centrally, in the *lem-2* mutant they remain close together. B) Analysis of nuclear separation distance (measured from the NE; arrows) after anaphase onset in wt and *tm1598* embryos. The absence of LEM-2 produces an abnormal movement of daughter nuclei, which initially separate like in wt embryos, but briefly reverse the separation (160-240 sec) and finally separates (280-320 sec) (see also Figure 46). n= 5 in each strain. Error bars indicate the standard deviation. Scale bar 10 µm.

2.3.6. **LEM-2 affects centrosomes behavior:** in the introduction it was mentioned that several groups have suggested a role of LEM-2 in the cytoskeleton or in the spindle pole body (Meyerzon, Gao et al. 2009, Gonzalez, Saito et al. 2012). When we were studying the defects in the nuclear migration in the *tm1582* embryos, we realized that *tm1582* mutants also showed an aberrant centrosome behavior in the AB and P1 cell division. At least in one of the two nucleus of each division, one of the centrosomes detach from the NE and moves to the cellular membrane, where it remains until the nucleus arrive to its normal position, and then is re-attached again to the nucleus surface. Immunofluorescence images with α-tubulin antibodies showed also this phenotype in *tm1582* mutants (Figure 32).

We also made measurements of the distance between the centrosomes attached to AB cells, after anaphase onset, in the wt and *tm1582* mutant background (Figure 32). The *tm1582* strain shows shorter distances between centrosomes that agree with the aberrant migration of the nucleus mentioned before

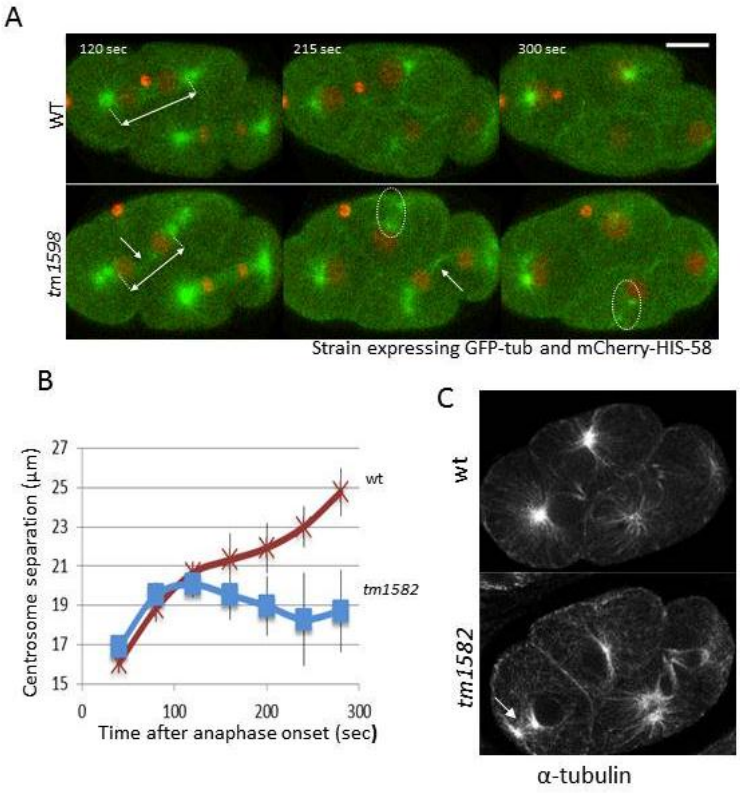

Figure 32. LEM-2 affects centrosomes behavior: A) Still images from time lapse confocal microscopy of embryos expressing GFP::tubulin and mCherry::HIS-58 in wt and *tm1582* background. An aberrant behavior of the centrosomes is observed in *tm1582* (ovals) and a strong accumulations of microtubules between the nucleus when they are spearing. Strain used BN245 and BN246. B) Analysis of distance between the two centrosomes most proximal to the NE (arrows in A) relative to anaphase onset reveals a defect in centrosome separation. n= 9 for each strain. Error bars indicate the standard deviation. C) Immunofluorescence analysis using α-tubulin antibodies demonstrate that the abnormal occurrence of a microtubule

To better understand these phenotypes we check several transgenic strains using *lem-2* RNAi or the *tm1582* mutant strain. The nuclear separation phenotype was shown in the cases of a transgenic strain expressing GFP::γ-tubulin and GFP::Hist and fed with control RNAi and *lem-2* RNAi (Figure 33). These images show that, in the case of the control RNAi embryo, centrosomes appear separated from the nucleus. To analyze if this centrosome was or not nucleating tubulin, we worked with wt and *lem-2* mutants strain expressing GFP::γ-tubulin and mCherry::β-tubulin. We saw that in the wt strain both centrosomes of each nucleus remain together and in *tm1582* embryos the centrioles show a bigger separation (no so evident as in the GFP::tub). We also measure the intensity of α and β tubulins in two different transgenic strains (GFP::tub

and mCherry::β-tub; GFP::γ-tubulin), in wt and mutant background, and the intensity values are more than two times fold in the mutant than in the wt strain.

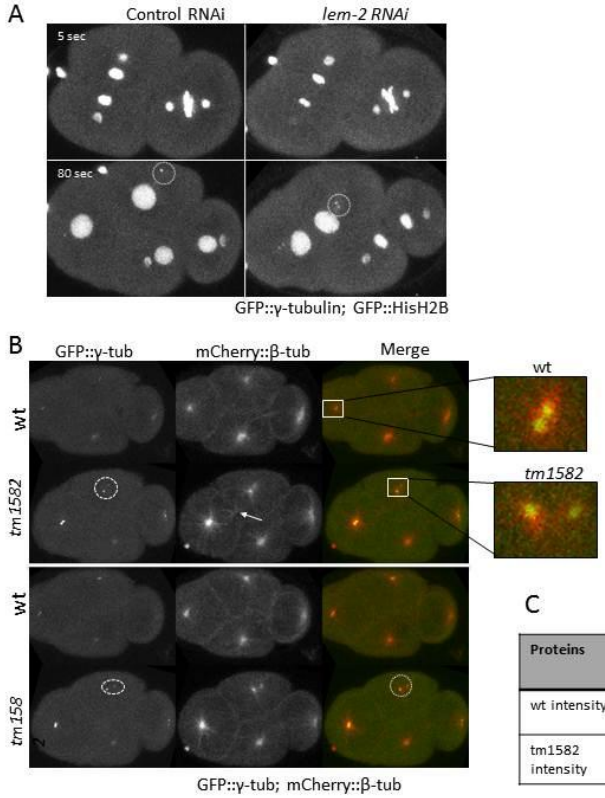

C

Proteins	GFP::tubulin	mCherry:: β-tubulin	AIR-2::GFP
wt intensity	10.6	6.8	64.7
tm1582 intensity	17.6	22.6	118.3

Figure 33. Analysis of the behavior of the different tubulins in *lem-2* mutant. A) Time lapse images of embryos expressing GFP::γ-tubulin; GFP::HisH2B in control and *lem-2* RNAi conditions. The *lem-2* RNAi (2nd column) produce the nuclear separation defect. In lower control condition image, γ-tubulin the centriole detaches from the nucleus (circle) but in this strain is not possible to observe if this centriole is nucleating or not.. Strain usednBN279. B) Still time lapse images of wt and *lem-2* mutant strains expressing GFP::γ-tubulin and mCherry::β-tubulin, corresponding to two consecutive time points. Mutant embryos show a detachment in the centrosomes (circle) that does not appear in the wt strain. In *tm1582* also appears an increased in the amounts of microtubules between the nuclei of AB division (arrow). Square show crop images of wt (up) and mutant (bottom) centrioles. Strain used BN289 and BN290. C) Measurement of the intensity of different fluorescent proteins in wt and lem-2 mutant strain,

2.3.7. *lem-2(tm1582)* shows a high expression level of AIR-2::GFP: Aurora B (AIR-2) is a kinase protein that forms part of the passenger complex (PC) and promotes multiple aspects of the cell division. At anaphase, AIR-2 localizes to the spindle midzone, a structure formed by antiparallel microtubules, where it promotes successful completion of the abscission cytokinesis, and is critical for the transduction of the abscission checkpoint. Chromatin obstructions induce hyperactive Aurora B at the midbody (Bembenek, Verbrugghe et al. 2013). We decided to check if this protein

was affected in the absence of LEM-2. In Figure 34 it is shown that the localization of AIR-1::GFP is not affected in the mutant strain, although there is a difference in the level of expression of AIR-1 that shows a higher intensity in the tm1582 strain. Together with other proteins we measure the intensity of AIR-1:: GFP in both strains and the mutant showed a value almost 2 fold higher comparing with the wt (table of Figure 33).

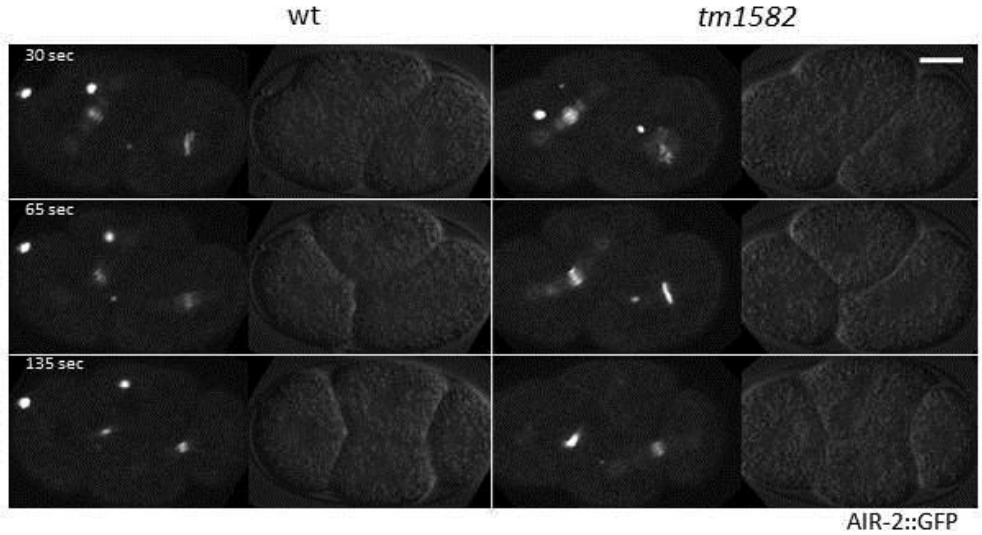

Figure 34. *lem-2(tm1582)* embryos show a high concentration of AIR-2::GFP: time lapse images of wt and *lem-2* mutant strain expressing AIR-2::GFP show that there is a higher accumulation of AIR-2 in the mitotic centrosome but also show higher levels in the DNA. Strain used OD27 and BN300.

2.3.8. <u>40 genes show interaction with LEM-2</u>: at the end of the genome wide RNAi screening we obtained 40 genes which when knocked down by RNAi produce strong phenotypes in the LEM-2 mutant strain but not in the wt strain. Some of them caused severe phenotypes such as Emb, Lva, Lvl or Ste, but also were observed post embryonic phenotypes such as Pvl, Muv, Rb or Grow (Table 3). Among them, there are known genes related with the cell cycle, transcription/ translation process, receptors, ubiquitination or ribosomal related genes. There were also 11 unknown genes that could be new NE related genes (Table 1). We also obtained two NE proteins, the nucleoporin, NPP-17, and EMR-1, which is known to show synthetic embryonic lethality with LEM-2. These results are a validation of the screening success.

Next we started analyzing the *lem-2* candidates, specially focusing on the unknown genes and the ones that produce stronger phenotypes in the *tm1582* strain. Some candidates did not show any phenotype in early development when they were visualized with the reporter gene EMR-1::mCherry, and other showed a drastic lethal phenotype both in the wt and mutant strains . A clear example of how variable RNAi efficiency it is, was the case of the candidate C27B7.7. After the validations round depletion of C27B7.7 by RNAi showed a 88% of Emb in *lem-2* mutant, and maintained this phenotype during several experiments. We did time lapse recordings and some genomic constructions to describe this unknown protein and its relation with LEM-2 but several month later its RNAi did not showed the Emb phenotype anymore, and after changing several conditions of the protocol without obtaining a positive result, we decided to stop working with C27B7.7.

After all, among all the candidates, we decided to analyze in more detail *ubc-12,* which is a neddylation related gene (Rabut and Peter 2008) that produces a high embryonic lethality in the *lem-2* mutant strain, and its RNAi efficiency seems to be very constant and reproducible.

LEM-2	Emb	Lva/Lvl	Ste	Stp	Pvl/ Muv	Gro/ Unc/ Rb
cuti-1						
fbxa-114						
npp-17	9.88% (9%-11%)					
ubc-12	68 %					
UPRTse						
WO4A4.5	100 %*	100%				
taf-1	100 % **					
K05C4.7	5 % (1%-9%)					
sago-2						
pkc-3	41 % (7%-81%)					
pro-1						
D2096.9	74 % *** (44%-87%)					
C27B7.7	88.8 % ** (80%-100%)					
ZK896.4	20% (5%-25%)					
srw-3						
sru-39						
nas-21						
rskn-1	53.6 % (32%-66%)					
apm-3						
tbc-11						
VY35H6BL-2						
C03B1.3						
unc-98						
zig-3						
T14G8.3						
emr-1	100 %					
skr-6						
T06E4.5						
F4719						
lip-2						
Y57G11B.5						
ceh-45						
oac-22						
T28F2.2						
dhs-6						
K10B3.6						
add-1						
coh-1						
T07H6.1						
sem-5						

Table 3. 40 candidate genes showed interaction with LEM-2: we obtained in our genome wide screen 40 genes, which when targeted by RNAi causes specific defects in the *tm1598* strain. Some of them produces Embryonic lethality (Emb; show are average percentage and range in brackets) but also post-embryonic phenotypes, such as Larval arrest (Lva), Larval lethality (Lvl), Sterility (Ste) , Sterile progeny (Stp), Protruding vulva (Pvl), Multivulva (Muv) or other defects.

* Produce a high % of Emb but in also high % of Lvl.

** Produces 100% of Emb also in wt.

*** After several experiments stops to produce the phenotype.

- **UBC-12 and LEM-2 show high synthetic lethal interaction**: for the 41 genes whose DNA causes a phenotype in the *tm1582* strain, *ubc-12* produces stronger embryonic lethality in the LEM-2 mutant than in the wt strain. This gene encodes an orthologous of yeast Ubc12p and is the conjugating enzyme (E2) in the neddylation process, using NED-8 as substrate.

Feeding RNAi experiments in LEM-2 mutant resulted in an embryonic lethality of 68%, while in the wt is 45 %, x^2 $p<0.001$ showed that this difference is statistically significant. Moreover, the effect of *ubc-12* RNAi also causes strong post-embryonic phenotypes in the *tm1582* strain, 88.3 %% of larval lethality and sterility in the few worms that reach adulthood (Figure 35).

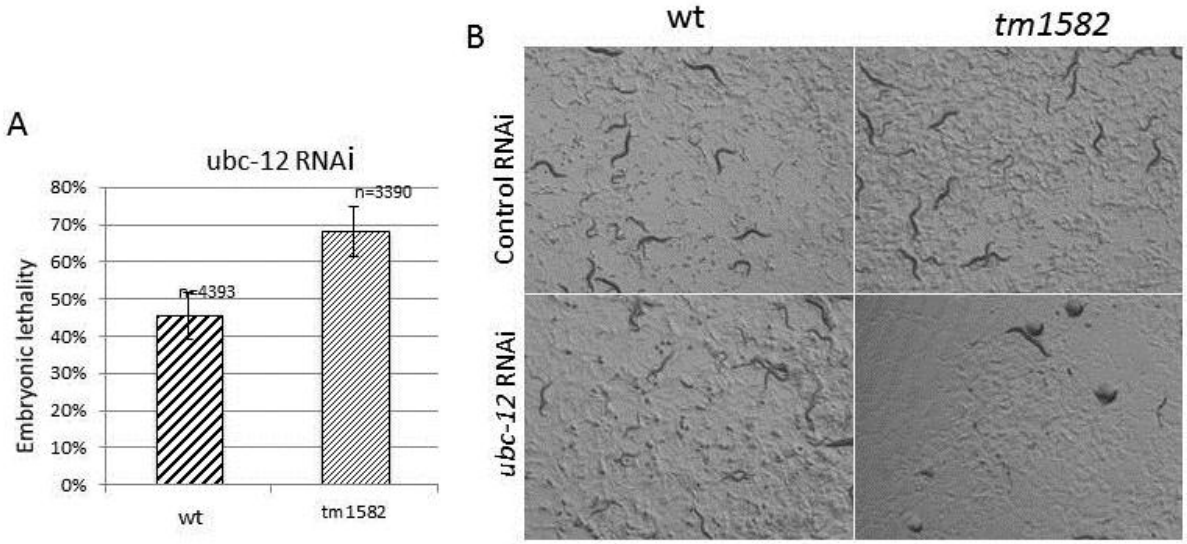

Figure 35. ubc-12 RNAi causes strong phenotypes in *lem-2* mutants: feeding worms with *ubc-12* RNAi causes a strong embryonic lethality in both strain but while this value is 45 % in the wt, it reaches 68 % in the mutant, showing a possible interaction between *ubc-12* and *lem-2*. B) To analyze post-embryonic phenotypes we took images from RNAi plates of control and *ubc-12* RNAi. In the case of the wt, the embryos depleted for UBC-12 reach adulthood and are fertile, whereas in the *lem-2* mutant the majority of embryos that hatch present larval lethality (88.3 %) and the few ones that reach adulthood are sterile. Error bars indicate the standard error of the mean.

Transgenic embryos expressing mCherry::HIS-58; GFP::α-tubulin of wt and LEM-2 mutants, fed with control and *ubc-12* RNAi, were recorded during 14h since early embryonic stage. The embryonic lethality was >90% in the mutant fed with ubc-12 RNAi and these died after 300 cell stage (Figure 36).

These results indicate that there is a relation between *lem-2* and *ubc-12* genes.

A

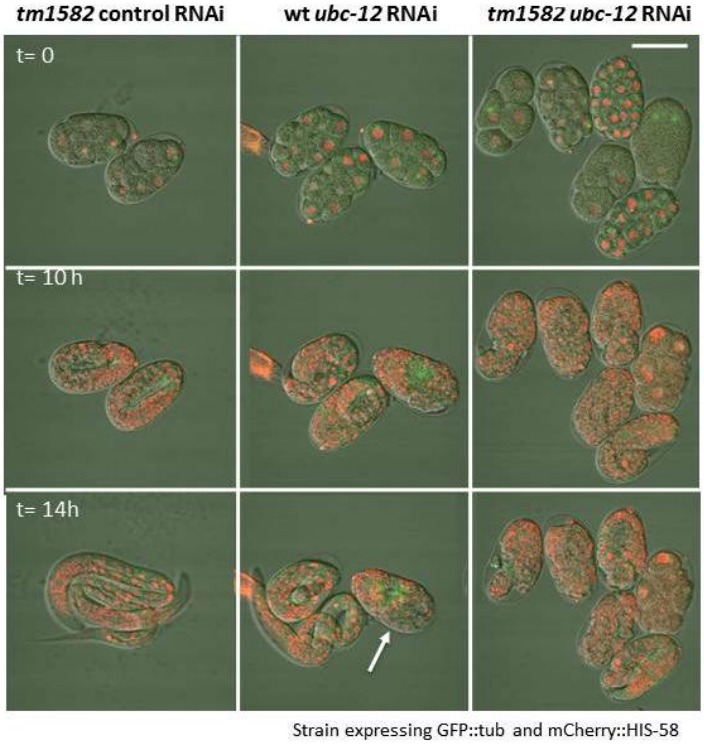

B

Strain/ RNAi	Embryos recorded	Dead embryos
wt/ *ubc-12*	9	3
tm1582/ control	5	0
tm1582/ *ubc-12*	11	10

Figure 36. *ubc-12* RNAi causes embryonic lethality after coma stage: A) the effect of ubc-12 RNAi in the development of wt and lem-2 mutant embryos was analyzed by recording of transgenic strains expressing mCherry::HIS-58 and GFP::tubulin. As control we recorded also tm1582 embryos fed with control RNAi and they develop properly, hatching after 14h (1st column). In the case of the wt fed with *ubc-12* RNAi, two out of three developed properly and hatched (2nd column, arrow point the dead embryo), whereas in tm1582 fed with *ubc-12* RNAi, all the embryos died, 5 of them after coma stage (3rd column). Scale bar 50 µm. B) Number of recorded and dead embryos recorded for each strain.- strain used BN245 and BN246.

- **<u>LEM-2 shows synthetic lethality with other neddylation pathway genes</u>**: we decided to check the relationship between LEM-2 and others genes involved in the neddylation pathway. This process is a post-translational protein modification similar to ubiquitination, in which the nedd-8 peptide is added to the substrate by an

isopeptide linkage: (Gly)76-Lys (protein). Few proteins have been reported to be neddylated such as cullins, p53, p73, some ribosomal proteins etc.

In this process are involved a precursor processing enzyme, an activating enzyme (E1, that is a complex form by ULA-1 and RFL-1) and a ligase (E3) that add the nedd-8 molecules (Rabut and Peter 2008).

To analyze if the relation between LEM-2 and UBC-12 proteins is allied to neddylation pathway, RNAi experiment against *rfl-1*, *ula-1* and *ned-8,* proteins involved in this processes, were performed.

Only the *ned-8* RNAi caused emb in both strains, but while in the wt the embryonic lethality was ~ 8%, in the LEM-2 mutant, the same phenotype was ~ 26%, x^2 $p<0.001$ showed that this difference is statistically significant, indicating that there is also a relation between *lem-2* and *ned-8* (Figure 37).

Neither *rfl-1* nor *ula-1* RNAi cause embryo*ni*c lethality or other post-embryonic phenotype either in the wt or *tm1582* strains.

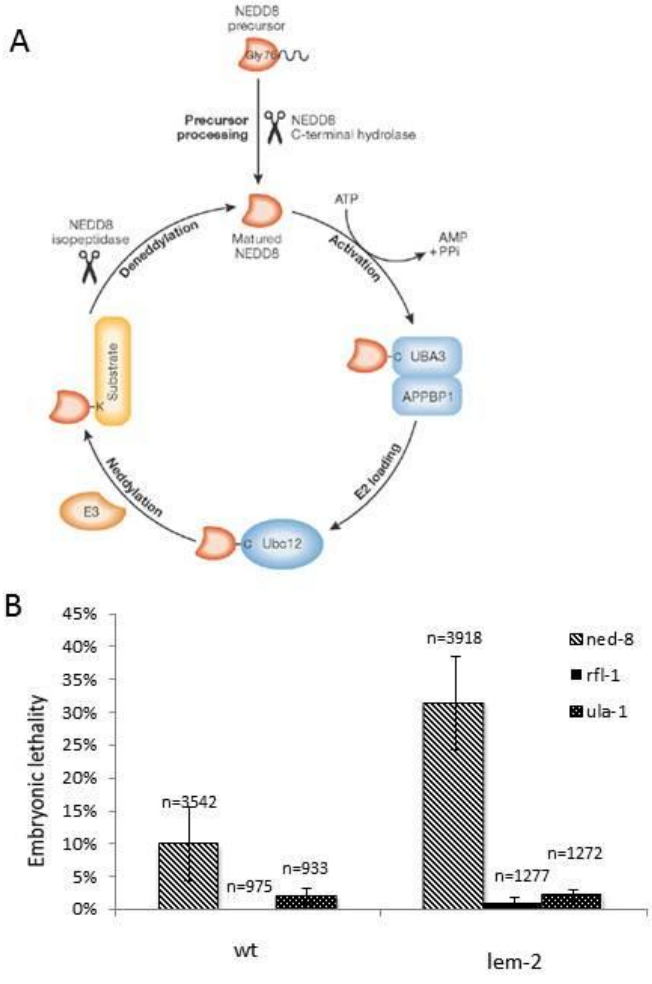

Figure 37. LEM-2 shows interactions with two proteins of the neddylation pathway: A) Scheme of the Neddylation pathway in yeast, in which act several enzymes: a C-terminal hydrolase processes precursor molecules (encoded by *ned-8* in *C. elegans)* to obtain mature NEDD8; an activating enzyme or E1 consisting of UBA-3 and APPBP1 (ULA-1 and RFL-1 in *C. elegans*); an E2 or conjugating enzyme Ubc12 (UBC-12); and an E3 ligase that loads the NEDD8 (NED-8) molecule onto the final substrate. This may imply a change in the conformation of the substrate, its activation or repression(Rabut and Peter 2008). B) RNAi feeding experiment for *ned-8*, *ula-1* and *rfl-1* performed in wt and *tm1582* strain showed that only in the cases of NED-8 there is a considerable embryonic lethal phenotype, consisting in 10% Emb in the wt and 31% Emb in *lem-2* mutant. Error bars indicate the standard error of the mean.

3. Discussion

In this work have characterized the nucleoporin NPP-16 and new features of the NET protein LEM-2. Moreover, this project had the objective to find proteins that interact with NPP-16 and/or LEM-2, was and to that end a genome wide RNAi screening, using the J. Ahringer library, was performed 54 candidate genes were obtained to show an interaction with NPP-16 or LEM-2. Between these candidates there were 14 unknown genes that could be nucleoporins or NETs proteins that have not been described yet in *C. elegans*.

3.1. RNAi technique: advantages and drawbacks

RNAi is one of the tools most used in functional studies in *C. elegans*, and the main one used in this thesis. This technique has advantages and disadvantages that have had fundamental impact on the present work.

On one hand, RNAi by feeding has allowed us to analyze almost the entire genome of *C. elegans*, and found 54 genes (Table 1) that showed interaction with NPP-16 or LEM-2. This would be difficult to perform by using direct genetic techniques or mutants for each gene, confirming that this technique is a very potent tool to perform high-throughput reverse genetic studies.

On the other hand, after obtaining the final candidates in the 2nd validation round of the screening, we could later not reproduce some of the phenotypes that we obtained in the screening. This was for instance the case of *npp-21* that showed ~90% of embryonic lethality with *npp-16(tm1596)* mutant in the 2nd validation round, or C27B7.7 that caused 88.8% of embryonic lethality in *lem-2(tm1582)*. These and other RNAi genes later gave none or very reduced phenotypes without a clear reason. To confirm if there was any condition that could affect RNAi efficiency, we did many RNAi experiments with several genes (for details see Materials and methods) testing whether different antibiotics, brand of agar, temperature, etc. affect the RNAi efficiency. Our conclusion was that, although those are very relevant parameters, such as the use of Carb instead of Amp, or to refresh the RNAi bacteria the day immediately before the preparation of RNAi plates, there is also a high intrinsic variation in RNAi efficiency for certain genes. There are cases such as *taf-1*, whose RNAi always causes

100% of embryonic lethality, while there are other such as *npp-21* whose RNAi sometimes produces embryonic lethality and sometimes not.

In the case of *npp-16* we could directly estimate RNAi efficiency. As demonstrated by Western blotting (Figure 14), the NPP-16 band was present in the wt sample with the control RNAi, but also in the wt treated with the *npp-16* RNAi, although strongly diminished. The immunofluorescence results (Figure 15) also showed that *npp-16* RNAi in wt strain produced a depletion of the mRNA that reduces the quantity of proteins but not completely. Moreover in the case of the *npp-16(tm1596)* mutant, which express a lower quantity of truncated protein, a decrease in the signal of NPP-16 between control and *npp-16* RNAi conditions was not observed. These results illustrate that the RNAi efficiency of a given gene is not always 100% constant and can oscillate.

Considering the RNAi variation, we have focused our work on the two candidates, *npp-2* and *ubc-12*, whose RNAi efficiencies were more constant and caused strong phenotypes (Emb, Lvl or Ste) in the mutant strains.

3.2. . Nup50/NPP-16 nucleoporin presents in the NPC and in the nucleoplasm

One of the main goals of this thesis was to characterize the putative nucleoporin NPP-16, which is homologous to Nup50 in mammals and considered a FG-nucleoporin that forms part of the nuclear basket in the NPC (Guan, Kehlenbach et al. 2000, Smitherman, Lee et al. 2000, Rabut, Doye et al. 2004, Kalverda, Pickersgill et al. 2010). We have shown that NPP-16 is enriched at the NE in C. elegans cells, strongly supporting the notion that NPP-16 is a nucleoporin. Firstly, we have shown that NPP-16 is expressed ubiquitously in the worm, presenting higher expression levels in germ line, and embryos (Figure 16), which is in agreement with the result observed in mouse where Nup50 displayed higher expression levels in adult testes and embryonic neural tube (Smitherman, Lee et al. 2000).(Smitherman, Lee et al. 2000).

We found that in pronuclei, NPP-16 has a uniform nuclear distribution, while this is more concentrated in the NE in a progressive manner during the embryo division (Figure 18). One cell embryos show a faint enrichment of NPP-16 in the NE, after the second division, in AB and P1 nuclei NPP-16 increases it localization in the NE, and continues increasing in 4 cell embryo stage. Although it is on 8-16 cell embryo stages

when NPP-16 is fully enriched in the NE. Cell type-specific localization was also observed by Fan and Liu (Fan, Liu et al. 1997) that found that Nup50 in rat has an intranuclear localization in premature male spermatids that change to a NE localization in the mature spermatozoa.

Regarding the localization of NPP-16 in different tissues, in this work we show that (Figures 17), in tail and intestine cells, in addition to the nucleoplasm, NPP-16 also accumulates in the NE, while in cells of the head (mainly neurons) this nucleoporin has an uniform distribution. Similar results were shown in rat cell, Nup50 localizes in the NE in liver nuclei, while in cultured NRK cells it also is abundant in intranuclear regions (Guan, Kehlenbach et al. 2000)

These results strengthen the idea of two pools of NPP-16, one that localizes in the NPC nuclear basket, and other that localizes in the nucleoplasm. Mobility assay of NPP-16::GFP (Figure 20) show that NPC-associated NPP-16 is more mobile than NPP-19 (Nup35), which is considered to be an adaptor protein (Rabut, Doye et al. 2004). NPP-16 at the NE is exchanged with a halftime of 53 sec, but when we measure this value in *npp-2*(RNAi) embryos (Figure 26), NPP-16 is exchanged six-fold faster, producing also a uniform distribution of NPP-16 along the nucleus, instead of the accumulation in the NE present in wt conditions. Knowing that NPP-2 is part of the scaffold structure of the NPC, *npp-2* RNAi most likely affects the NPC integrity. As result of this, under *npp-2* RNAi conditions, part of the NPC pool of NPP-16 would pass to the cytoplasm, showing a higher mobility and a uniform distribution, presenting some clumps or aggregates, due to the high quantity of protein in the nucleoplasm (Figure 26).

The distribution showed by NPP-16 could respond to a functional distribution. In mammals the pool of Nup50 bound to the NPC has been related to importin-α-mediated nuclear protein import (Lindsay, Plafker et al. 2002, Matsuura and Stewart 2005). In the present work we have analyzed whether the PIE-1 import pathway is affected in *npp-16(tm1596)* mutants. Measuring the PIE-1::GFP import rate in wt worms expressing this transgenic protein and treated with control or *npp-16* RNAi, indicated that the PIE-1 nuclear import pathway behaves normally under *npp-16* RNAi conditions. However, we do not discard a possible role of this nucleoporin in other

export and import pathways, as previously described in mammals (Guan, Kehlenbach et al. 2000, Makise, Mackay et al. 2012).

With respect to the nucleoplasmic pool of NPP-16, which appears increased in pronuclei stage and neurons, it function could be related with the role that has been proposed for Nup50 in Drosophila cells. In the work published by Kalverda et al. DamID experiments were used to identify the genomic regions where Nup98 and Nup50 bound. Although their work focused mainly on Nup98, authors differentiated the function of NPC-associated Nup98 from the nucleoplasmic Nup98 pool, but also show that Nup50 interact with a group of genes, related with development and cell cycle processes, stimulating their expression (Kalverda, Pickersgill et al. 2010). Based on sequence conservation, it is reasonable to speculate that *C. elegans* NPP-16 protein present in the nucleoplasm might similarly act to activate transcription. To test this, it would be relevant to combine DamID experiments with transcriptome analysis in wt and *npp-16(tm1596)* mutants to identify genes that are bound and regulated by NPP-16. For the DamID experiments, ideally one would use different *npp-16* constructs that localize exclusively to NPCs or to the nucleoplasm. However, such constructs would first need to be experimentally defined, for instance through truncation analysis.

To explain the different distribution of NPP-16 during development we propose two different hypotheses:

- Probably the pool of NPP-16 protein that localizes in the nuclear basket of NPC plays a role in mRNA export, as previously shown for other nucleoporins localized in the NPC basket, such as TPR or Nup153, or nucleoporins of the scaffold part of the NPC like Nup153 or Nup 160 (Vasu, Shah et al. 2001). Presumably, one to four cell stage embryos levels of nuclear export of mRNA is relatively low, because transcription activity is not yet very high and the embryo has a large batch of maternal proteins, and NPP-16 would stay in the nucleoplasm. In contrast, older embryos (i.e. from 16 cell stage and onwards) are characterized by higher nucleus-cytoplasmic transport rates of mRNA and other molecules. This coincides with the moment in which NPP-16 accumulates strongly at the NPC.

- Considering the possibility that, as proposed for Nup50, NPP-16 has a role in the regulation of gene expression, the high NPP-16 nucleoplasmic pool present during

pronuclei and very early embryos stages could be related to the fact that from pronuclei to eight cell embryos, almost 1.700 genes show changes in their expression (up-regulation or down-regulation) (Baugh, Hill et al. 2003).

3.2.1. NPP-16 is not essential in C. elegans

In mouse, Nup50 is essential for normal development of the neural tube, and presumably as a consequence, Nup50 mutant embryos die during late embryogenesis. Remarkably, other tissues, such as muscles, develop normally in the absence of Nup50, which led to the hypothesis of the existence of another (still unknown) protein that plays the same role (Smitherman, Lee et al. 2000).

We have seen that the absence of full-length NPP-16 in *C. elegans* does not have any concrete phenotype. One possibility is that there is another protein playing a redundant role,. Another possibility would be that this protein is dispensable in *C. elegans* but not in more complex organism like mouse. Finally, the reduced levels of truncated NPP-16 protein produced in *npp-16(tm1596)* mutants could potentially suffice to viability. We consider this unlikely because of both truncated isoforms lack most FG repeats. With the recent discovery of CRISPR-mediated gene disruption (Friedland, Tzur et al. 2013), we envision that this could be tested experimentally through the generation of a genetic null mutant.

3.2.2. . NPP-16 related with cell cycle check-point

It has been shown In *C. elegans* that *npp-16* plays a role in cell cycle regulation under stress condition, such as oxygen deprivation (Hajeri, Little et al. 2010). In anoxia stress conditions, CDK-1 is normally inactivated until normal air conditions are restored. In contrast, in a *npp-16* mutant strain, CDK-1 remains active, and the cell cycle is not arrested. In mammals it has been shown that Nup50 interacts with $p27^{kip1}$, a CDK/cyclin inhibitor (Smitherman, Lee et al. 2000) and that HeLa cells treated with Nup50 RNAi activate the Aurora B-mediated abscission checkpoint during cytokinesis (Mackay, Makise et al. 2010). The function of this checkpoint is to ensure that the daughter cells are generated only when chromosomes are segregated and enclosed in newly formed nuclei. Hence, CDK-1, $p27^{kip1}$ and Aurora-B, are proteins related to

checkpoints during the cell cycle, and they seem to interact with NPP-16 or Nup50. Related with this, one of the candidates resulting from our screen with *npp-16(tm1596)* was *cye-1*, which encodes the sole *C. elegans* E-type cyclin. Cyclin E is required for progression through the mitotic cell cycle during embryonic, larval, and germ line development (Aleem, Kiyokawa et al. 2005) and interacts with $p27^{kip1}$. Considering these observations, we propose that NPP-16 could be related with activation of several checkpoints but future experiments are required to determine the exact mechanisms.

2.3. NPP-16 and NPP-2

Between the 13 genes obtained with the *tm1596* mutant allele in our genome wide screen (Table 2), we chose *npp-2*, because when depleted by RNAi in the *npp-16(tm1596)*, it produces 96% embryonic lethality, while in the wt strain this phenotype was only 4% (Figure 22). The tm1596 *npp-2*(RNAi) embryos stop their development 4-5 h after fertilization with ~200 cells, while the few wt embryos that die as result of *npp-2* RNAi reach an older stage (Figure 25). Animals homozygous for the mutant allele *npp-2(tm2199)* arrest as young larvae, implying that this protein is essential for proper early development. This suggests that RNAi-mediated depletion of NPP-2 is relatively inefficient. However, the low *npp-2* RNAi efficiency has allowed us to uncover a novel interaction between these two nucleoporins.

npp-2 RNAi in wt strains affects the localization of nucleoporins, including NPP-7, NPP-16 and other FG nucleoporins recognized by mAb414 antibodies, resulting in a dashed NE, but still complete (Figures 23 and 26). In contrast, other NE proteins such as EMR-1, conserves it localization when NPP-2 is depleted (Figure 23). In the case of LMN-1, under *npp-2* RNAi conditions, it conserves it proper localization, but also aggregates around the centrosomes (Figure 24). The effects on other nucleoporins are not surprising, considering that our laboratory has described that *npp-2* plays a role in the maintenance of the NPC structure integrity (Rodenas, Gonzalez-Aguilera et al. 2012). However, the presence of LMN-1 assemblies around centrosome was unexpected. Multimerization of LMN-1 is normally restricted to assembly of the nuclear lamina. Disassembly of the nuclear lamina at mitotic entry requires its phosphorylation, whereas the process is reverted in telophase and interphase. We

speculate that proteins regulating LMN-1 phophorylation and hence multimerization may be mislocalized in *npp-2*(RNAi) embryos as consequence of NPC defects.

A main observation in this thesis is that depletion of NPP-2 in *npp-16* mutants produces dramatic defects in the early embryo (Figure 22) starting by an abnormal behavior of the two pronuclei that do not juxtapose correctly (data not shown), problems during the alignment and segregation of chromosomes, and a delay in the P1 division. The NE is also strongly affected in *npp-16* mutants under *npp-2* RNAi conditions, showing not only a dashed aspect, but also problems in DNA segregation, which eventually causes the formation of enucleated cells (Figure 23). The localization of other NE proteins such as EMR-1 is not affected, although the nuclei have an oval shape during their separation, presumably reflecting the DNA segregation problems (Figure 23). As observed in the wt strain treated with *npp-2* RNAi, lamin also localizes properly in *tm1596*, although with aberrant accumulations around the centrosomes (Figure 24).

Something similar, in the sense of the embryonic lethality, is observed with our control, NPP-5 (Nup107 in vertebrates) that forms part of the same complex as NPP-2. NPP-5 is not essential for the localization of most other proteins of the Nup107 complex, but *npp-5* null mutants show ~80% of larval lethality (Rodenas, Gonzalez-Aguilera et al. 2012). In contrast, when we deplete *npp-5* by RNAi in the wt strain, there is not any embryonic lethality or post-embryonic phenotype, which could mean that the efficiency of the RNAi depletion is not 100%. However, *npp-5* RNAi in *npp-16(tm1596)* mutant produces 97% embryonic lethality (Figure 16) implying a relation between these two nucleoporins.

It is known (Galy, Mattaj et al. 2003) that embryos that do not express NPP-2 are hypersensitive to depletion of other nucleoporins by RNAi. *npp-2* RNAi can affect partially the NPC structure but in a degree that the embryo can tolerate, and depletion of other nucleoporins of the same NPC subcomplex, such as NPP-5 or NPP-15, produces a collapse of the NPC structure and results in embryonic death.

However the interaction that we show here is different in the sense that NPP-16/Nup50 is not a member of the Nup107 complex, but rather localizes in the nuclear basket of the NPC. Morover until now NPP-16 has been related with nuclear transport

and control of gene expression and in mammals has been reported it relation with other nuclear basket protein such as Nup153, but not with structural nucleoporins such as NPP-2 or NPP-5 (Makise, Mackay et al. 2012)

The fact that the depletion of *npp-2* by RNAi in *tm1596* mutant produces dramatic effect in NE structure and DNA segregation could mean that NPP-16 has a not-yet described structural role that helps to maintain the NPC organization even when the structural Nup107 complex is inhibited by RNAi. Regarding the DNA segregation problem, it has been shown that, in anoxia conditions, the chromosomes in *npp-16* mutants, don´t bind to the NE waiting for normoxia conditions, remaining at the nucleoplasm (reference). In this case CDK-1 is also affected which could mean that NPP-16 has a relation with this check point protein that regulates the binding of the chromosome to the NE in stress situations, or that the NPC pool of NPP-16 plays a role in the binding of the DNA in stress conditions.

Finally, knowing that out of the 30 nucleoporins described in mammals and in yeast, only 23 has been described in *C. elegans*, a possibility exists, that any of the three unknown genes obtained from the screening with *tm1596* (Table 2) would be any of these "missing" nucleoporins. In fact the Nup107 complex is formed by 9 proteins in vertebrates while in *C. elegans* only 8 have been described, lacking the Nup37 protein. The fact that two nucleoporins, NPP-2 and NPP-21 were identified in the screening strengthens this hypothesis.

1. LEM-2 protein of the INM

The INM protein LEM-2 localizes in the NE and in a lesser manner in the ER, displaying a similar localization as EMR-1, another INM protein; however we demonstrate that the recruitment of LEM-2 to the NE occurs earlier than the recruitment of EMR-1. Worms express both proteins in all cell types but LEM-2 is concretely enriched in the germ line and intestine, relative to EMR-1 (Figure 27).

1.1. LEM-2/EMR-1 relation

As shown previously, LEM-2 and EMR-1 have overlapping functions: loss of either of them individually does not affect development or viability. Even one copy of EMR-1

is enough in *C. elegans* to allow the viability of the hypomorphics strain (*lem-2*$^{-/-}$ *emr-1*$^{-/+}$) whereas the double mutant is completely unviable (Liu, Lee et al. 2003). These two LEM-domain proteins have overlapping functions related to chromatin organization, cell proliferation, muscle differentiation and extracellular signaling (Huber, Guan et al. 2009, Bank, Ben-Harush et al. 2011, Barkan, Zahand et al. 2012). We have confirmed the embryonic lethal phenotype that *tm1582* displays in *emr-1* RNAi conditions and have demonstrated that these embryos show severe defects such as incomplete NE assembly and DNA missegregation. While previous work has reported phenotypes in embryos that have undergone several mitotic divisions (and hence may display the sum of primary and secondary effects) our experiments have revealed dramatic defects already after the first mitotic division (Figure 28).

We found that depletion of LEM-2 not only produces defects in the nuclear shape, resulting in lower nuclear circularity in the mutant, but additionally, presents nuclear invaginations containing EMR-1 (Figure 30). These results provide evidence that the relations between both proteins also include their location

The behavior of EMR-1 is also affected by LEM-2. Photoconversion assays with EMR-1::Dendra2 revealed a faster turnover of EMR-1 in *lem-2(tm1582)* neurons, hypodermal and muscle cells, whose red/green ratio decreases faster than in wt animals (Figure 29). In contrast, FRAP analysis performed in EMR-1::mCherry-expressing embryos showed that the absence of LEM-2 does not affect the short-term mobility of EMR-1 in the NE. It should be noted that although both assays address EMR-1 behavior in the absence of LEM-2, the two experiments were performed in stages very different and while Dendra experiment study the EMR-1 turnover during hours, the FRAP analysis study the mobility of this protein during few minutes.

1.2. The absence of LEM-2 affects nuclear separation during AB division and causes aberrant centrosomes behavior.

While working with *tm1582* strain we were surprised to realize that the absence of LEM-2 caused a defect in the nuclear separation during AB division (Figure 31, 32, 33). This phenotype consists of an abnormal movement of daughter nuclei, which initially

separates like in wt embryos, but briefly reverses the separation and finally separates (Figure 31 and 32). This phenotype has been observed in three different transgenic strains (EMR-1::mCherry, GFP::tub; mCherry::HIS-58 and GFP::γ-tubulin; GFP::HIS), thus excluding the possibility that this behavior was an artifact caused by the genetic background of a particular transgenic strain.

During mitosis, separation of the chromosome masses in anaphase and of the reforming nuclei in telophase relies on microtubule-dependent transport. Cortical pulling forces play a major role in movement of centrosomes away from each other, whereas the distance between chromosomes and centrosomes is relatively constant during anaphase. When we investigated centrosomes and chromatin in the *lem-2(tm1582)* strain we found also an aberrant behavior of the centrosomes. In *lem-2* mutants, one of the two centrosomes of each AB daughter cell detaches in late telophase from the NE and moves transiently to the cell membrane before positioning again close the nucleus when it becomes centered in the interphase cell.. In contrast, in the wt strain, both centrosomes of the AB daughter cells remain in close proximity of the NE in the majority of embryos. This NE centrosome detachment phenotype is also observed frequently in the EMS cell resulting from P1 division. In a similar manner, it has been shown that the absence of emerin (EMR-1) affects the centrosome attachment to the NE via microtubule association (Salpingidou, Smertenko et al. 2007). In normal human fibroblasts, the centrosomes are positioned next to the NE, whereas in the *emerin* mutant fibroblasts the centrosomes localize away from the NE. Salpingidou et al. also showed that probably neither SUN nor nesprin proteins are involved in the centrosome detachment, although they form part of the LINC complexes, which links the actin and intermediate filament cytoskeletons to the NE in mammalian cells (Crisp, Liu et al. 2006).

Considering our results, we propose that the detachment of a centrosome from the NE may reduce the total pulling force separating the two reforming nuclei and thereby contribute to the observed nuclear separation phenotype. Analysis of the distance between the two centrosomes most proximal to the NE of the two daughter cells, relative to anaphase onset, demonstrated that they are equally delayed in their separation (Figure 32).

Concomitantly with the NE-centrosome detachment we observed a 1.7-3.3 fold increased presence of central spindle microtubules in the *lem-2(tm1582)* mutant in telophase and cytokinesis (Figures 33). It has been observed that mutation of ZEN-4, which is involved in stabilization of central spindle microtubules, causes increased separation of centrosomes in anaphase (Canman, Lewellyn et al. 2008). Thus, it is plausible that the abnormal density of central spindle microtubules in *lem-2* mutants contributes to the reduced separation of both centrosomes and nuclei. To test this directly, we plan to evaluate if the depletion of ZEN-4 in *lem-2* mutants suppresses the *lem-2* nuclear separation phenotype. In addition, it will be important to test for the presence of central spindle proteins, such as ZEN-4 and CYK-4.

3.3. AIR-2::GFP protein accumulates to the spindle midzone in *lem-2(tm1582)*

Time lapse images of strains expressing AIR-2::GFP (Aurora B) and, its fluorescence intensity measurements, in wt and *lem-2* mutant strains showed that, in the absence of LEM-2, the fluoresce intensity of this protein in the spindle midzone is twice the intensity observed in wt (Figure 34). Aurora B is part of the Chromosomal Passenger Complex, which carries out checkpoint functions both at kinetochores to regulate anaphase onset and at the central spindle to influence cytokinesis (Agromayor and Martin-Serrano 2013). During cytokinesis, Aurora B is believed to phosphorylate different kind of filaments at the cleavage furrow, thereby delaying abscission until chromosomes have been separated away from the cleavage plane. However, we have not observed a higher incidence of lagging chromosomes in *lem-2* embryos, which suggests that the increased GFP::AIR-2 recruitment in these embryos is not due to a response to chromosome missegregation. It was recently reported that depletion of Nup50 (see above) or Nup153 causes a delay in cell abscission mediated by the Aurora B checkpoint, even in the absence of chromosome bridges (Mackay, Makise et al. 2010). NPC assembly is not visibly affected in *lem-2* mutants judged from immunostaining with MEL-28 or mAb414 (Figure 28), but we have not yet addressed to localization of NPP-7 (Nup153) or NPP-16. Related with this, one of the candidates resulted from ours screening with the *lem-2(1582)* mutant was the nucleoporin NPP-

17, whose RNAi causes 9.8 % of embryonic lethality, sterility and sterile progeny (Table 3).

3.2.3. LEM-2 related with the neddylation pathway

Among the 41 genes that showed phenotypes in the *tm1582* strain, we focused our work on *ubc-12* because it produces a strong and constant embryonic and post-embryonic phenotype. UBC-12 is the conjugating enzyme (E2) in the neddylation process. We show that *lem-2* mutants presented 68% embryonic lethality, whereas in the wt strain this RNAi produces 45% of embryonic lethality. Moreover the *tm1582 ubc-12(RNAi)* embryos that hatch showed 88.3% of larval lethality, and the few ones that reached adulthood were sterile. In contrast wt embryos under *ubc-12* RNAi conditions did not show any post-embryonic phenotype, showing a normal development (Figure 35). The mutant dead embryos, under *ubc-12* RNAi conditions, stopped their development ~10 h after fertilization, after they reached the coma stage (Figure 36).

Neddylation is a post-translational protein modification closely related with ubiquitination, although while ubiquitination usually targets proteins for degradation by the proteasome, neddylation can affect the subcellular localization of target proteins, their conformation and their association with other proteins. This pathway, which is highly conserved among eukaryotes and essential for many organism, consists in the addition of the molecule NEDD8 (NED-8 in *C. elegans*) to specific substrates. Several proteins are implied in this processes (Figure 37): a C-terminal hydrolase processes precursor molecules to obtain mature NEDD8; an activating enzyme or E1 consisting of UBA-3 and APPBP1 (ULA-1 and RFL-1 in *C. elegans*); an E2 or conjugating enzyme Ubc12 (UBC-12); and an E3 ligase that loads the NEDD8 (NED-8) molecule onto the final substrate (Rabut and Peter 2008).

To analyze if the interaction identified between *lem-2* and *ubc-12* implies a specific interaction of LEM-2 with this post-translational protein modification pathway (Figure 37), several related proteins (ULA-1, RFL-1 and NED-8) were depleted by RNAi in the *lem-2* mutant strain. Only *ned-8* RNAi cause embryonic lethality in both strains while in

the wt embryonic lethality was ~8%, in the LEM-2 mutant, the same phenotype was ~26%, indicating that there is also a relation between LEM-2 and NED-8 (Fig 41). The lack of a phenotype in *ula-1* and *rfl-1* RNAi experiments could possibly be due to residual protein levels.

The neddylation pathway targets many different substrates such as p73, p53, several ribosomal protein and cullins proteins (Rabut and Peter 2008). Cullin proteins are part of the E3 ubiquitin ligases together with F-box proteins, Skp-1 and RBX-1 (SCF complex), targeting different kinds of molecules such as cell-cycle regulators cyclin D, p73 or p130, cyclin E, c-myc oncoprotein or Notch (Tanaka, Nakatani et al. 2012) to promote their degradation in the proteasome and maintain cellular homeostasis. Many cancer cells are related with deregulation of these molecules, therefore regulators of neddylation and the components of SCF complexes are potential candidates in therapeutic strategies (Tanaka, Nakatani et al. 2012). Interestingly, another candidate identified in our screening with the *lem-2* mutant was *fbxa-114*, which encodes a F-box A protein that is considered part of the SCF complex by binding Skp-1 (Kipreos and Pagano 2000) *fbxa-114* RNAi produces Ste and Stp phenotypes specifically in the *lem-2* mutant, which potentially reflects the novel interaction between *lem-2* and the neddylation pathway identified in this thesis.

It has been shown that the neddylation pathway is essential for negative regulation of contractile activity, throughout the cortex of *C. elegans* early embryonic cells. Mutations or depletion by RNAi of the different proteins that form this pathway causes penetrant embryonic lethality phenotypes with nuclear misspositioning and formation of ectopic cleavage furrows (Bowerman 2001, Kurz, Pintard et al. 2002). Moreover, it has been shown in *rfl-1(or198)* that chromosomes separate slower during anaphase of one cell embryos and a smaller inter-centrosomal distance compared to the wt (Kurz, Pintard et al. 2002). These results resemble the phenotype that we observed in *lem-2(tm1582)* respect to the nuclear separation defect. We propose the possibility of the existence of two pathways that play a role in the separation of the nuclei in anaphase, one related with LEM-2 and the other regulated by neddylation pathway. Defects in any of the two pathways produce defects that the embryo can tolerate, but problems in both mechanisms produce embryonic lethality. An interesting question to address in

future studies is at which step the two pathways converge? It is conceivable that the phenotypes are related with neddylation of specific NE proteins interacting with *lem-2*. Another, not mutually exclusive possibility is that the effects of *lem-2* on centrosome behavior act through neddylated microtubule or centrosome-associated proteins.

4. Conclusions

Conclusions

1. A genome-wide RNAi screen using the Ahringer library in wt, *npp-16(tm1596)* and *lem-2(tm1582)* resulted in 13 genes that interact with *npp-16* and 40 genes that interact with *lem-2*.

2. RNAi efficiency varies a lot among genes. However, several parameters are critical that influence strength and reproducibility, e.g. the use of Carbecinillin instead of Ampicillin, refresh the RNAi bacteria strain the day before preparation of RNAi plates and dry them completely before adding the worms.

3. NPP-16 is ubiquitously expressed in *C. elegans* with highest level in the germ line. Its relative distribution between the NE and the nucleoplasm differs between tissues. In early embryos NPP-16 is mainly localized in the nucleoplasm and accumulates in the NE later in development.

4. *npp-16(tm1596)* allele has a 382 bp deletion , RT-PCR and immunofluorescence results indicate that it produces a low quantity of truncated protein which localizes properly.

5. NPP-16 is more dynamic than nucleoporin NPP-19, showing a faster recovering after photo bleaching.

6. NPP-16 is not essential in *C. elegans*.

7. NPP-16 could be related with activation of several checkpoints.

8. *npp-2* was identified as a strong genetic interaction partner of *npp-16(tm1596)*. Depletion of NPP-2 causes ~5% embryonic lethality the wt strain but almost complete lethality in the *npp-16* mutant.

9. The absence of both nucleoporins causes strong defect in DNA segregation and in NE structure. The absence of *npp-2* in both wt and *npp-16* mutants also produces accumulation of lamin around the centrosomes.

10. Similarly to EMR-1, LEM-2 localizes in the NE and to lesser extent in the ER during interphase but is recruited earlier during NE reformation.

11. Absence of LEM-2 does not affect EMR-1 mobility but affect its turnover rate in several tissues.

12. Depletion of LEM-2 affects nuclear shape, showing a decrease in circularity and produce invaginations structures were EMR-1::mCherry localized.

13. *lem-2(tm1582)* animals show defects in nuclear separation process and in centrosomes behavior during early embryonic divisions.

14. AIR-2::GFP present in the spindle midzone, in *lem-2(tm1582)* animals shows twice the intensity observed in the wt.

15. *lem-2(tm1582)* shows synthetic lethality with *ubc-12* and *ned-8*, genes implies in protein neddylation, indicating a role of LEM-2 in this post-translational pathway. Other of the final candidates obtain with the tm1582 mutant, *fbxa114* is a substrate of the neddylation pathway.

4. Materials and Methods

4.1. Nematode strains

In this thesis we have used the next nematode strain, to perform the different experiments.

Strain	Description/ Method/ Reference	Genotype
N2	Wild type Bristol strain.	
BN11	Homozygous *npp-16(tm1596)*. Made by backcrossing "raw" *npp-16(tm1596)* from JP KO with wt N2 five times.	*npp-16(tm1596)* III
BN14	Homozygous expression of GFP/LAP-tagged Nup35/NPP-19 and mCherry HisH2B. (Rodenas, Klerkx et al. 2009)	*unc-119*(ed3) III; bqIs07[*unc-119*(+); Ppie-1::LAP::*npp-19*] ?; ltIs37[Ppie-1::mCherry::his-58; *unc-119* (+)] IV
BN16	Homozygous expression of YFP-**lamin**/LMN-1 and Cherry His-H2B.(Rodenas, Klerkx et al. 2009)	*unc-119*(ed3) III; qaIs3502[*unc-119*(+) Ppie-1::YFP::*lmn-1*] ?; ltIs37[P*pie-1*::mCherry::his-58; *unc-119* (+)] IV
BN19	Homozygous *lem-2(tm1582)*. Made by outcrossing *lem-2(tm1582)* from Japan with wt N2 seven times.	*lem-2(tm1582)* II
BN20	Homozygous *emr-1(gk119)*. Made by backcrossing XA3524 with wt N2 four times.	*emr-1(gk119)* I
BN28	Homozygous Nup107 deletion; out-crossed with N2 six times.	*npp-5(ok1966)* II
BN46	Homozygous npp-19(tm2886) II expressing GFP/LAP-tagged Nup35/NPP-19. Made by crossing BN14 and BN38. Cherry H2B lost.	npp-19(tm2886) II; unc-119(ed3) or unc-119(+) III; bqIs07[unc-119(+); Ppie-1::LAP::npp-19]
BN78	Homozygous npp-19(tm2886), Ppie-1::gfp::lem-2 and Ppie-1::mCherry::H2B. Made by crossing BN38 and OD83.	npp-19(tm2886) II; Ppie-1::gfp::lem-2; ltIs37[Ppie-1::mCherry::his-58; unc-119 (+)] IV
BN142	Integrated P*emr-1*::*emr-1*::mCherry. Made by MosSCI injection of EG4322 w plasmid #934 pBN20 (+plasmids #881 pJL44 + #868 + #879 + #885). Outcrossed w N2 twice. Do not carry Mos. May carry unc-119(ed3) III	bqSi142[pBN20(unc-119(+) P*emr-1*::*emr-1*::mCherry)] II

BN160	Homozygous *lem-2(tm1582)* with integrated P*emr-1*::*emr-1*::mCherry. Made by crossing BN19 w BN142 (crossing 5x to BN19 to obtain recombination).	*lem-2(tm1582)* bqSi142[pBN20(*unc-119*(+) P*emr-1*::*emr-1*::mCherry)] II
BN177	Integrated emerin::Dendra2. Made by MosSCI injection of EG4322 with plasmid #1001 (+ plasmids #889 + #868 + #879 + #885).	*bqSi177[pBN43(unc-119(+) Pemr-1::emr-1::dendra2)] II*
BN181	Integrated P*npp-16*::gfp::*npp-16* with endogenous 3´UTR. Made by MosSCI injection of EG4322 with plasmid #1057 (+ plasmids #889 + #868 + #879 + #885). Outcrossed w N2 twice. Do not carry Mos.	bqSi181[p1057(*unc-119*(+) P*npp-16*::gfp::*npp-16*)] II
BN190	Homozygous *lem-2(tm1582)* and integrated *emerin*::Dendra2. Made by crossing BN19 with BN177.	*lem-2(tm1582)* bqSi177[pBN43(unc-119(+) P*emr-1*::*emr-1*::*dendra2*)] II
BN194	Integrated P*npp-2*::mCherry::*npp-2*. Made by MosSCI injection of EG4322 with plasmid #956 (+plasmids #889+ #1005+ #1008+ #973). Outcrossed w N2 twice. Does not carry the transposon.	bqSi189[pBN32(unc-119(+) Pn*pp-2*::mCherry::n*pp2*)] II
BN204	Balanced *npp-5(tm3039)* deletion strain expressing GFP-*tbb-2*, GFP-*tba-2* and mCherry-his-58. Made by crossing BN107 with OD57.	*npp-5(tm3039)*/mIn1[mIs14 dpy-10(e128)] II; ltIs37[Ppie-1::mCherry::his-58; *unc-119* (+)] IV; ojIs1[unc-119(+) P*pie-1*::GFP::*tbb-2*] V (?)
BN217	Integrated Pemr-1::mCherry::tbb-2::emr-1 3'UTR. Made by MosSCI injection of EG4322 with plasmid #1115 (+plasmids #889+ #1005+ #1008+ #973).	bqSi217[pBN92(unc-119(+) Pemr-1::mCherry::tbb-2)] II
BN227	Integrated Plem-2::lem-2::gfp and Pemr-1::emr-1::mcherry::emr-1 3'UTR. Made by crossing BN210 and BN225.	bqSi210[pBN21(unc-119(+) Plem-2::lem-2::gfp)] II; bqSi225[pBN34(unc-119(+) Pemr-1::emr-1::mcherry)] IV
BN230	Homozygous *npp-16(tm1596)* and P*npp-2*::*npp-2*::mCherry::*npp-2* 3´UTR. Made by crossing BN194 and BN11	bqSi217[pBN92(unc-119(+) P*emr-1*::mCherry::*tbb-2*)] II
BN231	Homozygous *npp-16(tm1596)* and P*emr-1*::*emr-1*::mcherry:emr-1 3´UTR. Made by crossing BN142 and BN11	P*emr-1*::emr-1::mcherry::*emr-1* 3'UTR
BN245	Homozygous strain expressing GFP-*tub* and mCherry-His-58. Made by crossing BN204 with N2. Carries GFP-*tba-2* and/or GFP-*tbb-2*	ltIs37[P*pie-1*::mCherry::his-58; *unc-119* (+)] IV; ojIs1[unc-119(+) P*pie-1*::GFP::*tbb-2*] V (?) and/or ltIs24[pAZ132; *pie-1*/GFP::*tba-2* + *unc-119*(+)] ?

BN246	Homozygous *lem-2 (tm1582)* strain expressing GFP-*tub* and mCherry-His-58. Made by crossing BN204 with BN19. Carries GFP-*tba-2* and/or GFP-*tbb-2*.	*lem-2(tm1582)* II; ltIs37[P*pie-1*::mCherry::*his-58*; *unc-119* (+)] IV; ojIs1[unc-119(+) Ppie-1::GFP::tbb-2] V (?) and/or ltIs24[pAZ132; *pie-1*/GFP::*tba-2* + *unc-119*(+)] ?.
BN247	Homozygous *npp-16(tm1596)* strain expressing GFP-tub and mCherry-His-58. Made by crossing BN204 with BN11. Carries GFP-*tba-2* and/or GFP-*tbb-2.*	*npp-16(tm1596)* III; ltIs37[P*pie-1::*mCherry::*his-58*; *unc-119* (+)] IV; ojIs1[unc-119(+) P*pie-1*::GFP::tbb-2] V (?) and/or ltIs24[pAZ132; *pie-1*/GFP::*tba-2* + unc-119(+)])?
BN279	*lem-2* mutant GFP-g-*tubuli*n (most likely from pie-1 promoter) + GFP-HisH2B (from *pie-1*) . Made by crossed BN19 males w TH30 hermaphrodites	*lem-2(tm1582)* II; *unc-119*(ed3) III; ddIs6[tbg-1::GFP + *unc-119*(+)]; ruIs32[pie-1::GFP::H2B + *unc-119*(+)].
BN280	GFP-g-tubulin (most likely from pie-1 promoter. Made by crossed N2 males w BN279 hermaphrodites	*unc-119*(ed3) III; *ddIs6*[tbg-1::GFP + unc-119(+)
BN281	*lem-2* mutant GFP-g-*tubulin* (most likely from pie-1 promoter). Made by crossed BN19 males w BN279 hermaphrodites	*lem-2(tm1582)* II; *unc-119*(ed3) III; ddIs6[tbg-1::GFP + *unc-119*(+)
BN289	GFP-g-tubulin; Pemr-1::mCherry::tbb-2::emr-1 3'UTR. Made by cressed BN280 with BN217	
BN290	Homozygous lem-2(tm1582) GFP-g-tubulin; Pemr-1::mCherry::tbb-2::emr-1 3'UTR. Made by cressed BN281 with BN217	
BN300	Homozygous *lem-2(tm1582)* GFP::AIR-2, integrated, relative bright expression. Made by crossed BN19 males with OD27 hermaphrodites.	*lem-2(tm1582)* II, *unc-119*(ed3) III; ltIs14[pASM05: *pie-1*::GFP-TEV-STag::air-2 + *unc-119*(+)] IV.
OD27	GFP::AIR-2, integrated, relative bright expression.(Audhya, Hyndman et al. 2005)	*unc-119*(ed3) III; ltIs14[pASM05: *pie-1*::GFP-TEV-STag::*air-2* + *unc-119*(+)] IV.
OD83	GFP::LEM-2; mCherry::HIS-58 / (Audhya, Hyndman et al. 2005)	ltIs37 [pAA64; pie-1::mCherry::HIS-58 + unc-119(+)] IV. qaIs3507 [pie-1::GFP::LEM-2 + unc-119(+)].
TH30	GFP-g-*tubulin* (most likely from pie-1 promoter) + GFP-HisH2B (from pie-1). Quintin et al EMBO Rep, 2003, "The mbk-2 kinase…"	unc-119(ed3) III; ddIs6[tbg-1::GFP + unc-119(+)]; ruIs32[pie-1::GFP::H2B + unc-119(+)].

XA3524	Homozygous Δ*emr-1/*GFP-MAN-1. Generated by crossing VC237 emr-1(gk119) with N2 males once and then with XA3507 three times.	*emr-1(gk119)* I; qaIs3507[unc-119(+) *pie-1*::gfp::*lem-2*
XA3524	Homozyous Δemr-1/GFP-MAN-1. Generated by crossing VC237 emr-1(gk119) with N2 males once and then with XA3507 three times.	emr-1(gk119) I; qaIs3507[unc-119(+) pie-1::gfp::lem-2] III

Table 4. Nematode strains used in this study.

4.2. Plasmid, RNAi and primers.

Construction	Vector	Description
# 338	L4440	*emr-1* cDNA fragment full length.
# 424	L4440	*lem-2* 682 bp gDNA fragment (Galy et al, MBoC, 2003)..
# 651	L4440	*npp-16* 512 bp cDNA fragment (Galy et al, MBoC, 2003).
#365	L4440	Npp-5 760 bp cDNA fragment (Galy et al, MBoC, 2003).
# 952	pCR II Blunt	*npp-16* ORF gDNA amplified with B274+B275 from gDNA, inserted into pCRII Blunt.
# 963	pCR II Blunt	*npp-16* promoter amplified w B276+B277, inserted into pCRII.
#964	pCR II Blunt	*npp-16* ORF+3'UTR amplified w B278+B279, inserted into pCRII.
# 965	pCR II Blunt	BsrGI site in vector backbone (#964) destroyed by Klenow fill-in.
# 966	pCR II Blunt	*npp-16* gene with unique BsrGI site after start codon. KpnI/BsrGI promoter fragment from #963 inserted into KpnI/BsrGI of #965
# 967	pBN28_hsp16.41 _gfp_npp-16_MSCI_II	XmaI/SpeI fragment from #952 inserted into NgoMIV/NheI of pBN16.
# 1055	pCRII(+)_npp-16_gene_GFP	Acc65I GFP fragment from #911 inserted into BsrGI of #966.
# 1057	pBN55_Pnpp-16_gfp_npp-16_MSCI_II	SpeI/NotI fragment from pCRII_*npp-16*_gfp #1055 inserted into SpeI/NotI of pBN8.
# 1124ah	pQE32	*npp-16* cDNA fragment amplified w B274+B382, cut XmaI/PstI, inserted into pQE32 XmaI/PstI.
#815	pGEX-GST His	Expression vector with N-term GST and C-term 6*his.
# 1125	pGEX-GST-npp-16frag_Klenow	BamHI/HindIII fragment from #1124ah pQE-32_npp-16_frag_clones_5_8 inserted into BamHI/HindIII of pGEX-GST. Reading frame corrected by BamHI->Klenow fill-in.

# 889	pJL43.1	Pglh-2::Mos1. Germ line expressed Mos1 transposase
# 885	pCFJ104	Pmyo-3::mCherry. Body wall muscle red fluorescence
# 879	pCFJ90	Pmyo2::mCherry. Pharyngeal muscle red fluorescence
# 868	PBN1	Plmn-1::mCherry::his-58::pie-1 3'UTR

Table 5. Constructions used in this thesis.

Apart of the controls RNAi construction, we used the J. Ahringer library to obtain the RNAi bacteria for the different genes.

Primmer	Description	Enzyme	Sequence
B022	M13 -29	EcoRI	CAGGAAACAGCTATGACC
B023	M13 -21	BglII/ HindIII	TGTAAAACGACGGCCAGT
B024	T7	SalI	TAATACGACTCACTATAGGG
B028	npp-16 IL		GAGTATTGGGGTGATGACTC
B029	npp-16 EL		GTCGTAGAGTGAGAGAACCA
B030	npp-16 IR		CGACGGTTTCCACCTTCGGA
B031	npp-16 ER		CACTGCATCCGGCTCCTGAT
B032	GFPfor		CGAAAAGAGAGACCACATGGTC
B033	SEQrev		CGCTTTCGCACCGTATTGTTC
B034	lem-2 IR		TGCGTTGTTGTCAGCGCGTA
B035	lem-2 ER		GCAGTTTTCGGGCGATGCGT
B036	lem-2 IL		GGCTTTCAGCTCATCGGGCA
B037	lem-2 EL		AGGCGTCGGTACAACGTGAG
B064	GSTfor	BamHI	ggcagatctATGTCCCCTATACTAGGTTATTG
B125	GFP int2		GTGTCTTGTAGTTCCCGTCA
B274	npp-16 forw	XmaI	tacccgggAATTCCCTAATTCCACCGCCA

B275	npp-16 rev	SpeI	agactagtgcTCAAACAGCGACTTCTAGA
B276	npp-16 promF	NotI	aGCGGCCGCaactcgaccactgccctcagt
B277	npp-16 promR	BsrGI	gatgtacaCATcacgaatctgaacgaaaatc
B278	npp-16 ORF	BsrGI	gatgtacaAATTCCCTAATTCCACCGCCA
B279	npp-16 3UTRR	SpeI	AGACTAGtcgaaatctactcgcggaaac
B321	npp-6_IL_ok		CATTGCTCAACGCAATCACTG
B353	Dendra2rev	NgoMIV	atgccggcAACACCTGAATCACCAGACC
B381	npp-16 rev pQE	PstI	GCGCGCTGCAGgcTCAAACAGCGACTTCTAGAA
B382	npp-16 rev trunk	PstI	GCGCGCTGCAGTCActCTTTTCCCAAAAATGCGAAAAG
B448	tba-2_rev		Ctgggagatgattctgttgaggt
B449	L4440_for	BglII/ HindIII	GAGTCAGTGAGCGAGGAAGCAA

Table 6: Primers used in this study.

4.3. RNAi

4.3.1. . RNAi liquid genome wide screening.

For the genome wide screening were used the Julie Ahringer library that contains ~17,000 bacteria clones organized by chromosomes in 384 well plates. To analyze each gene in the N2, BN11 an BN19 strains we used flat 96 well flat plates from (VWR Ref: 732-7585) (4 96 well plates for each 384 well plate) and they were processed using the robot Precision XS, Bio Tek. The programs indicated and the receipts of the recipes of the media used are in the supplementary material.

Day 0

Take shallow 96 well plates from freezer: Use a sterile 96-pin (bioX) replicator to spot bacteria from a glycerol stock to a 14 cm LB plate (C. Viral) containing 100 µg/ml ampicillin and 10 µg/ml tetracycline. Grow overnight at 37°C. Due to the design of the original library, many 96 well plates have positions without growth.

Day 1

Prepare 96 deep well plates (VWR Ref: 732-7585) with 1 ml LB medium containing 100 µg/ml ampicillin (Robot program Nº 1). To inoculate the deep well plates, touch the bacteria colonies with a sterile 96-pin replicator and move the replicator to the 96-well deep well plates. Move the replicator around the walls of the 96-well plate, remove the replicator and seal the plate with gas permeable sticker. Prepare the controls: two tubes, each one with 1 ml of LB with 100 µg/ml ampicillin and inoculate with RNAi #7 (*emr-1*) and with RNAi #17 (*npp-5*). Grow cultures for 13h at 20°C +1h 37°C, shaking (220 rpm).

Wash worms (N2, BN11 *npp-16*, BN19 *lem-2*) of two 10 cm NGM plates using M9. Collect in 15 ml tubes. Centrifuge 500 rpm 2' in swinging buckets (Sorvall T21 Benchtop Centrifuge). Remove supernatant. Add 15 ml M9. Centrifuge 500 rpm 2' in swinging buckets. Remove supernatant. Add 2 ml freshly prepared bleach solution (5 ml H2O; 3 ml household bleach; 2 ml NaOH 5M). Shake until worms break up. Add 13 ml S-medium. Centrifuge 2200 rpm 1'. Remove supernatant. Add 15 ml S-medium. Centrifuge 2200 rpm 1'. Remove supernatant. Add 15 ml S-medium. Centrifuge 2200 rpm 1'. Remove supernatant. Add 5 ml S-medium containing 0.01% Tween-20, 100 ug/ml ampicillin, and 5 ug/ml cholesterol. Take out a couple of 30 ul aliquots to count embryo. Leave embryos to hatch into L1s overnight at 20°C, rocking.

Day 2

Spin the 96-well plates in centrifuge at 4000 rpm (Sorvall T21 Benchtop Centrifuge)., 8 min. Discard the supernatant by inversion. Leave the plates inverted on top of paper soaked with EtOH to minimize cross-contamination. Add with robot 160 µl S-medium containing 100 ug/ml ampicillin, 5 ug/ml cholesterol, 1mM IPTG. Mix by pipetting up/down 3x with robot using VWR wide orifice Pippet Tip (Robot program Nº 2). Shake at 30°C for 3 hours or 37° 2 hours.

Count number of L1s and unhatched embryos in several aliquots of 30 ul. Dilute by adding S-medium containing 0.01% Tween-20, 100 ug/ml ampicillin, and 5 ug/ml cholesterol to a concentration of 10 worms/30 µl. 2.88 ml is needed for each 96-well

bacteria plate + minimum 2 ml dead volume in reservoir. Add to the worm solution Fungizone (1:1000) to minimize fungal contamination.

Use robot to aliquot 30 µl of bacteria suspension (Robot program Nº 3) and 30 µl worm solution (Robot program Nº 4) into shallow flat bottomed 96-well plates (Clinicord Ref: 989000011.00). We use VWE Bevel Pipet Tips and VWE Non-Bevel Pipet Tips for worms. The number of worms/well will probably range from 5–15.

Cover plates with lids and put plates in a humid chamber at 20°C. Score 4–7 days later for phenotypes.

4.3.2. RNAi plates.

6 cm RNAi plates were done using NGM agar and adding Carbecinillin (Carb) to 25 µg/ml and IPTG to 1mM just before pouring. It is important that the plates are dry before seeding the bacteria to avoid diluting the RNAi effect. Desired bacterial strains, from a glycerol stock, were streaked on a LB plate containing 25 µg/ml Carb and 10 µg/ml tetracycline (Tet) and grown overnight at 37°C. The next day we grew the cultures in LB medium containing 50 µg/ml Carb and 10 µg/ml Tet, with shaking at 220 rpm for 8 hours. Each RNAi plate was seeded with 100µl of the bacterial culture, left to dry and incubated overnight at room temperature.

4.3.3. RNAi feeding on plates

RNAi feeding was performed from two different worm stages:

From L1: three adult worms were placed in a small drop (XX µl) of bleach on each RNAi plate and the embryos were left during 42 h at 20°C for RNAi to take effect. Phenotypes such as Lva, Ste, and Stp of these worms and other such as Emb in their progeny were scored at different point time.

From L4: 9-10 L4 worms per plate were left during 36 h at 20°C for RNAi to take effect, then three adults were moved to each of three replica plates seeded with the same bacteria. After 4 hours, the adults were removed from the replica plates. To score for embryonic lethality, the number of embryos laid and the number of death

embryos after 24 h later were counted. Post-embryonic phenotypes such as Lva, Lvl or Ste also were scored later at appropriate time points.

The two validation rounds of the screening were performed on RNAi plate, the 1st was done from L1, whereas the 2nd validation was performed from L4 allowing the quantification of embryonic lethality. Apart from the genome wide screening, feeding RNAi has been used as a main tool for different experiments in the present work, and usually has been perform from L4 worm.

4.3.4. Test of different conditions for RNAi feeding

After the second validation of the screening, we stated to have a lot of problems with the reproducibility of the RNAi phenotypes obtained. Not only with candidates genes, but also with the controls, RNAi *npp-5* and *emr-1*, we obtained decrease/disappearance of previously observed phenotypes. With the goal of analyze how different factors could affect the RNAi and obtain the best conditions. Several RNAi experiments were done from L4.

Conditions		*npp-16(tm1596)* *npp-5* RNAi	*lem-2(tm1582)* *emr-1* RNAi	*lem-2(tm1582)* *ubc-12* RNAi
Antibiotic in the liquid culture	Amp	27 % (22%-35%)	100 %	
	Amp + Tet	58 % (54%-62%)	100 %	
Agar brand	Sigma	40 % (34%-63%)	89 % (77%-98%)	64 % (34%-85%)
	Pronadisa	55 % (91%-36%)	75 % (64%-81%)	41 % (0%-68%)
	Labotaq	35 % (39%-75%)	64 % (48%-88%)	30 % (12%-52%)
Temperature of the plates before adding the RNAi bacteria	Pre-heat 1h 37	40 % (25%-50%)	100 %	70 % (30%-80%)
	No pre-heat	49 % (30%-69%)	69 % (52%-85%)	42 % (13%-56%)
Bacteria	Original glycerol stock			96 % (91%-100%)
	HT115 freshly transformed with RNAi plasmid			62 % (56%-70%)

Table 7: Analysis of the RNAi efficiency measured as percentage embryonic lethality in different conditions. Shown are average and range.

From this experiments we start to use Tetracycline in the liquid cultured because the efficiency in *npp-5* RNAi is increased. Respect to the other conditions, we did not

conclude anything clear about how ,the different brand of agar or the temperature bacteria, increase or not the efficiency, in fact the different conditions affect in a different way to the genes checked. In the case of use bacteria from the original glycerol stock or HTT115 freshly transformed with RNAi plasmid, the numbers show that HT115 freshly transformed bacteria did not has higher efficiency, so we continued using the original ones.

At the same time we check how different temperatures could affect the efficiency of the RNAi, and for that we check several candidates genes at 16º, 20º and 25º doing RNAi from embryos.

NPP-16 candidates				
Gene/ Code	16º	20º	25º	Phenotype showed after 2nd round of validation
cye-1 / I3Q2D3	BN11: Grow, Sck	BN11: F2 Ste, Grow, Sck	BN11: strong Sck, Lvl N2: F2 Ste	BN11: 32% Emb, Stp, enhanced Pvl, Stp N2: Stp
npp-2/ I4Q1D2	BN11: Ste, Lva, Sck	BN11: Ste, Lva, Sck	Lethal in both	BN11: 70% Emb, Stp N2: 25% Emb, Lva, Stp
skr-1/ I4Q3G6	BN11: Grow	BN11: F2 Emb, Lva		BN11: 80% Emb N2: 50% Emb

LEM-2 candidates				
Gene/ Code	16º	20º	25º	Phenotype showed in 2nd validation round
C03B1.3/ X3Q2F12	BN19: Stp	No phenotype	No phenotype	BN19: Stp
D2096.9/ IV4Q1G1	No	BN19: F2 Lva, Ste	BN19: Grow	BN19: 74% Emb, F2 emb
sago-2/ I7Q4H4	BN19: reduced brood size	BN19: reduced brood size	BN19: reduced brood size	BN19: Rb
ubc-12/ I5Q4H11	BN19: Emb	BN19: Ste, Lva	BN19: Ste	BN19: 60% Emb N2: 20% Emb Both Ste
rskn-1/ I4Q1H7	BN19: Lva, Ste, Grow	BN19: Grow	Lethal in both	BN19: 53,6% Emb N2: 17% Emb
cuti-1 / I3Q1C10	Lva and Lvl in both but stronger in BN19	Lva and Lvl in both but stronger in BN19	Lva and Lvl in both but stronger in BN19	Dpy, Unc (also in N2), mild Pvl
npp-17/ I5Q1B8	BN19: F2 Ste	No phenotype	BN19: Lva Sck	BN19: 9.8% Emb, Ste, Pvl N2: 5% Emb, Ste

Table 8.Different temperature RNAi assay. Analysis of several candidate genes at different temperatures and comparison with the phenotype that they showed after the 2nd round of validation in the RNAi screening.

From these experiments, we conclude that the different temperatures did not recover the phenotype observed in the 2nd round of validation with these candidates. Only in some of them the effect at 25º was stronger, even lethal in wt and mutant strains, as is the case of *npp-2* and *rskn-1*. So we decides continue doing the RNAi experiment at 20ºC

Having experienced a decrease in efficiency with the RNAi by feeding, we induced RNAi of some of our candidates (*npp-21*, *ubc-12*, *C2B7.7*, *ned-8*, *rfl-1*, *ula-1* and *lem-2*) and controls (*npp-5* and *lem-2*) using injection and soaking protocols. However, despite the controls producing robust phenotypes, we did not observe an enhancement of the phenotypes produced through RNAi by feeding.

4.3.5. RNAi by other methods

- **dsRNA molecule production**

DH5-α bacteria were transformed with the L4440 RNAi plasmids to obtain better plasmid quantity and quality. PCR were performed using these DNAs as templates and the universal primers B023 and B449. PCR products were gel purified and used as templates for the in vitro transcription reaction.

We used the kit Mega script T7 (Ambion) to obtain the dsRNA, performing 10 µl reactions. Typical yields are ~0.4 µg/µl of RNA (4µg total). Then the transcription reaction was diluted 4x with 20 µl sterile DEPC water, and 2 µl were run on a gel for visual inspection of dsRNA quality.

- **RNAi by injection:**

Young adults were injected with the dsRNA solution without purification into the intestine, body cavity or gonad. Immediately, the injected worms were put onto plates. They were moved to new plates every 24 hours and the progeny produced was scored at different times after injection (Ahringer 2006).

4.3.6. RNAi by soaking:

Purification of the RNAi molecules was needed to prevent death during the soaking process. We did Lithium chloride precipitation, using the same kit. Then 8 µl of this reaction were put in a 200 µl PCR tube with 2 µl of 5x soaking buffer (Ahringer 2006).

L4 worms were picked to a fresh NGM plate without bacteria, and let them crawl for several minutes to remove bacteria completely. We put 10 L4 in the dsRNA solution, and they were incubated at 20°C for 24 hours. These worms were transferred to NGM plates and phenotypes in the P0 or F1 progeny were scored.

4.4. Production and purification of antibodies

NPP-16 antibodies were raised in rabbits against a recombinant NPP-16 (274-382 aa). These antibodies were affinity purified from sera using an Immobile-P (Millipore) membrane coated with the NPP-16 antigen.

The antigen was obtained by overexpression of the antigen from plasmid #1125 and #815 in BLD21(DE3)pREP4 bacteria. The bacteria were grown on 12 ml LB with Amp and 2% glucose O/N. 500 ml of pre-warmed LB/Amp/2% glucose were inoculated with 12,5 ml of growth culture. This was growth at 37ºC for 4 h, to reach an OD ~600, then IPTG to 1mM was added to the culture, leaving it 3h more at 37ºC. This cultured was harvest in 250 ml tubes at 18ºC. Next day pellet was re-suspended in Buffer B (supplementary material) and sonicate with Bandson digital Sonifier in 15ml Falcon tubes on ice. (programs in supplementary material part). Samples were rotate 30 min at 4ºC and later spin at 12.000rpm (Sorvall T21 Benchtop Centrifuge). The supernatant was mixed with 250 µl of Talon beads from Clonotech (previously washed 3 times with PBS 1X and Triton-100% and centrifuges at 500 g for 2 min) and rotate at 4ºC during 3h. After that the beads were spin at 500g for 3.5 min and washed with PBS 1X and Trition-100%. Then the protein was eluted six times with 1ml of elution buffer. 10 µl of the different samples taken during all the processes (total, pellet, unbound) and 10 µl of each elution were run in a gel with SDS buffer and β-Mercaptoethanol, to check in the majority of the protein is in the eluted fractions. Later this was quantified on an agarose gel running a sample of the protein next to different BSA concentrations.

To reduce the quantity of Tris in the sample we dialyzed it by osmosis with PBS 1X and three step for dilute the quantity of Tris. Spectra/Por molecular porous membrane tubing (Spectrum laboratories) was used for this process.

A total of 11 ml of NPP-16 antigen was recovered at a concentration of 0.4 µg/µl. The antigen was injected into two rabbits at Abyntek, which later provided us with 150 ml of final bleeds from two different rabbits (300 ml in total). To continue the protocol, after the affinity purification, we chose the one that gave a better signal in the WB and IF experiment.

The antigen (200 µl) was then coupled to an Inmobilon P membrane (Milipore) of 50 cm^2, and then 300µl of the antibodies were incubated with the membrane.

Bound antibodies were eluted with 1 ml 0.1 M glycine (pH 2.5) and immediately neutralized with 0.1 ml of 1M Tris (pH 8.0).

4.5. Western blot

Embryos were obtained using a hypochlorite treatment (1N NaOH, 30% bleach solution). Then they were disrupted by boiling and vortexing in SDS sample buffer together with 0.5 µm diameter glass beads and separated by 10%SDS-PAGE. Proteins were transferred to Inmobilon P membranes (Milipore), previously blocked with PBS containing 0.05% Tween-20 and 3% low-fat milk (PBST-M). Then the membrane was probed for 2 h at room temperature with first antibodies diluted in PBST-M (1:300) and after that, was washed with PBST-M for 1 h. Next, the membranes were washed with PBST for 1 h, incubated with peroxidase-conjugated secondary antibodies (Sigma-Aldrich, 1:5000-1:10,000) for 2 h at room temperature. Finally the membrane was developed with ECL Plus (GE Amersham).

4.6. Immunofluorescence

Gravid hermaphrodites were dissected in 3 µl M9 directly on poly-L-lysine-coated glass slides and covered with 12x12 mm coverslips. To break the eggshells, slides were transferred immediately to metal plates on top of dry ice and stored O/N at -80º. After that coverslips were flicked off and slides were placed in methanol for 15-18 min at -18°C, and slides were rehydrated for 30 min in PBS with 0.1% Tween 20 (PBST) and

blocked for 30 min with 10% fetal calf serum in PBST. Then the embryos were incubated for 2 h with primary antibodies diluted in PBST-F as indicate in Table 9. Embryos were washed for 1 h in PBST followed by incubation for 2 h with secondary antibodies diluted in PBST-F. Secondary antibodies were Alexa Fluor 546-conjugated goat anti-mouse antibodies (Invitrogen 1:1000) and Alexa Fluor 633-conjugated goat anti-rabbit antibodies (Invitrogen 1:1000). Slides were washed again for 1 h in PBST and finally mounted with Mowiol containing 5 mg/ ml Hoechst 33258. All the process was at room temperature. Confocal images were obtained with a Leica confocal SPE microscope equipped with a ACS APO 63X/1.3 objective and processed with Fiji.

111

Antibody	Western blot	Inmuno-fluorescence	Description	Reference
NPP-16/ Nup50	1:300	1:50	Rabbit polyclonal affinity purified (against recombinant NPP-16 (274-382 aa)	This study
NPP-7/ Nup153	-	1:300	Rabbit polyclonal antiserum BUBU	Galy et al.,2003
LMN-1	-	1:300	Rabbit	(Liu, Rolef Ben-Shahar et al. 2000)
mAb414	-	1:250	Mouse monoclonal against FG nucleoporins	Covance MMS-120R
α-tubulin	-	1:300	Mouse monoclonal DM1 alpha	Sigma T9026
MEL-28/ ELYS	-	1:300	Rabbit polyclonal antiserum BUD3	Galy et al., 2006

Table 9 : Antibodies used in this study.

4.7. Single copy integration transgenic generated by microinjection (MosSCI)

Transgenic worms were made by injection into EG4322 (TTtI5605 ii; unc-119 (ed-3)) worms. The standard injection mix consisted of 50 ng/ml repair template, 50 ng/ml Mos1 transposase pJL43.1 (P_{glh-2}::transposase), 10 ng/ml pBN1($_{Plmn-1}$::mCherry::his-58), 5 ng/ml pCFJ104 (P_{myo-3}::mCherry) and 1.25 ng/ml pCFJ90 (P_{myo-2}::mCherry). *unc-119* worms are severely paralyzed and egg-laying defective, so L1-L2 worms were manually distributed across a lawn of OP50, and very young adults were selected for injection. Injected worms were individually transferred to standard NGM plates and placed at 16°C for a few hours to recover followed by incubation at 25 °C. Plates were scored for the number of phenotypically rescued F1 worms 3 days after injection.

Individual injected worms were allowed to exhaust the food source. Once starved, plates containing transgenic lines were screened for insertion events on a fluorescence dissection microscope based on wild-type movement but complete lack of fluorescent coinjection markers. Plates containing insertion events typically had a large proportion of non-fluorescent moving worms, although some plates only had a few. Integrated strains were outcrossed to wild type N2 twice.

4.8. Live embryo imaging

Embryos were mounted in M9 buffer between a cover slip and a 2% agarose pad. Epifluorescence and transmitted light were recorded with a NIKON-A1R confocal microscope through a 60x/1.4 objective, captured using integral Nikon software and processed with Fiji. The laser intensity was adjusted so that no effect on development was observed. Images were collected at 5 sec interval for a total of 20-40 min, except for Figure 35 and Figure 36B where z stacks consisting of three focal planes separated by 2 µm were acquired at 35 s intervals. For extended recording up to 14 h (Figure 28 and 40), samples were sealed with VALAP and 6 z-stacks were acquire at 5 min intervals (1.5 µm per stack; total 6 µm). Images of Figures 18 and 20 were captured using the 10x objective.

Images of Figure 36B were acquired with the microscope Spinning Disk Roper Scientific, samples were sealed with VALAP and 6 z-stacks were acquire at 5 s intervals (1.5 µm per stack; total 6 µm).

4.9. Fluorescence recovery after photobleaching (FRAP) analyses

FRAP analyses were performed with 4-cell embryos, bleaching with a high intensity laser light a small region of interest (ROI) along the nuclear envelope. Fluorescence then recovers as the population of bleached molecules is replaced by unbleached molecules from outside the ROI. FRAP experiments were performed using NIKON-A1R confocal microscope through a 60x/1.4 objective. Images were processed using Fiji.

FRAP analysis of Figure 22 were performed using the laser 402 nm to make the bleaching for 3 sec, and images were acquire using the Resonant scanner. In the case of figure 29, bleaching was done using the laser 488 nm during for 3 sec and images were acquired using the Galvano scanner.

4.10. Dendra2 photo-conversion assay

Young adults were put in a drop of 4 µl 5mM levamisole, on a slide with agarose. Images were captured using the NIKON-A1R confocal microscope through 10x objective. To produce the photo-conversion 100% laser 402 nm, with a scan speed of 2s/frame, was used during 20 sec and 11 loops.

After stimulation, worms were put on a plate with 20 µl of M9 to recover and they were kept at 20°C. Every 24 h, 3 images per worm (3-4 worms) were taken (head, tail and the area of the vulva) with 60x objective.

5. Supplementary material

Media	1000 ml	MW [g/mol]	M [mmol/L]
NGM Agar			
NaCl [g]	**3,00**	58,44	51,3
agar [g]	**17,00**		
peptone [g]	**2,50**		
cholesterol (5 mg/ml in EtOH) [ml]	**1,00**		
H2O [ml]	**972,00**		
autooclave			
CaCl2 1M [ml]	**1,00**		1,0
MgSO4 1M [ml]	**1,00**		1,0
potassium phosphate 1M pH6 [ml]	**25,00**		25,0
OPTI-Growth Agar	Same as NGM Agar but with 5 g/L peptone		
S Medium			
NaCl 5M [ml]	**20,00**		100,0
potassium phosphate 1M pH6 [ml]	**50,00**		50,0
potassium citrate 1M pH6 [ml]	**10,00**		10,0
trace metals solution [ml]	**10,00**		
CaCl2 1M [ml]	**3,00**		3,0
MgSO4 1M [ml]	**3,00**		3,0
filter and keep in dark			
cholesterol (5 mg/ml in EtOH) [ml]	**1,00**		
Trace Metal Solution			
Disodium EDTA [g]	**1,860**	372,24	5,0
FeSO4 7*H2O	**0,690**	278,02	2,5
MnCl2 4*H2O	**0,200**	197,91	1,0
ZnSO4 7*H2O	**0,290**	287,54	1,0
CuSO4 5*H2O [g]	**0,025**	249,68	0,1
autoclave and keep in dark			
5*TBE (pH 8.3)			
Trizma base [g]	**54,00**	121,14	445,8
Boric acid [g]	**27,50**	61,83	444,8
EDTA (Na-salt) [g]	**4,65**	372,24	12,5
Check that pH is ~8.3			
M9 Buffer			
KH2PO4 [g]	**3,00**	136,09	22,0
Na2HPO4 [g]	**6,00**	177,99	33,7
NaCl [g]	**5,00**	58,44	85,6
MgSO4, 1M [mL]	**1,00**		1,0
T-low-E pH 8.0	**100 ml**	**50 ml**	
Tris 1M pH 8.0 -> 10 mM	1 ml	0.5 ml	
EDTA 0.5M pH 8.0 -> 0.2 mM	40 ul	20 ul	
25*PBS (pH 7.4)			
KH2PO4 [g]	**6,00**	136,09	44,1
Na2HPO4 [g]	**36,00**	177,99	202,3
NaCl [g]	**200,00**	58,44	3422,3
KCl [g]	**5,00**	74,56	67,1
Adjust pH to 7.4			
Buffer B (Ab Production)			10ml
Roche Complete Mini			½ tablet
10mM Tris pH 8.0			100 µl
1mM EDTA			50 µl

1M DTT	50 µl
30% Sarcosyl	500 µl
PMSF 100mM	20 µl
Elution buffer (AB Production)	1600 µl
20mM glutathione	320 µl
100 mM Tris pH 8.0	160 µl
120 mM NaCl	192 µl
10% glycerol	320 µl

Table 10: Medias used in the different experiments

Robot programs

Program nº1: LB in 96 deep well plates:

Loop Max times [Level 1]

DISPENSE 1000 µl into Sta E column 1 (+1) using Dispenser normal

Loop off

Loop Max times [Level 1]

DISPENSE 1000 µl into Sta F column 1 (+1) using Dispenser normal

Loop off

Loop Max times [Level 1]

DISPENSE 1000 µl into Sta C column 1 (+1) using Dispenser normal

Loop off

Loop Max times [Level 1]

DISPENSE 1000 µl into Sta B column 1 (+1) using Dispenser normal

Loop off

Program nº 2: S-Medium

Loop Max times [Level 1]

DISPENSE 320 µl into Sta E column 1 (+1) using Dispenser normal

Loop off

Loop Max times [Level 1]

TIPS from Sta A column 1 (+1) using Rack for tips, waste for residual.

ASPIRATE 50 µl from Sta E column 1 (+1) using s-medium (name given to the 96 liquid content)

DISPENSE 50 µl into Sta E column 1 (+1) using DP_Mix_bacteria

Loop off

Put a new box of tips (white ones with the wide mouth)

Loop Max times [Level 1]

DISPENSE 320 µl into Sta F column 1 (+1) using Dispenser normal

Loop off

Loop Max times [Level 1]

TIPS from Sta A column 1 (+1) using Rack for tips, waste for residual.

ASPIRATE 50 µl from Sta F column 1 (+1) using s-medium (name given to the 96 liquid content)

DISPENSE 50 µl into Sta F column 1 (+1) using DP_Mix_bacteria

Loop off

Put a new box of tips (white ones with the wide mouth)

Loop Max times [Level 1]

DISPENSE 320 µl into Sta C column 1 (+1) using Dispenser normal

Loop off

Loop Max times [Level 1]

TIPS from Sta A column 1 (+1) using Rack for tips, waste for residual.

ASPIRATE 50 l from Sta C column 1 (+1) using s-medium (name given to the 96 liquid content)

DISPENSE 50 l into Sta C column 1 (+1) using DP_Mix_bacteria

Loop off

Put a new box of tips (white ones with the wide mouth)

Loop Max times [Level 1]

DISPENSE 320 l into Sta B column 1 (+1) using Dispenser normal

Loop off

Loop Max times [Level 1]

TIPS from Sta A column 1 (+1) using Rack for tips, waste for residual.

ASPIRATE 50 l from Sta B column 1 (+1) using s-medium (name given to the 96 liquid content)

DISPENSE 50 l into Sta B column 1 (+1) using DP_Mix_bacteria

Loop off

The DP Mix-bacteria is defined in the robot:

Program nº 3: Bact (mix) aliquots

Remarks:

Load Sta A with 96 Tips yellow narrow tips

Load Sta B, Sta C and Station F with 96 small well plates

Load Sta D with 96 Deep Well plate that has the pelleted bacteria in S-medium

LOOP 4 times [Level 1]

TPS from Sta A column 1 (+1) using Rack for tips. Waste for residual

ASPIRATE 109 l from Sta D column 1 (+1)

DISPENSE 109 l into Sta D column 1 (+1) using DP__Mix bacteria

Remark “ALIQUOT Sta F” clones row 1-4

ASPIRATE 90 l from Sta. D column 1 (+1) using Paulo Aspirate

DISPENSE 30 l into Sta F column 1 (+3) using Adela Disp

DISPENSE 30 l into Sta F column 2 (+3) using Adela Disp

DISPENSE 30 l into Sta F column 3 (+3) using Adela Disp

LOOP off

LOOP 4 times [Level 1]

TIPS from Sta A column 5 (+1) using Rack for tips. Waste for residual

ASPIRATE 109 l from Sta D column 5(+1)

DISPENSE 109 l into Sta D column 5 (+1) using DP__Mix bacteria

Remark “ALIQUOT Sta B” clones row 5-8

ASPIRATE 90 l from Sta. D column 5 (+1) using Paulo Aspirate

DISPENSE 30 l into Sta B column 1 (+3) using Adela Disp

DISPENSE 30 l into Sta B column 2 (+3) using Adela Disp

DISPENSE 30 l into Sta B column 3 (+3) using Adela Disp

LOOP off

LOOP 4 times [Level 1]

TIPS from Sta A column 9 (+1) using Rack for tips. Waste for residual

ASPIRATE 109 l from Sta D column 9 (+1)

DISPENSE 109 µl into Sta D column 9 (+1) using DP__Mix bacteria

Remark “ALIQUOT Sta B” clones row 9-12

ASPIRATE 90 µl from Sta. D column 9(+1) using Paulo Aspirate

DISPENSE 30 µl into Sta C column 1 (+3) using Adela Disp

DISPENSE 30 µl into Sta C column 2 (+3) using Adela Disp

DISPENSE 30 µl into Sta C column 3 (+3) using Adela Disp

LOOP off

Program nº 4: Worms’s aliquot

Remark: Load Sta. A with 4 row of yellow wide tips.

Remark: Load Sta. D with 3X 50 µl wells with Mutant 1, Wt, and Mutant 2 worms

Remark: Load Sta. B, C and F with 96 small well plates containing bacteria aliquots

Remark: Mutant 1 worms add

TPS from Sta. A column 1 (+0) using Rack for tips. Waste for residual.

Remark “Sta B”

ASPIRATE 120 µl fom Sta. D column 1 (+0) using Paulo Asp DEEP

DISPENSE 120 µl into Sta D column 1 (+0) using P_MIX_Worms

ASPIRATE 120 µl fom Sta. D column 1 (+0) using Paulo Asp DEEP

DISPENSE 30 µl into Sta B column 1 (+0) using Adela Disp 1

DISPENSE 30 µl into Sta B column 4 (+0) using Adela Disp 1

DISPENSE 30 µl into Sta B column 7 (+0) using Adela Disp 1

DISPENSE 30 µl into Sta B column 10 (+0) using Adela Disp 1

Remark “Sta C”

ASPIRATE 120 l fom Sta. D column 1 (+0) using Paulo Asp DEEP

DISPENSE 120 l into Sta D column 1 (+0) using P_MIX_Worms

ASPIRATE 120 l fom Sta. D column 1 (+0) using Paulo Asp DEEP

DISPENSE 30 l into Sta C column 1 (+0) using Adela Disp 1

DISPENSE 30 l into Sta C column 4 (+0) using Adela Disp 1

DISPENSE 30 l into Sta C column 7 (+0) using Adela Disp 1

DISPENSE 30 l into Sta C column 10 (+0) using Adela Disp 1

Remark “Sta F”

ASPIRATE 120 l fom Sta. D column 1 (+0) using Paulo Asp DEEP

DISPENSE 120 l into Sta D column 1 (+0) using P_MIX_Worms

ASPIRATE 120 l fom Sta. D column 1 (+0) using Paulo Asp DEEP

DISPENSE 30 l into Sta F column 1 (+0) using Adela Disp 1

DISPENSE 30 l into Sta F column 4 (+0) using Adela Disp 1

DISPENSE 30 l into Sta F column 7 (+0) using Adela Disp 1

DISPENSE 30 l into Sta F column 10 (+0) using Adela Disp 1

Remark: WT worms add

TPS from Sta. A column 2(+0) using Rack for tips. Waste for residual.

Remark “Sta B”

ASPIRATE 120 l fom Sta. D column 2 (+0) using Paulo Asp DEEP

DISPENSE 120 l into Sta D column 2(+0) using P_MIX_Worms

ASPIRATE 120 l fom Sta. D column 2 (+0) using Paulo Asp DEEP

DISPENSE 30 l into Sta B column 2 (+0) using Adela Disp 1

DISPENSE 30 l into Sta B column 5 (+0) using Adela Disp 1

DISPENSE 30 l into Sta B column 8 (+0) using Adela Disp 1

DISPENSE 30 l into Sta B column 11 (+0) using Adela Disp 1

Remark “Sta C”

ASPIRATE 120 l fom Sta. D column 2 (+0) using Paulo Asp DEEP

DISPENSE 120 l into Sta D column 2(+0) using P_MIX_Worms

ASPIRATE 120 l fom Sta. D column 2 (+0) using Paulo Asp DEEP

DISPENSE 30 l into Sta C column 2 (+0) using Adela Disp 1

DISPENSE 30 l into Sta C column 5 (+0) using Adela Disp 1

DISPENSE 30 l into Sta C column 8 (+0) using Adela Disp 1

DISPENSE 30 l into Sta C column 11 (+0) using Adela Disp 1

Remark “Sta F”

ASPIRATE 120 l fom Sta. D column 2 (+0) using Paulo Asp DEEP

DISPENSE 120 l into Sta D column 2(+0) using P_MIX_Worms

ASPIRATE 120 l fom Sta. D column 2 (+0) using Paulo Asp DEEP

DISPENSE 30 l into Sta F column 2 (+0) using Adela Disp 1

DISPENSE 30 l into Sta F column 5 (+0) using Adela Disp 1

DISPENSE 30 l into Sta F column 8 (+0) using Adela Disp 1

DISPENSE 30 l into Sta F column 11 (+0) using Adela Disp 1

Remark: Mutant 2 worms add

TPS from Sta. A column 3(+0) using Rack for tips. Waste for residual.

Remark “Sta B”

ASPIRATE 120 l fom Sta. D column 3 (+0) using Paulo Asp DEEP

DISPENSE 120 l into Sta D column 3(+0) using P_MIX_Worms

ASPIRATE 120 l fom Sta. D column 3 (+0) using Paulo Asp DEEP

DISPENSE 30 l into Sta B column 3 (+0) using Adela Disp 1

DISPENSE 30 l into Sta B column 6 (+0) using Adela Disp 1

DISPENSE 30 l into Sta B column 9 (+0) using Adela Disp 1

DISPENSE 30 l into Sta B column 12 (+0) using Adela Disp 1

Remark “Sta C”

ASPIRATE 120 l fom Sta. D column 3 (+0) using Paulo Asp DEEP

DISPENSE 120 l into Sta D column 3(+0) using P_MIX_Worms

ASPIRATE 120 l fom Sta. D column 3 (+0) using Paulo Asp DEEP

DISPENSE 30 l into Sta C column 3 (+0) using Adela Disp 1

DISPENSE 30 l into Sta C column 6 (+0) using Adela Disp 1

DISPENSE 30 l into Sta C column 9 (+0) using Adela Disp 1

DISPENSE 30 l into Sta C column 12 (+0) using Adela Disp 1

Remark “Sta F”

ASPIRATE 120 l fom Sta. D column 3 (+0) using Paulo Asp DEEP

DISPENSE 120 l into Sta D column 3(+0) using P_MIX_Worms

ASPIRATE 120 l fom Sta. D column 3 (+0) using Paulo Asp DEEP

DISPENSE 30 l into Sta F column 3 (+0) using Adela Disp 1

DISPENSE 30 l into Sta F column 6 (+0) using Adela Disp 1

DISPENSE 30 l into Sta F column 9 (+0) using Adela Disp 1

DISPENSE 30 l into Sta F column 12 (+0) using Adela Disp 1

Sonication program:

15% intensity: loops: 10 sec ON; 20 sec OFF. Total 2 min

20% intensity: loops: 10 sec ON; 20 sec OFF. Total 1 min.

6. References

References

. "Genome-wide RNAi screening in C. elegans." from http://www.gurdon.cam.ac.uk/~ahringerlab/pages/res_rnai.html.
A. V. Sorokin, E. R. K., and L. P. Ovchinnikov (2007). "Nucleocytoplasmic Transport of Proteins."
Agrawal, N., P. V. Dasaradhi, A. Mohmmed, P. Malhotra, R. K. Bhatnagar and S. K. Mukherjee (2003). "RNA interference: biology, mechanism, and applications." Microbiol Mol Biol Rev **67**(4): 657-685.
Agromayor, M. and J. Martin-Serrano (2013). "Knowing when to cut and run: mechanisms that control cytokinetic abscission." Trends Cell Biol **23**(9): 433-441.
Ahringer, J. (2006). "Reverse genetics." WormBook.
Aleem, E., H. Kiyokawa and P. Kaldis (2005). "Cdc2-cyclin E complexes regulate the G1/S phase transition." Nat Cell Biol **7**(8): 831-836.
Altun, Z. F. a. H., D.H (2009). "Introduction." WormAtlas.
Audhya, A., F. Hyndman, I. X. McLeod, A. S. Maddox, J. R. Yates, 3rd, A. Desai and K. Oegema (2005). "A complex containing the Sm protein CAR-1 and the RNA helicase CGH-1 is required for embryonic cytokinesis in Caenorhabditis elegans." J Cell Biol **171**(2): 267-279.
Bank, E. M., K. Ben-Harush, N. Wiesel-Motiuk, R. Barkan, N. Feinstein, O. Lotan, O. Medalia and Y. Gruenbaum (2011). "A laminopathic mutation disrupting lamin filament assembly causes disease-like phenotypes in Caenorhabditis elegans." Mol Biol Cell **22**(15): 2716-2728.
Barkan, R., A. J. Zahand, K. Sharabi, A. T. Lamm, N. Feinstein, E. Haithcock, K. L. Wilson, J. Liu and Y. Gruenbaum (2012). "Ce-emerin and LEM-2: essential roles in Caenorhabditis elegans development, muscle function, and mitosis." Mol Biol Cell **23**(4): 543-552.
Baugh, L. R., A. A. Hill, D. K. Slonim, E. L. Brown and C. P. Hunter (2003). "Composition and dynamics of the Caenorhabditis elegans early embryonic transcriptome." Development **130**(5): 889-900.
Bembenek, J. N., K. J. Verbrugghe, J. Khanikar, G. Csankovszki and R. C. Chan (2013). "Condensin and the spindle midzone prevent cytokinesis failure induced by chromatin bridges in C. elegans embryos." Curr Biol **23**(11): 937-946.
Bercher, M., J. Wahl, B. E. Vogel, C. Lu, E. M. Hedgecock, D. H. Hall and J. D. Plenefisch (2001). "mua-3, a gene required for mechanical tissue integrity in Caenorhabditis elegans, encodes a novel transmembrane protein of epithelial attachment complexes." J Cell Biol **154**(2): 415-426.
Bernstein, E., A. A. Caudy, S. M. Hammond and G. J. Hannon (2001). "Role for a bidentate ribonuclease in the initiation step of RNA interference." Nature **409**(6818): 363-366.
Blobel, G. (1985). "Gene gating: a hypothesis." Proc Natl Acad Sci U S A **82**(24): 8527-8529.
Boutros, M. and J. Ahringer (2008). "The art and design of genetic screens: RNA interference." Nat Rev Genet **9**(7): 554-566.
Bowerman, B. (2001). "Cytokinesis in the C. elegans embryo: regulating contractile forces and a late role for the central spindle." Cell Struct Funct **26**(6): 603-607.
Brachner, A., S. Reipert, R. Foisner and J. Gotzmann (2005). "LEM2 is a novel MAN1-related inner nuclear membrane protein associated with A-type lamins." J Cell Sci **118**(Pt 24): 5797-5810.
Broers, J. L., F. C. Ramaekers, G. Bonne, R. B. Yaou and C. J. Hutchison (2006). "Nuclear lamins: laminopathies and their role in premature ageing." Physiol Rev **86**(3): 967-1008.
Callan, H. G. and S. G. Tomlin (1950). "Experimental studies on amphibian oocyte nuclei. I. Investigation of the structure of the nuclear membrane by means of the electron microscope." Proc R Soc Lond B Biol Sci **137**(888): 367-378.
Canman, J. C., L. Lewellyn, K. Laband, S. J. Smerdon, A. Desai, B. Bowerman and K. Oegema (2008). "Inhibition of Rac by the GAP activity of centralspindlin is essential for cytokinesis." Science **322**(5907): 1543-1546.
Casolari, J. M., C. R. Brown, S. Komili, J. West, H. Hieronymus and P. A. Silver (2004). "Genome-wide localization of the nuclear transport machinery couples transcriptional status and nuclear organization." Cell **117**(4): 427-439.

Cogoni, C., J. T. Irelan, M. Schumacher, T. J. Schmidhauser, E. U. Selker and G. Macino (1996). "Transgene silencing of the al-1 gene in vegetative cells of Neurospora is mediated by a cytoplasmic effector and does not depend on DNA-DNA interactions or DNA methylation." EMBO J **15**(12): 3153-3163.

Consortium, C. e. S. (1998). "Genome sequence of the nematode C. elegans: a platform for investigating biology." Science **282**(5396): 2012-2018.

Cordes, V. C., S. Reidenbach, H. R. Rackwitz and W. W. Franke (1997). "Identification of protein p270/Tpr as a constitutive component of the nuclear pore complex-attached intranuclear filaments." J Cell Biol **136**(3): 515-529.

Cowan, C. R. and A. A. Hyman (2004). "Asymmetric cell division in C. elegans: cortical polarity and spindle positioning." Annu Rev Cell Dev Biol **20**: 427-453.

Crisp, M., Q. Liu, K. Roux, J. B. Rattner, C. Shanahan, B. Burke, P. D. Stahl and D. Hodzic (2006). "Coupling of the nucleus and cytoplasm: role of the LINC complex." J Cell Biol **172**(1): 41-53.

Cheeks, R. J., J. C. Canman, W. N. Gabriel, N. Meyer, S. Strome and B. Goldstein (2004). "C. elegans PAR proteins function by mobilizing and stabilizing asymmetrically localized protein complexes." Curr Biol **14**(10): 851-862.

Doucet, C. M. and M. W. Hetzer (2010). "Nuclear pore biogenesis into an intact nuclear envelope." Chromosoma **119**(5): 469-477.

Duchaine, T. F., J. A. Wohlschlegel, S. Kennedy, Y. Bei, D. Conte, Jr., K. Pang, D. R. Brownell, S. Harding, S. Mitani, G. Ruvkun, J. R. Yates, 3rd and C. C. Mello (2006). "Functional proteomics reveals the biochemical niche of C. elegans DCR-1 in multiple small-RNA-mediated pathways." Cell **124**(2): 343-354.

Fan, F., C. P. Liu, O. Korobova, C. Heyting, H. H. Offenberg, G. Trump and N. Arnheim (1997). "cDNA cloning and characterization of Npap60: a novel rat nuclear pore-associated protein with an unusual subcellular localization during male germ cell differentiation." Genomics **40**(3): 444-453.

Fievet, B. T., J. Rodriguez, S. Naganathan, C. Lee, E. Zeiser, T. Ishidate, M. Shirayama, S. Grill and J. Ahringer (2013). "Systematic genetic interaction screens uncover cell polarity regulators and functional redundancy." Nat Cell Biol **15**(1): 103-112.

Fire, A., S. Xu, M. K. Montgomery, S. A. Kostas, S. E. Driver and C. C. Mello (1998). "Potent and specific genetic interference by double-stranded RNA in Caenorhabditis elegans." Nature **391**(6669): 806-811.

Fontoura, B. M., G. Blobel and M. J. Matunis (1999). "A conserved biogenesis pathway for nucleoporins: proteolytic processing of a 186-kilodalton precursor generates Nup98 and the novel nucleoporin, Nup96." J Cell Biol **144**(6): 1097-1112.

Friedland, A. E., Y. B. Tzur, K. M. Esvelt, M. P. Colaiacovo, G. M. Church and J. A. Calarco (2013). "Heritable genome editing in C. elegans via a CRISPR-Cas9 system." Nat Methods **10**(8): 741-743.

Galy, V., I. W. Mattaj and P. Askjaer (2003). "Caenorhabditis elegans nucleoporins Nup93 and Nup205 determine the limit of nuclear pore complex size exclusion in vivo." Mol Biol Cell **14**(12): 5104-5115.

Gavilano, L. B., N. P. Coleman, L. E. Burnley, M. L. Bowman, N. E. Kalengamaliro, A. Hayes, L. Bush and B. Siminszky (2006). "Genetic engineering of Nicotiana tabacum for reduced nornicotine content." J Agric Food Chem **54**(24): 9071-9078.

Gerstein, M. B., Z. J. Lu, E. L. Van Nostrand, C. Cheng, B. I. Arshinoff, T. Liu, K. Y. Yip, R. Robilotto, A. Rechtsteiner, K. Ikegami, P. Alves, A. Chateigner, M. Perry, M. Morris, R. K. Auerbach, X. Feng, J. Leng, A. Vielle, W. Niu, K. Rhrissorrakrai, A. Agarwal, R. P. Alexander, G. Barber, C. M. Brdlik, J. Brennan, J. J. Brouillet, A. Carr, M. S. Cheung, H. Clawson, S. Contrino, L. O. Dannenberg, A. F. Dernburg, A. Desai, L. Dick, A. C. Dose, J. Du, T. Egelhofer, S. Ercan, G. Euskirchen, B. Ewing, E. A. Feingold, R. Gassmann, P. J. Good, P. Green, F. Gullier, M. Gutwein, M. S. Guyer, L. Habegger, T. Han, J. G. Henikoff, S. R. Henz, A. Hinrichs, H. Holster, T. Hyman, A. L. Iniguez, J. Janette, M. Jensen, M. Kato, W. J. Kent, E. Kephart, V. Khivansara, E. Khurana, J. K.

Kim, P. Kolasinska-Zwierz, E. C. Lai, I. Latorre, A. Leahey, S. Lewis, P. Lloyd, L. Lochovsky, R. F. Lowdon, Y. Lubling, R. Lyne, M. MacCoss, S. D. Mackowiak, M. Mangone, S. McKay, D. Mecenas, G. Merrihew, D. M. Miller, 3rd, A. Muroyama, J. I. Murray, S. L. Ooi, H. Pham, T. Phippen, E. A. Preston, N. Rajewsky, G. Ratsch, H. Rosenbaum, J. Rozowsky, K. Rutherford, P. Ruzanov, M. Sarov, R. Sasidharan, A. Sboner, P. Scheid, E. Segal, H. Shin, C. Shou, F. J. Slack, C. Slightam, R. Smith, W. C. Spencer, E. O. Stinson, S. Taing, T. Takasaki, D. Vafeados, K. Voronina, G. Wang, N. L. Washington, C. M. Whittle, B. Wu, K. K. Yan, G. Zeller, Z. Zha, M. Zhong, X. Zhou, E. C. mod, J. Ahringer, S. Strome, K. C. Gunsalus, G. Micklem, X. S. Liu, V. Reinke, S. K. Kim, L. W. Hillier, S. Henikoff, F. Piano, M. Snyder, L. Stein, J. D. Lieb and R. H. Waterston (2010). "Integrative analysis of the Caenorhabditis elegans genome by the modENCODE project." Science **330**(6012): 1775-1787.

Ghosh, D. and G. Seydoux (2008). "Inhibition of transcription by the Caenorhabditis elegans germline protein PIE-1: genetic evidence for distinct mechanisms targeting initiation and elongation." Genetics **178**(1): 235-243.

Goldstein, B. and S. N. Hird (1996). "Specification of the anteroposterior axis in Caenorhabditis elegans." Development **122**(5): 1467-1474.

Gonczy, P., C. Echeverri, K. Oegema, A. Coulson, S. J. Jones, R. R. Copley, J. Duperon, J. Oegema, M. Brehm, E. Cassin, E. Hannak, M. Kirkham, S. Pichler, K. Flohrs, A. Goessen, S. Leidel, A. M. Alleaume, C. Martin, N. Ozlu, P. Bork and A. A. Hyman (2000). "Functional genomic analysis of cell division in C. elegans using RNAi of genes on chromosome III." Nature **408**(6810): 331-336.

Gonczy, P. and L. S. Rose (2005). "Asymmetric cell division and axis formation in the embryo." WormBook: 1-20.

Gonzalez, Y., A. Saito and S. Sazer (2012). "Fission yeast Lem2 and Man1 perform fundamental functions of the animal cell nuclear lamina." Nucleus **3**(1): 60-76.

Grewal, P. S. a. R., P. N. (1991). "Effects of Caenorhabditis elegans (Nematoda: Rhabditidae) on yield and quality of the cultivated mushroom Agaricus bisporus." Annals of Applied Biology.

Grishok, A., A. E. Pasquinelli, D. Conte, N. Li, S. Parrish, I. Ha, D. L. Baillie, A. Fire, G. Ruvkun and C. C. Mello (2001). "Genes and mechanisms related to RNA interference regulate expression of the small temporal RNAs that control C. elegans developmental timing." Cell **106**(1): 23-34.

Grosshans, H. and W. Filipowicz (2008). "Molecular biology: the expanding world of small RNAs." Nature **451**(7177): 414-416.

Gruenbaum, Y., K. K. Lee, J. Liu, M. Cohen and K. L. Wilson (2002). "The expression, lamin-dependent localization and RNAi depletion phenotype for emerin in C. elegans." J Cell Sci **115**(Pt 5): 923-929.

Guan, T., R. H. Kehlenbach, E. C. Schirmer, A. Kehlenbach, F. Fan, B. E. Clurman, N. Arnheim and L. Gerace (2000). "Nup50, a nucleoplasmically oriented nucleoporin with a role in nuclear protein export." Mol Cell Biol **20**(15): 5619-5630.

Guo, S. and K. J. Kemphues (1995). "par-1, a gene required for establishing polarity in C. elegans embryos, encodes a putative Ser/Thr kinase that is asymmetrically distributed." Cell **81**(4): 611-620.

Hajeri, V. A., B. A. Little, M. L. Ladage and P. A. Padilla (2010). "NPP-16/Nup50 function and CDK-1 inactivation are associated with anoxia-induced prophase arrest in Caenorhabditis elegans." Mol Biol Cell **21**(5): 712-724.

Hannon, G. J. (2002). "RNA interference." Nature **418**(6894): 244-251.

Hetzer, M. W. (2010). "The nuclear envelope." Cold Spring Harb Perspect Biol **2**(3): a000539.

Hetzer, M. W. and S. R. Wente (2009). "Border control at the nucleus: biogenesis and organization of the nuclear membrane and pore complexes." Dev Cell **17**(5): 606-616.

Huber, M. D., T. Guan and L. Gerace (2009). "Overlapping functions of nuclear envelope proteins NET25 (Lem2) and emerin in regulation of extracellular signal-regulated kinase signaling in myoblast differentiation." Mol Cell Biol **29**(21): 5718-5728.

References

Ikegami, K., T. A. Egelhofer, S. Strome and J. D. Lieb (2010). "Caenorhabditis elegans chromosome arms are anchored to the nuclear membrane via discontinuous association with LEM-2." Genome Biol **11**(12): R120.

Izquierdo, M. (2005). "Short interfering RNAs as a tool for cancer gene therapy." Cancer Gene Ther **12**(3): 217-227.

Jose, A. M., J. J. Smith and C. P. Hunter (2009). "Export of RNA silencing from C. elegans tissues does not require the RNA channel SID-1." Proc Natl Acad Sci U S A **106**(7): 2283-2288.

Kalverda, B., H. Pickersgill, V. V. Shloma and M. Fornerod (2010). "Nucleoporins directly stimulate expression of developmental and cell-cycle genes inside the nucleoplasm." Cell **140**(3): 360-371.

Kamath, R. S., A. G. Fraser, Y. Dong, G. Poulin, R. Durbin, M. Gotta, A. Kanapin, N. Le Bot, S. Moreno, M. Sohrmann, D. P. Welchman, P. Zipperlen and J. Ahringer (2003). "Systematic functional analysis of the Caenorhabditis elegans genome using RNAi." Nature **421**(6920): 231-237.

Kamath, R. S., M. Martinez-Campos, P. Zipperlen, A. G. Fraser and J. Ahringer (2001). "Effectiveness of specific RNA-mediated interference through ingested double-stranded RNA in Caenorhabditis elegans." Genome Biol **2**(1): RESEARCH0002.

Kim, S. K. (2001). "Http://C. elegans: mining the functional genomic landscape." Nat Rev Genet **2**(9): 681-689.

Kipreos, E. T. and M. Pagano (2000). "The F-box protein family." Genome Biol **1**(5): REVIEWS3002.

Kurz, T., L. Pintard, J. H. Willis, D. R. Hamill, P. Gonczy, M. Peter and B. Bowerman (2002). "Cytoskeletal regulation by the Nedd8 ubiquitin-like protein modification pathway." Science **295**(5558): 1294-1298.

Le, L. Q., Y. Lorenz, S. Scheurer, K. Fotisch, E. Enrique, J. Bartra, S. Biemelt, S. Vieths and U. Sonnewald (2006). "Design of tomato fruits with reduced allergenicity by dsRNAi-mediated inhibition of ns-LTP (Lyc e 3) expression." Plant Biotechnol J **4**(2): 231-242.

Lee, K. K., Y. Gruenbaum, P. Spann, J. Liu and K. L. Wilson (2000). "C. elegans nuclear envelope proteins emerin, MAN1, lamin, and nucleoporins reveal unique timing of nuclear envelope breakdown during mitosis." Mol Biol Cell **11**(9): 3089-3099.

Lee, K. K. and K. L. Wilson (2004). "All in the family: evidence for four new LEM-domain proteins Lem2 (NET-25), Lem3, Lem4 and Lem5 in the human genome." Symp Soc Exp Biol(56): 329-339.

Li, C. X., A. Parker, E. Menocal, S. Xiang, L. Borodyansky and J. H. Fruehauf (2006). "Delivery of RNA interference." Cell Cycle **5**(18): 2103-2109.

Lindsay, M. E., K. Plafker, A. E. Smith, B. E. Clurman and I. G. Macara (2002). "Npap60/Nup50 is a tri-stable switch that stimulates importin-alpha:beta-mediated nuclear protein import." Cell **110**(3): 349-360.

Liu, J., K. K. Lee, M. Segura-Totten, E. Neufeld, K. L. Wilson and Y. Gruenbaum (2003). "MAN1 and emerin have overlapping function(s) essential for chromosome segregation and cell division in Caenorhabditis elegans." Proc Natl Acad Sci U S A **100**(8): 4598-4603.

Liu, J., T. Rolef Ben-Shahar, D. Riemer, M. Treinin, P. Spann, K. Weber, A. Fire and Y. Gruenbaum (2000). "Essential roles for Caenorhabditis elegans lamin gene in nuclear organization, cell cycle progression, and spatial organization of nuclear pore complexes." Mol Biol Cell **11**(11): 3937-3947.

Mackay, D. R., M. Makise and K. S. Ullman (2010). "Defects in nuclear pore assembly lead to activation of an Aurora B-mediated abscission checkpoint." J Cell Biol **191**(5): 923-931.

Maeda, I., Y. Kohara, M. Yamamoto and A. Sugimoto (2001). "Large-scale analysis of gene function in Caenorhabditis elegans by high-throughput RNAi." Curr Biol **11**(3): 171-176.

Makise, M., D. R. Mackay, S. Elgort, S. S. Shankaran, S. A. Adam and K. S. Ullman (2012). "The Nup153-Nup50 protein interface and its role in nuclear import." J Biol Chem **287**(46): 38515-38522.

Matsuura, Y., A. Lange, M. T. Harreman, A. H. Corbett and M. Stewart (2003). "Structural basis for Nup2p function in cargo release and karyopherin recycling in nuclear import." EMBO J **22**(20): 5358-5369.
Matsuura, Y. and M. Stewart (2005). "Nup50/Npap60 function in nuclear protein import complex disassembly and importin recycling." EMBO J **24**(21): 3681-3689.
Meyerzon, M., Z. Gao, J. Liu, J. C. Wu, C. J. Malone and D. A. Starr (2009). "Centrosome attachment to the C. elegans male pronucleus is dependent on the surface area of the nuclear envelope." Dev Biol **327**(2): 433-446.
Napoli, C., C. Lemieux and R. Jorgensen (1990). "Introduction of a Chimeric Chalcone Synthase Gene into Petunia Results in Reversible Co-Suppression of Homologous Genes in trans." Plant Cell **2**(4): 279-289.
Ogawa, Y., Y. Miyamoto, M. Asally, M. Oka, Y. Yasuda and Y. Yoneda (2010). "Two isoforms of Npap60 (Nup50) differentially regulate nuclear protein import." Mol Biol Cell **21**(4): 630-638.
Pak, J., J. M. Maniar, C. C. Mello and A. Fire (2012). "Protection from feed-forward amplification in an amplified RNAi mechanism." Cell **151**(4): 885-899.
Parrish, S. and A. Fire (2001). "Distinct roles for RDE-1 and RDE-4 during RNA interference in Caenorhabditis elegans." RNA **7**(10): 1397-1402.
Poole, R. J., E. Bashllari, L. Cochella, E. B. Flowers and O. Hobert (2011). "A Genome-Wide RNAi Screen for Factors Involved in Neuronal Specification in Caenorhabditis elegans." PLoS Genet **7**(6): e1002109.
Pukatzki, S., N. Tordilla, J. Franke and R. H. Kessin (1998). "A novel component involved in ubiquitination is required for development of Dictyostelium discoideum." J Biol Chem **273**(37): 24131-24138.
Pumroy, R. A., J. D. Nardozzi, D. J. Hart, M. J. Root and G. Cingolani (2012). "Nucleoporin Nup50 stabilizes closed conformation of armadillo repeat 10 in importin alpha5." J Biol Chem **287**(3): 2022-2031.
Rabut, G., V. Doye and J. Ellenberg (2004). "Mapping the dynamic organization of the nuclear pore complex inside single living cells." Nat Cell Biol **6**(11): 1114-1121.
Rabut, G. and M. Peter (2008). "Function and regulation of protein neddylation. 'Protein modifications: beyond the usual suspects' review series." EMBO Rep **9**(10): 969-976.
Raices, M. and M. A. D'Angelo (2012). "Nuclear pore complex composition: a new regulator of tissue-specific and developmental functions." Nat Rev Mol Cell Biol **13**(11): 687-699.
Rodenas, E., C. Gonzalez-Aguilera, C. Ayuso and P. Askjaer (2012). "Dissection of the NUP107 nuclear pore subcomplex reveals a novel interaction with spindle assembly checkpoint protein MAD1 in Caenorhabditis elegans." Mol Biol Cell **23**(5): 930-944.
Rodenas, E., E. P. Klerkx, C. Ayuso, A. Audhya and P. Askjaer (2009). "Early embryonic requirement for nucleoporin Nup35/NPP-19 in nuclear assembly." Dev Biol **327**(2): 399-409.
Rothballer, A. and U. Kutay (2013). "Poring over pores: nuclear pore complex insertion into the nuclear envelope." Trends Biochem Sci **38**(6): 292-301.
Saleh, M. C., R. P. van Rij, A. Hekele, A. Gillis, E. Foley, P. H. O'Farrell and R. Andino (2006). "The endocytic pathway mediates cell entry of dsRNA to induce RNAi silencing." Nat Cell Biol **8**(8): 793-802.
Salpingidou, G., A. Smertenko, I. Hausmanowa-Petrucewicz, P. J. Hussey and C. J. Hutchison (2007). "A novel role for the nuclear membrane protein emerin in association of the centrosome to the outer nuclear membrane." J Cell Biol **178**(6): 897-904.
Savas, J. N., B. H. Toyama, T. Xu, J. R. Yates, 3rd and M. W. Hetzer (2012). Extremely long-lived nuclear pore proteins in the rat brain. Science. **335:** 942.
Schirmer, E. C. and L. Gerace (2002). "Organellar proteomics: the prizes and pitfalls of opening the nuclear envelope." Genome Biol **3**(4): REVIEWS1008.
Schneider, S. Q. and B. Bowerman (2003). "Cell polarity and the cytoskeleton in the Caenorhabditis elegans zygote." Annu Rev Genet **37**: 221-249.

References

Sijen, T., J. Fleenor, F. Simmer, K. L. Thijssen, S. Parrish, L. Timmons, R. H. Plasterk and A. Fire (2001). "On the role of RNA amplification in dsRNA-triggered gene silencing." Cell **107**(4): 465-476.

Simmer, F., C. Moorman, A. M. van der Linden, E. Kuijk, P. V. van den Berghe, R. S. Kamath, A. G. Fraser, J. Ahringer and R. H. Plasterk (2003). "Genome-wide RNAi of C. elegans using the hypersensitive rrf-3 strain reveals novel gene functions." PLoS Biol **1**(1): E12.

Smitherman, M., K. Lee, J. Swanger, R. Kapur and B. E. Clurman (2000). "Characterization and targeted disruption of murine Nup50, a p27(Kip1)-interacting component of the nuclear pore complex." Mol Cell Biol **20**(15): 5631-5642.

Sun, C., W. Yang, L. C. Tu and S. M. Musser (2008). "Single-molecule measurements of importin alpha/cargo complex dissociation at the nuclear pore." Proc Natl Acad Sci U S A **105**(25): 8613-8618.

Sundaram, P., B. Echalier, W. Han, D. Hull and L. Timmons (2006). "ATP-binding cassette transporters are required for efficient RNA interference in Caenorhabditis elegans." Mol Biol Cell **17**(8): 3678-3688.

Tabara, H., A. Grishok and C. C. Mello (1998). "RNAi in C. elegans: soaking in the genome sequence." Science **282**(5388): 430-431.

Tabara, H., M. Sarkissian, W. G. Kelly, J. Fleenor, A. Grishok, L. Timmons, A. Fire and C. C. Mello (1999). "The rde-1 gene, RNA interference, and transposon silencing in C. elegans." Cell **99**(2): 123-132.

Tabara, H., E. Yigit, H. Siomi and C. C. Mello (2002). "The dsRNA binding protein RDE-4 interacts with RDE-1, DCR-1, and a DExH-box helicase to direct RNAi in C. elegans." Cell **109**(7): 861-871.

Tanaka, T., T. Nakatani and T. Kamitani (2012). "Inhibition of NEDD8-conjugation pathway by novel molecules: potential approaches to anticancer therapy." Mol Oncol **6**(3): 267-275.

Tavernarakis, N., S. L. Wang, M. Dorovkov, A. Ryazanov and M. Driscoll (2000). "Heritable and inducible genetic interference by double-stranded RNA encoded by transgenes." Nat Genet **24**(2): 180-183.

Tijsterman, M., R. C. May, F. Simmer, K. L. Okihara and R. H. Plasterk (2004). "Genes required for systemic RNA interference in Caenorhabditis elegans." Curr Biol **14**(2): 111-116.

Timmons, L., D. L. Court and A. Fire (2001). "Ingestion of bacterially expressed dsRNAs can produce specific and potent genetic interference in Caenorhabditis elegans." Gene **263**(1-2): 103-112.

Timmons, L. and A. Fire (1998). "Specific interference by ingested dsRNA." Nature **395**(6705): 854.

Tran, E. J. and S. R. Wente (2006). "Dynamic nuclear pore complexes: life on the edge." Cell **125**(6): 1041-1053.

Tzur, Y. B., K. L. Wilson and Y. Gruenbaum (2006). "SUN-domain proteins: 'Velcro' that links the nucleoskeleton to the cytoskeleton." Nat Rev Mol Cell Biol **7**(10): 782-788.

Ulbert, S., W. Antonin, M. Platani and I. W. Mattaj (2006). "The inner nuclear membrane protein Lem2 is critical for normal nuclear envelope morphology." FEBS Lett **580**(27): 6435-6441.

van Steensel, B., J. Delrow and S. Henikoff (2001). "Chromatin profiling using targeted DNA adenine methyltransferase." Nat Genet **27**(3): 304-308.

Vasu, S., S. Shah, A. Orjalo, M. Park, W. H. Fischer and D. J. Forbes (2001). "Novel vertebrate nucleoporins Nup133 and Nup160 play a role in mRNA export." J Cell Biol **155**(3): 339-354.

Wilkins, C., R. Dishongh, S. C. Moore, M. A. Whitt, M. Chow and K. Machaca (2005). "RNA interference is an antiviral defence mechanism in Caenorhabditis elegans." Nature **436**(7053): 1044-1047.

Winston, W. M., C. Molodowitch and C. P. Hunter (2002). "Systemic RNAi in C. elegans requires the putative transmembrane protein SID-1." Science **295**(5564): 2456-2459.

Worman, H. J. and G. Bonne (2007). ""Laminopathies": a wide spectrum of human diseases." Exp Cell Res **313**(10): 2121-2133.

Yigit, E., P. J. Batista, Y. Bei, K. M. Pang, C. C. Chen, N. H. Tolia, L. Joshua-Tor, S. Mitani, M. J. Simard and C. C. Mello (2006). "Analysis of the C. elegans Argonaute family reveals that distinct Argonautes act sequentially during RNAi." Cell **127**(4): 747-757.

References